DEPARTMENT OF NUCLEAR ENGINEERING

NOTICE OF DOCTORAL DEFENSE

STABILITY LIMITS AND WAVES IN TOROIDAL CONFIGURATIONS WITH FINITE PLASMA PRESSURE

Ph. D. THESIS

by

ANTONIO CARLOS DE ALMEIDA FERREIRA

1981

DEPARTMENT OF NUCLEAR ENGINEERING

NOTICE OF DOCTORAL DEFENSE

STABILITY LIMITS AND WAVES IN TOROIDAL CONFIGURATIONS WITH FINITE PLASMA PRESSURE

by

Antonio Carlos de Almeida Ferreira

Date: Wednesday, February 11, 1981

2:00 p.m.

Room: 24-407

Thesis Supervisor: Professor Bruno Coppi

Thesis Reader: Professor Jeffrey Freidberg

STABILITY LIMITS AND WAVES IN TORCIDAL CONFIGURATIONS WITH FINITE PLASMA PRESSURE

by

ANTONIO CARLOS DE ALMEIDA FERREIRA

SUBMITTED IN PARTIAL FULFILLMENT

OF THE REQUIREMENTS FOR THE

DEGREE OF DOCTOR OF

PHILOSOPHY

at the

MASSACHUSETTS INSTITUTE OF TECHNOLOGY

February, 1981

Signature of Author: Antonio Carlos Ferreira
Department of Nuclear Engineering
January, 1981

Certified by: Bruno Coppi
Thesis Supervisor

Certified by: G P Lavidy
Thesis Reader

Accepted by: A F Henry
Chairman, Departmental Committee on Graduate Students

STABILITY LIMITS AND WAVES IN TORCIDAL CONFIGURATIONS WITH FINITE PLASMA PRESSURE

by

ANTONIO CARLOS DE ALMEIDA FERREIRA

Submitted to the Department of Nuclear Engineering
January, 1981, in partial fulfillment of the
requirements for the Degree of Doctor of Philosophy in
Nuclear Engineering

ABSTRACT

A study of the ideal MHD spectrum of low frequency modes with long parallel wavelength, short perpendicular wavelength was made. By applying a two-scale perturbation analysis to the two coupled equations that in general describe the modes, an equation was derived that is valid in the vicinity of the magnetic axis of an axisymmetric high-beta configuration. By solving it, the stability boundaries to ballooning instabilities and the growth rates of unstable modes are obtained. The connection between ballooning and interchange modes is discussed. From the asymptotic solutions of this equation, the continuous spectrum of shear-Alfvén waves and slow sound waves can be generated. The time-dependent problem is solved to determine the amplification of stable perturbations and to examine the transition from shear-Alfvén waves to ballooning instabilities.

Thesis Supervisor: Dr. Bruno Coppi

Title: Professor of Physics

Thesis Reader: Dr. Jeffrey P. Freidberg

Title: Professor of Nuclear Engineering

ACKNOWLEDGEMENTS

I am thankful to the following persons and institutions:

Professor Bruno Coppi, my thesis adviser, who offered me a most interesting topic;

Drs. Thomas M. Antonsen, Jr. and Jesus J. Ramos, my close collaborators, who watched and participated in the development of this thesis;

Barton Lane, for many useful discussions, comments and advice on the manuscript;

Sow Toh Chu, who taught me that computers are not to be feared;

Drs. Nicholas Sharky and Ronald Englade, for their assistance in the use of computers;

Geoffrey Crew, for help with some computations and graphs;

Drs. James W.-K. Mark and Linda Sugiyama, for their interest in the development of this work;

Instituto de Energia Atômica e Pesquisas Energéticas in São Paulo, Brazil, for a fellowship;

Yamato Miyao, my attorney in Brazil, for his loyalty and generosity in the defense of my interests;

Profs. Sidney Yip and Robert Hulsizer for moral support during the completion of this thesis;

Maggie Carracino, for her good will and efficiency in typing the manuscript;

Andy Pornoy, for his care in the preparation of drawings.

TABLE OF CONTENTS

LIST OF FIGURES

Chapter I

INTRODUCTION

In the past few years, a considerable effort has been expended in the theoretical understanding of ballooning modes. Practical reasons justify this, since ballooning modes are generally seen as a potentially dangerous form of instability, that could limit the maximum beta achievable in tokamaks. Beta, defined as the ratio of the average plasma pressure to the magnetic field pressure, is perhaps the most important single parameter to characterizing the merit of a fusion device as a prospective reactor. A limitation to a low value of beta would pose a serious threat to the economic feasibility of fusion reactors of the tokamak design, since the power output is directly proportional to the square of beta[1]. In addition, we cannot expect that the strength of the magnets necessary to produce strong confining fields can be increased without meeting technological barriers. It is then crucial to asses how much room is available, in increasing beta, without creating conditions that would lead to loss of confinement.

To critics, the weakness of a fusion program based on the assumption of reactors operating at low beta did not pass unnoticed. In an article published in the magazine Science in 1976,[2] just before the beginnings of intense research on ballooning modes, Mertz, quoting comparative studies on the

fusion cost, pointed out that "to make a tokamak reactor competitive, ways would have to be found to increase the beta value from the currently assumed value, between 1.9 and 5.6 percent to at least 10 percent." We may take these figures as representative.

In fact, the limitations on beta at that time, for engineering design, were dictated not only by stability considerations, but also by the equilibrium. It is known that a plasma has a tendency to expand along the major radius of the chamber, and to counteract this, a vertical field has to be applied. As the pressure is raised, the plasma must be kept in position by a stronger vertical field, and at a value of poloidal beta (the ratio of the plasma pressure to the magnetic poloidal field pressure) typically of the order of the inverse aspect ratio, the applied field cancels the poloidal field on the inner side of the torus. In terms of beta, this limit corresponds to $\beta \sim \epsilon/q^2$ (3), where q is the safety factor, and $\epsilon = a/R_o$, for a circular tokamak with minor radius a and major R_o. With the formation of a second magnetic axis inside the column, the flux surfaces would intersect the wall, and once the plasma is carried to the wall, the confinement is destroyed.

One way to relax this equilibrium limit is by tailoring non-circular cross sections. But probably it was the development of the concept of the flux-conserving tokamak that opened new ways in the search of high-beta systems and shifted the emphasis from the equilibrium to stability considerations. The idea can be traced back to a review paper of 1971 by

Mukhovatov and Shafranov[4], where we find the observation that "if a plasma is heated sufficiently rapidly so that the condition of 'freezing' of the magnetic field in the plasma is satisfied, then the topology of the magnetic confinement cannot be disturbed, i.e., even on unlimited increase of pressure the topology of the enclosed toroidal magnetic surfaces with one magnetic axis theoretically remains unchanged." The condition of "freezing" is equilivalent to the condition that, in the process of pressure raising, the q-profile is held fixed. With this simple prescription, sequences of equilibria can then be obtained with arbitrarily large values of beta without the undesirable shifting of the separatrix to the interior of the chamber and consequent loss of confinement. The principle found a fertile development in the hands of the Oak Ridge researchers; in 1977, Clark and Sigmar[5] proposed an analytical model to explain the evolution of the macroscopic parameters of the equilibrium under the constraint of flux conservation, and Dory and Peng[6] reported the results of numerically computed equilibria with β values above 20%. Since then, flux conservation has become a common computational method of generating high-pressure configurations for stability studies.

With the obstacle of the equilibrium out of the way, it seemed that magnetohydrodynamic stability considerations would set the limit to the maximum pressure that could be contained. Indeed, by 1977, following a paper by the Princeton group[7], it was clear that ballooning modes would impose very severe limitations on the attainable value of beta, of the order of 1.5 percent.

First reports on ballooning instabilities, however, go as far back as three papers dating from 1965[8-10]. There we find already the main ingredients of our present conceptual characterization of ballooning, as modes that can be driven unstable by locally unfavorable magnetic curvature. In a toroidal axisymmetric configuration, particles moving along a field line would see a magnetic curvature that is periodically varying with respect to the direction of the confined plasma pressure gradient. Favorable regions then alternate with adverse ones from the point of view of the stability. Perturbations are possible for which the amplitude is largest in the "bad" regions, and can evolve in a relatively localized ballooning instability. In these original papers a criterion was given for the critical beta against the onset of the instabilities, of the form $\beta \sim rR_c/L^2$, where r is the plasma radius, L is the length along field lines between "good" and "bad" regions, and R_c is the mean radius of curvature.

Apparently, ballooning modes remained in relative oblivion in the following ten years. The work done in Princeton in 1976-77 was essentially a numerical one, making use of the recently developed PEST package. A wealth of beautiful figures, showing the displacement vector fields, that seem to drag the plasma from the center to the outer surface of the chamber, and providing a vivid picture of the structure of the mode did not fail to motivate the community of physicists. Ballooning modes rapidly became the fashion. Soon after a talk given by Greene at MIT late in 1976, Coppi[11], examining the characteristics of

the mode revealed by the Princeton code, formulated a simple analytical theory to explain its topology and to identify the main physical parameters affecting the mode. From this theory a criterion for stability was obtained, that in the case of shearless systems, can be stated as $G = 1/2$, where $G = -q^2 R_o (2dP/dr/B^2)$, B being the magnetic field strength and dP/dr the pressure gradient. If we assume that the typical length of modulation of the magnetic field is $L \sim qR_o$, this relation gives the same scaling law for the critical beta of ten years before. Coppi also found that, around the most unstable flux surface, the radial distribution of the mode can be approximated by a Gaussian curve and -- although not stated explicitly -- that the most unstable modes occur in the limit of infinite toroidal number.

The theory of Coppi was based on an equilibrium configuration described by circular concentric flux surfaces. For the form of the perturbed quantities, as the displacement, he wrote $\xi = \tilde{\xi}(r,\theta)e^{iN(\phi - q(r)\theta)}$, where ϕ is the toroidal coordinate, θ the poloidal angle, q(r) is the inverse rotational transform on a surface of radius r, and N is the toroidal number, assumed to be a large integer. This is one instance of the widely used "eikonal representation," to which we shall give some attention later in this chapter. The difficulty with this representation is that, if Nq is not an integer, in order to produce a displacement ξ that is periodic in the poloidal angle, the "amplitude" $\tilde{\xi}$ cannot be periodic. This is inconvenient, because the mode equation ultimately will refer to the quantity $\tilde{\xi}$, and

instead of usual boundary conditions, we find that $\tilde{\xi}$ has to satisfy a difference relation of the type $\tilde{\xi}(\theta+\pi) = \tilde{\xi}(\theta-\pi)e^{-i2\pi Nq}$. One way to circumvent this difficulty is just to assume that $\tilde{\xi}$ vanishes at the angles $\theta = \pm\pi$. This was, again, suggested by the numerical results of the Princeton group, that showed, consistent with the physical mechanism of the instability, that the amplitude becomes quite small at the inner edge of the torus. Coppi baptized this boundary conditon the "disconnected mode approximation," because the modes appear as if they were acting independently on periodically spaced, successive regions along a given magnetic line. Strictly, this approximation does not generate fully periodic, analytic solutions, since it introduces a discontinuity in the derivative of $\tilde{\xi}$ that, in principle, would be removed by a more adequate treatment of the problem in a narrow layer around $\theta = \pm\pi$. For systems with strong shear, however, the eigenmodes do decay very quickly in the poloidal angle as we move from the outer to the inner side of the torus, and the approximation provides reasonably good estimates for the critical conditions of stability and growth rates of unstable modes.

In the same year of 1977, Dobrott et al.[12], working at the General Atomic Company in San Diego, California, derived the high-N equation for ballooning modes at marginal stability for arbitrary equilibria. Starting from the ideal MHD energy principle, they carried out a systematic minimization procedure, which, to lowest order in powers of 1/N, gives an equation that describes the structure of the mode along the field lines on a

given magnetic surface. This derivation showed that, in the high-N limit, kinks, that are driven by the interaction of the parallel equilibrium current with the perturbed magnetic field, decouple from ballooning. The minimization process eliminates the terms in the energy functional usually associated with the fast and slow magnetosonic waves, leaving only the term that drives the shear-Alfvén waves (stabilizing) and the term containing the interaction of the pressure gradient with the curvature (de-stabilizing). To solve the mode equation, Dobrott and co-workers used the same boundary conditions as Coppi, i.e., they considered even modes that vanish at $\theta = \pm\pi$.

The next step in the development of the theory of ballooning modes came as a new approach to the question of the representation of the mode, and to the boundary condition to be applied to the mode equations. Y.C. Lee and VanDam[13], at the Workshop on Finite Beta Theory held in September 1977, in Varenna, Italy, noticed that, in the high wave number limit, there is local translational invariance among the harmonics of the perturbations, and, using this fact and the Poisson summation formula from the theory of Fourier transforms, they derived a representation of the mode as an infinite series. Each of the terms of the series has the "eikonal form" that we mentioned previously, but shifted by 2π in the poloidal angle. In this way, the periodicity of the overall mode is automatically guaranteed, with no need for the individual terms of the series to satisfy any periodicity requirement. At the same Conference, Glasser proposed an identical representation.[14]

Pegoraro and Schep[15] had also arrived at the infinite series of quasi-modes, by exploring the symmetries of the mode equation in the local approximation, and developed arguments quite similar to the ones of Lee and VanDam. This formalism, that is now usually referred to as the "ballooning representation," is an important gain to the theory because it finally solves the problem of reconciliation of the eikonal form, which is desirable to preserve, with the physical requirement of periodicity of the mode in a sheared magnetic field.

Apparently, the new representation received wide acceptance after the paper by Connor, Hastie and Taylor[16] appeared in 1978. In this paper, the "ballooning representation" was given as an infinite summation of Fourier transforms, rather than a series of quasi-modes with shifted arguments, which is indeed more convenient for theoretical purposes. Connor, Hastie and Taylor rederived the mode equation, that has exactly the same form of the equation previously obtained by Dobrott and co-workers, but noticed the fact that because of the introduction of the "ballooning transformation," the independent variable is no longer to be interpreted as the physical poloidal angle, and ranges over an infinite interval. As a consequence, the appropriate boundary conditions have to be redefined, and this leads to stricter conditions for marginal stability than found previously. Exploring further the new mathematical terms in which the problem was re-stated, they carried out an asymptotic analysis of the mode equation, and recovered the Mercier criterion for stability against localized interchanges.

All these results appeared again in 1979, in an expanded version of the original paper[17], but with an important addition. Connor, Hastie and Taylor observed that, by use of the "ballooning representation," to lowest order in an expansion in powers of 1/N, one obtains an ordinary differential equation that describes the oscillations on each magnetic surface. No coupling occurs in the radial direction, and the eigenvalue that results is a "local" one, depending parametrically on the equilibrium quantities of the considered surface. The radial structure of the mode, of course, remains undetermined to this order. To complement the local theory, they carried out a higher-order analysis, that permitted them to evaluate the "global" eigenvalue and to determine the radial profile of the mode. A quite general proof was then given that the most unstable modes correspond to the limit $N \to \infty$.

In fact, the equations derived by Connor, Hastie and Taylor are strictly valid only at marginal stability, although this does not affect in the least the general conclusions that they obtained concerning growth rates and finite-N dependencies of the mode. The limitation came from the fact that they had assumed that the divergence of the displacement vanished to all orders and this does not actually minimize the full Lagrangian (the kinetic energy term included in the energy functional). The correct treatment was given by the Princeton group by the middle of 1978[18], which showed that, in general, modes with long parallel wavelength, short perpendicular wavelength across the field lines, and low frequencies — in other words, modes

with the ballooning characteristics — are described by two coupled equations, rather than one. In the same paper, they proposed an alternate method of treating the problem of the global eigenvalue, and the N-dependencies of the mode, that makes use of the phase integral quantization condition.

The Second Stability Region

Up to now, in this historical overview, we have followed the path of development of what we could call the "general MHD theory of ballooning modes." Parallel to this, there was the search of concrete stability limits, both using numerical codes and analytic or semi-analytic models for the equilibrium.

In the first studies on ballooning modes, we found already a scaling law for the critical beta, that can be written as $\beta \sim \epsilon/q^2$. It seemed an obstinacy of Nature that the same limit formerly set by the equilibrium reappeared now imposed by the stability against ballooning. The simple model for the equilibrium adopted by Coppi, corresponding to an almost pressureless plasma, reproduced this scaling law and indicated that the growth rates of unstable modes increase in an approximately linear relation with the pressure gradient (more precisely, with the parameter G); also, that increase of shear is uniformly stabilizing. He pointed out, however, that the consistent determination of the stability limits would have to take into account the modifications in the equilibrium introduced by the finite values of beta at which the instability actually appears, in particular the shortening of the effective

connection length[19]. This could be accomplished in a model by assuming a simple law of variation of the poloidal magnetic field over a given magnetic surface, of the form $B_\theta \propto (1 - \alpha_\theta(G) \cos\theta)^{-1}$, where $\alpha_\theta(G)$ is a positive monotonically increasing function of G. In addition to the increase of the poloidal magnetic field in the outer regions of the torus, an equilibrium model for finite beta configurations should include the weakening of the local shear around $\theta = 0$, the simplest choice being an expression of the type: shear (local) = shear (average) - $\alpha_q(G) \cos\theta$, where $\alpha_q(G)$ has a behaviour with G similar to $\alpha_\theta(G)$. In fact, we can show that an equilibrium with these characteristics is described, geometrically, by shifted, rather than concentric, circular flux surfaces. In the first half of 1978, the MIT group found the surprising result that such an equilibrium predicts that the modes are first de-estabilized at some critical threshold of the pressure gradient, but then, by further increase of the pressure, can again become stable[20]. At the Innsbruck Conference of 1978, it was reported that "when β increases, at first a critical value β_c is found such that for $\beta > \beta_c$, a mode with positive growth rate is obtained. Then by increasing β further, the mode growth rate does not appear to increase and in certain cases it decreases and even vanishes"[21]. This phenomenon has been referred to later as the "second stable region" of high pressures. The interpretation given then for the appearance of two points of marginal stability was that the pressure gradient enters twice the effects of the equilibrium on the mode, first

as an unfavorable factor, as in the Raleigh-Taylor instability, and second, as a stabilizing factor such as by shortening the characteristic scale lengths of the mode amplitude along the field lines. In fact, if we analyse the mode equation appropriate to this equilibrium using a variational form, because of the dependence of the poloidal field and shear on the pressure gradient, we obtain a quadratic algebraic equation for the critical G, that admits two real, positive roots.

At the Innsbruck Conference, similar findings to ours were communicated by European researchers, namely Mercier[22], Sykes, Turner, Fielding and Haas[23], and, from the Soviet Union by Zakharov[24]. Basically, their results were also derived from simplified analytical solutions of the equilibrium, that, in one way or another, contained the essential ingredients that lead to the stabilization of the mode at high pressures. Because the calculations based on such models are strictly valid only in the vicinities of the magnetic axis, it was not clear, however, if equilibria which are globally stable could be obtained by increasing the pressure beyond the first critical threshold. In the United States, numerical codes finally confirmed that high-beta configurations could be produced with flux surfaces lying in the second region of stability at an average beta of the order of 8%, far above the limit of 1% of the first region[25]. It appeared then, for the second time, that the restriction $\beta \lesssim \varepsilon/q^2$ could be beaten.

A Simple Model for Ballooning Instabilities

In this thesis, we assume that the plasma is described by the equations of ideal MHD. In the system of rationalized natural units, they are written as:

Equation of motion: $$\rho_m \frac{d\vec{v}}{dt} = - \nabla P + \vec{J} \times \vec{B} \qquad (1\text{-}1a)$$

Equation of continuity: $$\frac{\partial \rho_m}{\partial t} + \nabla \cdot (\rho_m \vec{v}) = 0 \qquad (1\text{-}1b)$$

Faraday's Law: $$\frac{\partial \vec{B}}{\partial t} = - \nabla \times \vec{E} \qquad (1\text{-}1c)$$

Ampere's Law: $$\vec{J} = \nabla \times \vec{B} \qquad (1\text{-}1d)$$

where ρ_m is the mass density of the fluid, P is the scalar pressure, $\vec{J}$ is the current density, $\vec{E}$ and $\vec{B}$ are, respectively, the electric and magnetic field. The basic MHD constraint, usually called the "frozen-in-law":

$$\vec{E} + \vec{v} \times \vec{B} = 0 \ , \qquad (1\text{-}1e)$$

which characterizes the plasma as a perfectly conducting fluid, is assumed to be valid. This set of equations, in general, is not sufficient to specify completely the fluid behavior, and has to be complemented with an equation of state. For phenomena that occur in a time scale much shorter than the typical transport time scale, we may assume that the equation for adiabatic processes is obeyed:

$$\frac{d}{dt}\left(\frac{P}{\rho_m^{\gamma_c}}\right) = 0 \qquad (1\text{-}1f)$$

where γ_c is the ratio of specific heats. We shall always consider equilibrium states for which there is no flow velocity.

We now develop, within this general framework, a rudimentary model that illustrates the physical factors affecting the stability of ideal MHD ballooning modes[26]. We consider an infinite plasma slab imbedded in a uniform magnetic field directed along the z-axis. The equilibrium density is nonhomogeneous along the x-axis with a characteristic length scale

$$r_p = -\frac{1}{\rho_m}\frac{d\rho_m}{dx} \qquad (1\text{-}2)$$

To simulate effects of magnetic curvature in this one-dimensional model, we introduce an artificial gravity g along the diretion of the pressure gradient that acts upon the fluid mass oscillations, but not on the fluid at rest (Fig. 1.1). We will see, in subsequent chapters, that the incompressible fluctuations are subject to the least favorable stability condition. Thus, we take:

$$\nabla \cdot \vec{\xi} = 0 \ , \qquad (1\text{-}3)$$

a strict constraint that can be viewed as an equation of state and closes the set of the fluid-magnetic equations, making the use of Eq. (1-1f) unnecessary. Here, $\vec{\xi}$ is the fluid displacement, that we assume to vary harmonically with time:

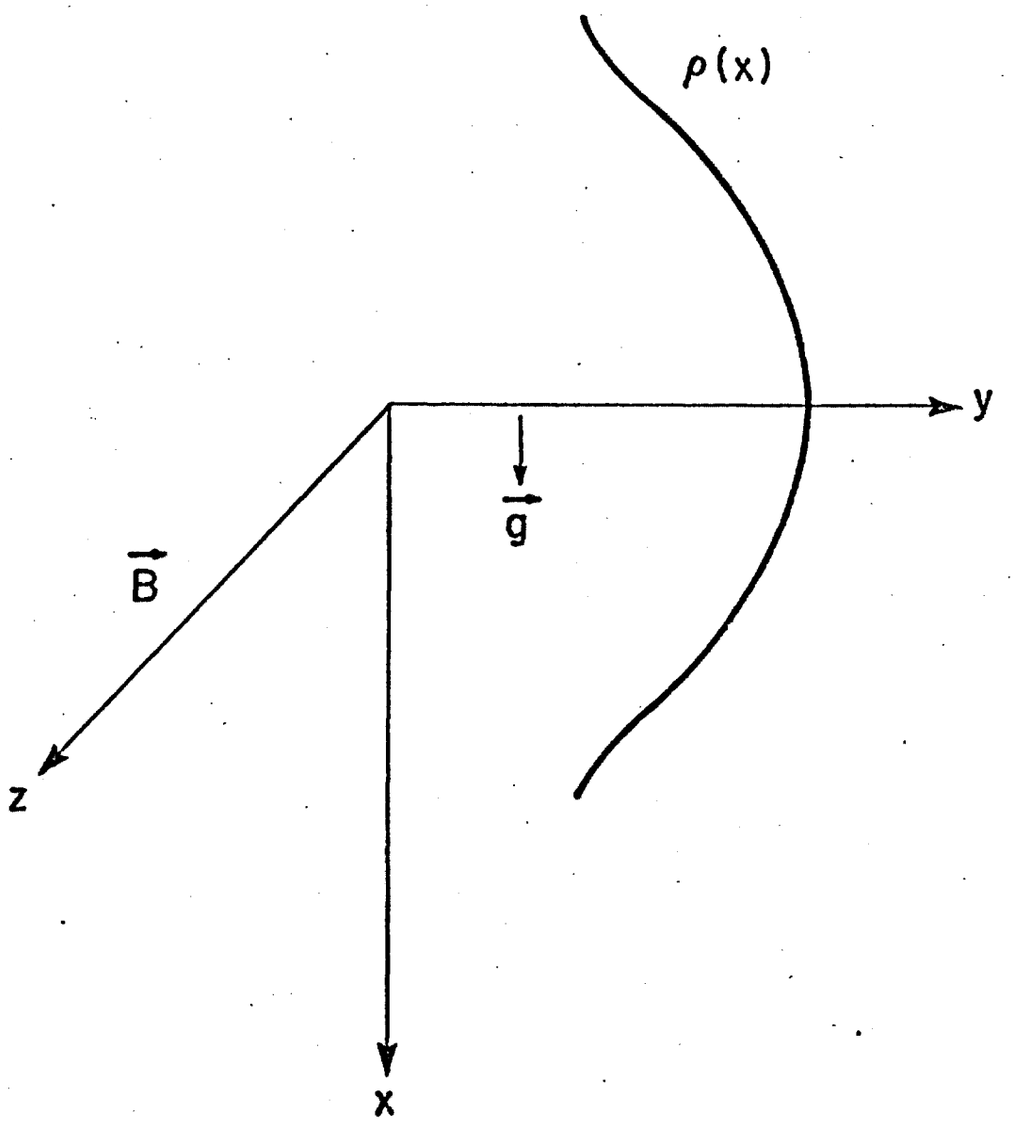

Figure 1.1: A Plasma Slab Model to Interpret the Gravitational Instability. The Applied Magnetic Field and the Gravitational Field are Uniform.

$$\vec{\xi}\ (\vec{r})\ e^{-i\omega t} = \int^{t} \vec{v}\ dt. \qquad (1\text{-}4)$$

Linearizing the equation of motion for small deviations of the equilibrium, we obtain:

$$-\omega^2\ \rho_m \vec{\xi} = -\nabla(P_1 + \vec{B}\cdot\vec{B}_1) + \vec{B}\cdot\nabla\vec{B}_1 + \vec{B}_1\cdot\nabla\vec{B} + \rho_1\vec{g}\ , \qquad (1\text{-}5)$$

where the subscripts 1 apply to perturbed quantities. The equation of mass conservation gives

$$\rho_1 + \vec{\xi}\cdot\nabla\rho_m = 0\ , \qquad (1\text{-}5)$$

and, by combining Faraday's law with the frozen-in law, we obtain for the perturbed magnetic field:

$$\vec{B}_1 = \nabla \times (\vec{\xi} \times \vec{B}) \qquad (1\text{-}6)$$

We next Fourier-analyse the perturbed quantities, and write the displacement, for example, as:

$$\vec{\xi}(\vec{r}) = \hat{\vec{\xi}}\ e^{ik_x + ik_y y + ik_{\parallel} z} \qquad (1\text{-}7)$$

We choose to consider perturbations with $\vec{\xi}_z = 0$ and assume further that, in the directions transverse to the applied magnetic field, the scale of variation of the mode is much shorter than the equilibrium scale:

$$k_y \sim k_x >> r_p \tag{1-8}$$

The incompressibility condition can then be used to eliminate the y-component of the displacement:

$$\hat{\xi}_y = -\frac{k_x}{k_y}\,\hat{\xi}_x \tag{1-9}$$

Eq. (1-5) gives immediately:

$$\hat{\rho} = -\hat{\xi}_x \frac{d\rho_m}{dx} \tag{1-10}$$

and, from the x-component of Eq. (1-6), we obtain:

$$\hat{B}_x = i\, k_{\parallel} B\, \hat{\xi}_x \tag{1-11}$$

Taking the z-component of the curl of Eq. (1-5), we have:

$$-\omega^2 \rho_m k_\perp^2 \hat{\xi} = i(k_{\parallel} B)\, k_\perp^2 \hat{B}_x + k_y^2 g \hat{\rho} \tag{1-12}$$

where $k_\perp^2 = k_x^2 + k_y^2$. With the already known expressions for the perturbed density and magnetic field, this last equation finally yields:

$$\omega^2 = k_{\parallel}^2 V_A^2 - \frac{1}{1 + (k_x/k_y)^2}\,\frac{g}{r_p} \tag{1-13}$$

where $V_A^2 = B^2/\rho_m$ defines the Alfvén speed. This dispersion relation is a composition of the dispersion relations for the

Alfvén waves and the Raleigh-Taylor instability. The first term, in particular, is due to the bending of the field lines and is stabilizing. Eq. (1-13) tells us that the modes, because they stretch the field lines, require a minimum plasma pressure before developing into the gravitational instability. The condition of marginal stability is reached when

$$\frac{g}{r_p V_A^2} = k_{\parallel}^2 \left(1 + \frac{k_x^2}{k_y^2}\right) \qquad (1\text{-}14)$$

Now, in a realistic configuration, because of the curvature of the magnetic field, particles moving along a field line experience an acceleration $m\, v_{th}^2/R_c$, where R_c is the radius of curvature, m is the mass and v_{th} in the average is the thermal velocity. This suggests that the analogy between the effects of curvature and gravity in a planar model can be achieved by the substitution:

$$\frac{g}{r_p} \longrightarrow \frac{P}{\rho_m r_p R_c} \qquad (1\text{-}15)$$

The scale of variation of the mode along the field lines is typically of the order of magnitude of the periodicity length of the magnetic field, and we replace

$$k_{\parallel} \longrightarrow \frac{2\pi}{L} \qquad (1\text{-}16)$$

Defining beta as $\beta = 2P/B^2$, the condition expressed by Eq. (1-14) provides then a rough estimate for the critical value of beta as:

$$\beta \sim \frac{r_p R_c}{(L/2\pi)^2} \sim \frac{r_p}{R_c q^2} \qquad (1\text{-}17)$$

where we have assumed that $k_x \sim k_y$.

The dispersion relation, Eq. (1-13) can also be interpreted as follows. If the Alfvén term is large, meaning that the field lines behave as stretched strings under strong tension, ripples that are formed in the "bad" regions tend to propagate quickly to the inside of the torus, and have no time to be effectively de-stabilized by the local unfavorable curvature. They will just experience a transient growth, that occurs in a time scale larger than the time of transit between the regions of bad and good curvature. On the other hand, if the combined effects of the pressure gradient and curvature expressed in the second term of the dispersion relation is large enough, as the fluctuations travel along the outside of the torus, they are first slowed down, and then trapped in the gravitational "well", eventually developing into an instability (Fig. 1.2).

Advantages of a High-N Theory

In Chapter II we shall present the reasons that make the eikonal form a natural choice for the representation of the most unstable perturbations. However, even remaining in the level of general considerations, we can find intuitive arguments to make it plausible[27]. A plasma, because of the strong confining magnetic field, is a highly anisotropic medium. The magnetic

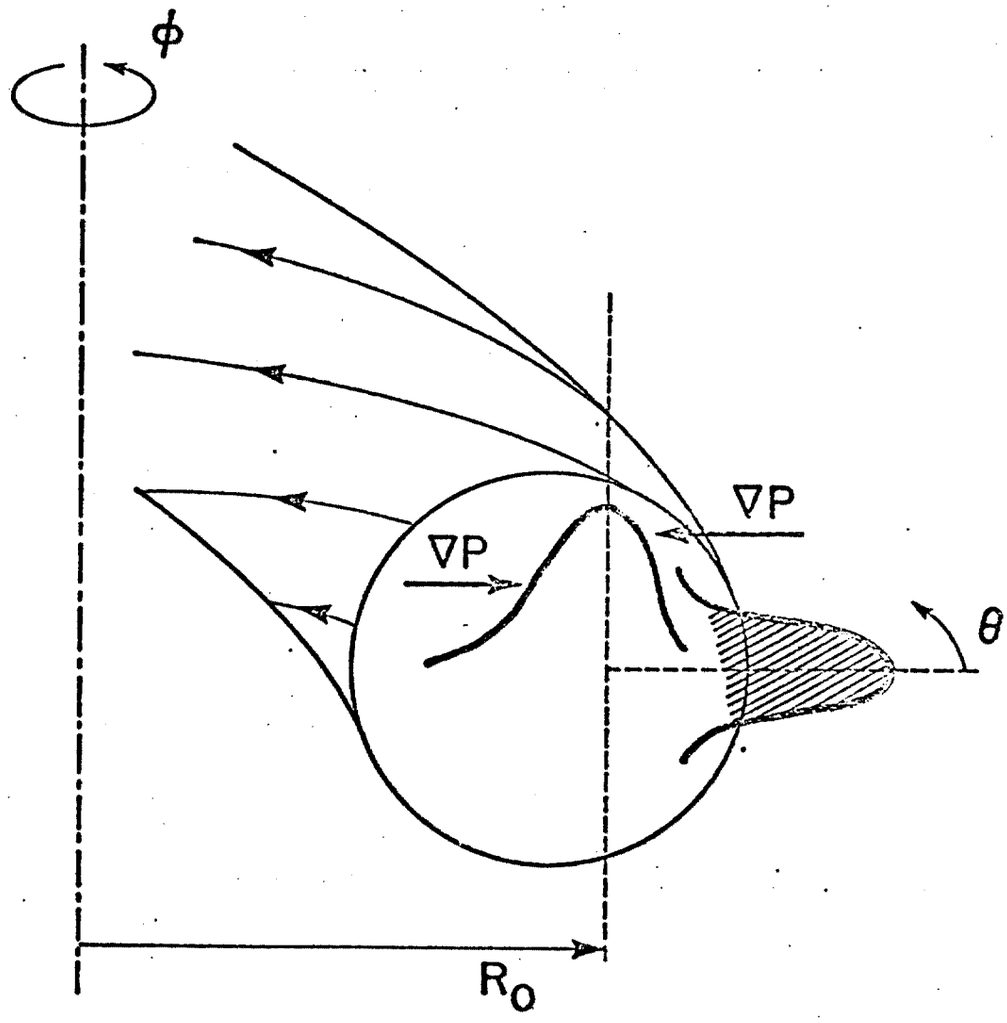

Figure 1.2: Evolution of a Fluctuation into a Ballooning Instability in a Torus.

field tends to tie the motion of the particles to the field lines, in this way isolating the plasma on adjacent field lines. Thus, the plasma supports rapid variations of perturbed quantities across the field. Along the parallel direction, however, the free motion of particles is hindered only by their own inertia, and for low frequency phenomena, in particular, this rules out the possibility of large unbalanced forces associated with rapid variations in perturbed quantities. Because they bend the field lines, variations along the parallel direction have a stabilizing influence. Therefore, we may argue that the most unstable modes are those that maximize the ratio $k_\perp/k_{\parallel}$, being characterized by long wavelengths in the direction of the magnetic field and short perpendicular wavelengths. Perturbations of this type are conveniently represented as:

$$\vec{\xi} = \hat{\vec{\xi}}(\vec{x})\, e^{i\alpha} \tag{1-18}$$

where all fast variations across the field are isolated in the eikonal α, and the large scale variation along the line of force is contained in the amplitude $\hat{\vec{\xi}}(\vec{x})$. Specifically, we require that

$$|\nabla_\perp \alpha| \gg \left| \frac{\partial \vec{\xi}}{\partial \ell} \right| \tag{1-19}$$

where ℓ represents a coordinate along the field line. Since $\nabla\alpha$ involves large derivatives, to make effective that the amplitude, alone, gives the slow parallel variation of the mode, we demand further that

$$\frac{\partial \alpha}{\partial \ell_{\parallel}} = 0 \quad , \tag{1-20}$$

id est, the eikonal must be constant along the field lines.

For example, in an axisymmetric toroidal confinement described by circular concentric flux surfaces, where the field lines are helices of uniform pitch on a given flux surface, the appropriate representation of such modes is

$$\vec{\xi} = \hat{\vec{\xi}}(\vec{x})\, e^{iN(\phi - q\theta)} \tag{1-21}$$

Short perpendicular wavelength is represented by the large number N in the phase factor. To make the mode periodic in the toroidal coordinate, N must be chosen to be an integer. On the other hand, the parallel wavelength of the oscillation is contained in the amplitude, with a much slower variation, such that parallel derivatives remain of order unity.

A high-N theory of ballooning modes has many advantages. The first of these is that it deals with the modes that impose the strictest conditions of stability. In the second place, high-N number modes provide a natural expansion parameter, and this makes it possible to obtain mode equations for absolutely general equilibria. For modes with low toroidal numbers, in contrast, because of the lack of an expansion parameter embodied in the structure of the mode itself, we have to look for a suitable parameter in the equilibrium, usually the aspect ratio. This leads to mode equations that are less than general,

limiting the scope and amplitude of the theory. In the third place, the lowest order equations in a high-N expansion corresponding to infinite N, can be shown to be ordinary differential equations, describing the structure of the mode over decoupled lines of force, and are sufficient to determine the boundaries of marginal instability. This greatly simplifies the problem, that in principle would require a two-dimensional formulation. Stabilizing effects of finite N and the radial structure of the mode are fixed by higher-order equations in the expansion. However, once again because of the large parameter involved, asymptotic methods are available that make unnecessary a precise picture of the radial profile to determine the effects on the instability boundaries by the finite value of N. Thus, higher-order equations are not really needed, all relevant information being contained in the lowest order theory. Finally, for large N numbers, computational methods of minimization of the energy functional find difficulty in resolving the fine structure of the mode, and have to be complemented by the differential equations provided by the asymptotic theory.

Retrospective View of the Development of this Thesis

The object of this thesis is to study low-frequency modes with long parallel wavelengths and short perpendicular wavelengths in a realistic equilibrium configuration. Because of the difficulty of a global treatment of the problem, we restricted our attention to the vicinities of the magnetic axis, where equilibrium solutions can be obtained in the form of power series.

Sacrifices are imposed by the analytical attitude, not only concerning the domain of validity of the analysis, but also because the complexity of the equations still require further simplification of the description of the equilibrium. This precludes a systematic investigation of the local effects of boundary conditions of the equilibrium on the modes. However, we believe that shaping studies, with its important applications for the design of optimal geometries for confinement, become more meaningful in the context of global analyses, that require a full numerical approach. They can be left outside of our study with no harm to the substance of its conclusion.

The starting point and basic motivation of the work presented here was to determine the stability limits against ballooning modes by using simplified equilibrium models that would mimic the most important effects expected to be found in realistic, high-beta configurations. We could expect that, conceived as models, these descriptions of the equilibrium would portray more accurately the actual conditions prevailing in the neighborhood of the magnetic axis. In the development of the work, it became clear that, because of the specific ways by which the equilibrium affects the mode, a fairly more detailed solution of the equilibrium equations, even in that tiny particular region, was required. We mean by this that, with the available tool of the power series expansions, the lowest order solutions of the mode equations could be found only after going much farther in the orders of the equilibrium. This sensitivity of the ballooning modes to the equilibrium is in sharp contrast

with other MHD modes, as the localized interchanges, for which local criteria of stability can be determined with much less complete information about the equilibrium. Then, the location of the precise boundaries to ballooning instabilities at the axis involve not only a knowledge about the amount of relative shift of the flux surfaces, but also about distortions in shape as fine as of the fifth harmonic in the poloidal angle.

The complete understanding of this problem was reached only by the application of an appropriate mathematical technique to the mode equations that makes use of two distinct scales. In the ballooning equations, because of the periodicities of the equilibrium, the poloidal-like variable appears as the argument of periodic functions but, by effect of the non-vanishing shear also in secular, non periodic terms. We note that, because of the dependence of $\nabla\alpha$ along a field line, shear effects are retained in the equations that describe the structure of the mode, although these equations apply to each single surface individually. As we follow a field line winding around a given flux surface, it departs more and more from the path of a field line lying on an adjacent flux surface with a different rate of twisting, although at the starting point they would run very close. Then secularities appear mixed with periodicities. The introduction of two-scales permits us to treat separately the two different dependences on the poloidal-like variable. By appropriate averages, it is possible to compress all information regarding the effects of the equilibrium on the mode in the coefficients of a much simpler, second order differential

equation involving only a secular variable. This provides a compact description of shear-Alfvén waves, slow sound waves and ballooning and interchange instabilities in the neighborhood of the magnetic axis, id est, of all types of oscillations that are present in the general equations. Because of the way that this equation is generated, we call it a "distilled" equation.*

We then arrived at a rich and, nonetheless, simple analytical model for the investigation of the low-frequency MHD spectrum, that reproduces faithfully the effects of the physical environment around the magnetic axis on an important class of modes. This model is the conducting thread of this thesis, and integrates our study of ballooning modes in a unifying frame that comprises a variety of other aspects.

It should be noted that, because of the specific conditions surrounding the magnetic axis (we have in mind the weak values of the shear), this region of the plasma is not accessible to numerical solutions of the mode equations. Within this perspective, analytical results presented here can be considered a useful reference for the extrapolation of the numerical ones.

This dissertation is organized as follows. Chapter II is devoted to a review of the general MHD theory of ballooning modes. We discuss the question of representation, and going through the arguments developed by Lee and VanDam, and Pegoraro and Schep, we show how the ballooning transformation solves the

---

*This expression was coined by J. J. Ramos.

dilemma of the eikonal form and periodicity. The energy principle is used only as a guide to model the most unstable perturbations; to obtain the mode equations, we use directly the general differential equations of MHD. This derivation, that we present in detail, was communicated to us by Thomas Antonsen, Jr., and we believe that it is simpler than other derivations that are available, in more or less concise form, in the literature. We give a brief account of the method envisaged by Connor, Hastie and Taylor to bridge the local theory to a global one, and reproduce their formula for the global eigenvalue using the WKB method. Finally, we summarize the results concerning the boundary conditions and the asymptotic behavior of the solutions.

In Chapter III, using the method of Solovev and Shafranov, we obtain the equilibrium solution that is needed for the subsequent work. We compute the equilibrium quantities that are relevant to the problem, as the rotational transform and the curvatures, and derive the appropriate expansions for the coefficient functions of the mode equations in the vicinity of the magnetic axis.

The next two chapters contain most of the original contributions of this work. Most of Chapter IV is devoted to the unstable side of the spectrum. We describe in detail the method of the averages, and deduce the "distilled" equation. The stability limits against ballooning are then obtained as the eigenvalues of this equation, and a simple approximated dispersion relation for growing modes is given. Next, we

compute analytically small growth rates for both ballooning and interchange instabilities and examine the transition from the infinite sequence of interchange modes to a single unstable ballooning mode. We conclude the chapter by obtaining the representation of the eigenfunctions in the "real", physical space of the poloidal variable at marginal conditions of stability.

In Chapter V we address our attention mainly to the stable side of the spectrum. We review briefly some general theorems stated by Barston concerning the structure of the continuum and show how they must be applied to modes constructed by the use of the ballooning infinite series. A simple rule to generate the continuum then follows, and is applied to determine the dispersion relation for shear-Alfven waves and slow sound waves in the neighborhood of the magnetic axis. We then solve the time-dependent problem to examine the evolution of shear-Alfvén waves into ballooning instabilities and to determine the rate of amplification of perturbations in stable regimes of equilibrium. In this chapter we make extensive use of a slab plasma model in order to clarify certain concepts associated with the continuous spectrum, and we find here an opportunity to formulate a more elaborate planar model for toroidal effects, that illuminates the meaning of the "distilled" equation. In Chapter VI we return to general considerations, discussing some tendencies in the current approach to ballooning modes, and give suggestions for future work.

Chapter II

THE GENERAL MHD THEORY OF BALLOONING MODES

Review of MHD Equilibrium

In this section we review briefly the equilibrium equation of ideal MHD for axisymmetric systems, in order to have the basic concepts and results available. We follow closely the treatment given by Callen and Dory[28].

The basic equations to be solved are:

$$\nabla P = \vec{J} \times \vec{B} \tag{2-1}$$

$$\nabla \times \vec{B} = \vec{J} \tag{2-2}$$

$$\nabla \cdot \vec{B} = 0 \tag{2-3}$$

where P is the scalar pressure, $\vec{J}$ is the current density and $\vec{B}$ is the magnetic field. From the first equation, it follows that $\vec{B} \cdot \nabla P = 0$ and $\vec{J} \cdot \nabla P = 0$, and therefore field lines and current lines lie on surfaces of constant pressure. We refer to these surfaces as "magnetic surfaces." We introduce then a function $\psi(\vec{x})$, such that each of the magnetic surfaces is specified by a constant value of ψ.

Magnetic surfaces provide a natural set of coordinate surfaces to describe the configuration. For axisymmetric toroids, the azimuthal angle ϕ around the axis of symmetry is an ignorable coordinate and provides another convenient choice. To complement these two, we introduce a poloidal coordinate χ, such

that surfaces of constant χ are orthogonal to both the magnetic surfaces and the meridian plane of ϕ = constant. The construction of the orthogonal coordinate system (Ψ,χ,ϕ) will then be completed if it can be associated with a metric that gives the differential length between two neighboring points. The expression for the line element, in general, is

$$d\vec{\ell} = h_\Psi \, d\Psi \, \vec{e}_\Psi + h_\chi \, d\chi \, \vec{e}_\chi + h_\phi \, d\phi \, \vec{e}_\phi \quad , \tag{2-4}$$

where h_ϕ, h_χ and h_ϕ are scale factors, and $\vec{e}_\Psi$, $\vec{e}_\chi$, $\vec{e}_\phi$ are unity vectors that, at any point, are directed perpendicularly to the coordinate surfaces. The volume element is $dV = J_o \, d\Psi d\chi d\phi$, where J_o si the Jacobian in this coordinate system, given by the product $h_\Psi \; h_\chi \; h_\phi$.

The scale factor h_ϕ is simply $1/|\nabla\phi| = R$, the distance away from the axis of symmetry. To determine the scale factor h_Ψ, we have first to specify the function Ψ, which, besides the condition that it takes constant values on surfaces of constant pressure, still remains arbitrary. It could be chosen to be the pressure itself, but it is preferable to define Ψ in terms of the poloidal flux.

Since field lines lie on magnetic surfaces, the magnetic field in this coordinate system is represented only in terms of its poloidal and toroidal components, $\vec{B} = B_\chi \, \vec{e}_\chi + B_\phi \, \vec{e}_\phi$. The magnetic flux across a ribbon of width dr between two neighbor magnetic surfaces Ψ and $\Psi + d\Psi$, all the long way around the torus, is defined to be $2\pi \, d\Psi$. From this definition, it follows that

$$d\Psi = RB_\chi \, dr \tag{2-5}$$

and the scale length h_ψ is

$$h_\psi = \frac{1}{|\nabla\Psi|} = \frac{1}{RB_\chi} \tag{2-6}$$

The magnetic field can then be rewritten as

$$\vec{B} = T \nabla\phi + \nabla\phi \times \nabla\Psi \tag{2-7}$$

where $T = R B_\phi$. Since the pressure is only a function of Ψ, the two components of the pressure balance equation

$$\nabla P = (\nabla \times \vec{B}) \times \vec{B} \tag{2-8}$$

along the $\vec{e_\chi}$ and $\vec{e_\phi}$ directions must vanish. With the above form for the magnetic field, this constraint can be satisfied in an axisymmetric configuration in which $\partial T/\partial\phi = 0$ only if we also have $\partial T/\partial\chi = 0$. Thus, the function T, the same as the pressure and the poloidal flux, is a surface quantity, in the sense that it depends only on the coordinate Ψ, $T = T(\Psi)$.

The remaining component of Eq. (2-8), along the $\vec{e\psi}$ direction gives a nonlinear partial differential equation for the flux function ψ:

$$\frac{dP}{d\Psi} = -\frac{1}{R^2} T \frac{dT}{d\Psi} - \nabla\cdot\left(\frac{1}{R^2} \nabla\Psi\right) \tag{2-9}$$

This equation represents a reduction of the original set of equilibrium equations for an axisymmetric toroid, and is frequently referred in the literature as the Grad-Shafranov equation. For specified functional dependences of P and T on Ψ, under suitable boundary conditions, it can be solved for the flux function Ψ in some convenient system of coordinates, and once the distribution of flux surfaces is known, all equilibrium quantities can be obtained. Alternatively, Eq. (2-9) can be viewed as an equation for the Jacobian, that completes the geometric description of the equilibrium through the last metric coefficient:

$$h_\chi = J_o B_\chi \tag{2-10}$$

The quasi-Laplacian operator in the right-hand side of Eq. (2-9) is usually denoted by the symbol Δ^*:

$$\Delta^* \Psi = \nabla \cdot \left(\frac{1}{R^2} \nabla \Psi \right) = \frac{1}{J} \frac{\partial}{\partial \Psi} (J B_\chi^2) \tag{2-11}$$

This term clearly represents that part of the confinement coming from the interaction between the toroidal current and the poloidal flux, and is related to the toroidal current density by:

$$J_T = R \Delta^* \Psi \tag{2-12}$$

The first term on the right-hand side results from the crossing of the poloidal current with the toroidal field, and, in fact, it can be shown[29] that the stream function $T(\Psi)$, except for a factor 2π, is the total poloidal current.

As a field line winds around a flux surface, the toroidal angle changes with the poloidal coordinate at the rate

$$q_\ell\ (\Psi,\chi) \equiv \frac{d\phi}{d\chi} = \frac{J_o B_T}{R} \quad , \tag{2-13}$$

as can be readily obtained from the equation of the field lines, $d\vec{\ell} \times \vec{B} = 0$. This is not an invariant quantity, since it depends on the choice of the poloidal coordinate that is effectively used in the representation of J_o. An invariant quantity can be obtained by taking the average of q_ℓ over one period of χ:

$$q(\Psi) = \frac{1}{2\pi} \oint \frac{J_o B_\chi}{R}\, d\chi \tag{2-14}$$

which is commonly referred in the literature as the safety factor, or, more appropriately, as the inverse rotational transform. After a complete turn the short way around the torus, the field line has proceeded on angle $\Delta\phi$ the long way, that is given precisely by $2\pi q$.

In general, a field line does not close upon itself after a finite number of circuits around the torus; as we follow a field line, it traces out a net that covers the magnetic surface densely. For some particular surfaces, however, the angle $\Delta\phi$ is

a rational fraction of 2π; in this case, after n complete turns the short way and m complete turns the long way, we are back to the initial position. The q-value, for these rational surfaces, is the ratio of the integers m and n.

The inverse rotational transform is an important parameter in the characterization of an equilibrium configuration, and appears frequently in the formulation of stability criteria. An alternative definition can be given as follows. The toroidal magnetic flux between two close magnetic surfaces Ψ and $\Psi + \Delta\Psi$ is

$$\Delta\Phi_{tor} = \oint B_\phi \, h_\chi \, d\chi \, h_\psi \, \Delta\Psi = \oint \frac{JB_\phi}{R} \, d\chi \, \Delta\Psi \, , \qquad (2\text{-}15)$$

and, by comparison with Eq. (2-14), we see that

$$q(\Psi) = \frac{1}{2\pi} \frac{d\Phi_{tor}}{d\Psi} = \frac{d\Phi_{tor}}{d\Phi_{pol}} \, , \qquad (2\text{-}16)$$

remembering the original definition of the poloidal flux.

To conclude this overview of MHD equilibrium, we recall that the curvature vector $\vec{\kappa}$ of a field line is defined as the gradient along the field line of the unity vector $\vec{b} = \vec{B}/B$:

$$\vec{\kappa} \equiv (\vec{b} \cdot \nabla)\vec{b} = \frac{1}{B^4} \left[\vec{B} \times \nabla \left(P + \frac{B^2}{2}\right)\right] \times \vec{B} \qquad (2\text{-}17)$$

and is everywhere perpendicular to $\vec{b}$. The component normal to the magnetic surface is the normal curvature:

$$\kappa_n = \frac{1}{B^2} \frac{1}{h_\psi} \frac{\partial}{\partial \psi} \left(P + \frac{B^2}{2}\right) \tag{2-18}$$

and the component lying on the magnetic surface, but perpendicular to the field line, is called the geodesic curvature given by:

$$\kappa_s = \frac{B_\phi}{B^3 B_\chi} \frac{1}{J} \frac{\partial}{\partial \chi} \left(\frac{B^2}{2}\right) \tag{2-19}$$

In a circular cylinder, field lines are geodesics on the surfaces, and κ_s is identically zero. In a torus, since the magnetic field is not uniform on a magnetic surface, this is not the case, but it can be shown[30] that the surface average of the geodesic curvature always vanishes.

The Orderings for Ballooning Modes

We shall derive the equations for ballooning modes using the fluid equations, rather than by minimizing the Lagrangian of ideal MHD. However, in order to identify the essential features of the most unstable modes, and to model the perturbations, we shall use the energy principle as a convenient starting point and a guide. The following form is particularly useful for this purpose[31]:

$$L = \frac{1}{2}\int dV \left[\frac{1}{B^2} (\vec{B}_1 \cdot \vec{B} - \vec{\xi}\cdot\nabla P)^2 + B_{1_\perp}^2 + \gamma_c P(\nabla\cdot\vec{\xi})^2 \right.$$

$$\left. - \frac{\vec{J}\cdot\vec{B}}{B^2} (\vec{\xi} \times \vec{B})\cdot\vec{B}_1 - 2(\vec{\xi}\cdot\nabla P)(\vec{\xi}\cdot\vec{\kappa}) + \rho_m \omega^2 \xi^2 \right] \qquad (2\text{-}20)$$

the last term representing the kinetic energy and the sum of all others the total potential energy. Here, $\vec{\xi}$ is the fluid displacement, γ_c is the ratio of specific heats, ρ_m is the fluid mass density and ω is the frequency. The vector $\vec{B}_1$ represents the perturbed magnetic field and is given by

$$\vec{B}_1 \equiv \nabla \times (\vec{\xi} \times \vec{B}) \qquad (2\text{-}21)$$

The first term of the potential energy contains the component of $\vec{B}_1$ in the direction of the equilibrium field, indicating that this term represents the work done in compressing the field lines. The perpendicular component gives the second term, which can be interpreted as the energy associated to the bending of the field lines. The third term on the other hand, measures the amount of work required to compress the fluid. These three terms are responsible for the stable side of the MHD spectrum. It is an approximation commonly made to assume that they individually drive three modes, respectively the fast magnetosonic, the shear-Alfvén and the slow sound waves. In the case of an infinite homogeneous medium, in particular, in the limit of long parallel wavelength:

$$k_{||} \equiv \vec{k} \cdot \frac{\vec{B}}{B} << |\vec{k}| \qquad (2\text{-}22)$$

where $\vec{k}$ is the wave vector, they effectively decouple. As it is well known[32], the dispersion relation in this case reduces to:

fast magnetosonic waves: $$\omega^2 = k^2 \left(\frac{V_A^4}{V_A^2 - V_S^2} \right) \qquad (2\text{-}23a)$$

shear-Alfvén waves: $$\omega^2 = k_{||}^2 V_A^2 \qquad (2\text{-}23b)$$

slow magnetosonic waves: $$\omega^2 = k_{||}^2 V_S^2 \qquad (2\text{-}23c)$$

where V_A is the Alfvén speed, given by $V_A^2 = B^2/\rho_m$ and the velocity of the slow magnetosonic waves is defined by:

$$V_S^2 = \frac{\gamma_c P}{\gamma_c P + B^2} \left(\frac{B^2}{\rho_m} \right) \qquad (2\text{-}24)$$

The two other terms in the expression for the potential energy are destabilizing. The first of these contains the force-free (parallel) equilibrium current, and drives the kink mode. We shall see later that, in the limit of high-toroidal number modes, it decouples entirely from the other terms, and disappears from the final equations. We may concentrate then our attention in the term that contains the curvature and the pressure gradient which is responsible for the interchange and ballooning instabilities. To derive an equation for ballooning modes, we have to manufacture a perturbation that emphasizes the

effect of this term by reducing the stabilizing influence of the other three.

We start with the assumption that, by applying the operator ∇ to the perturbed quantities, due to the large mode number N, we generate large derivatives, of the order of N. Variations of the equilibrium quantities are assumed to be much smaller, and we refer to them as of order "unity." Then the ballooning term itself is of order unity, while the stabilizing terms, if no further condition is introduced, become of order N^2. To see more clearly this point, we expand the expression for the perturbed magnetic field as

$$\vec{B}_1 = (\vec{B} \cdot \nabla)\vec{\xi} - \vec{B}\, \nabla \cdot \vec{\xi} - (\vec{\xi} \cdot \nabla)\vec{B} \qquad (2\text{-}25)$$

making use of familiar vector identities. It becomes apparent that the sources of large stabilization by the terms resulting from the bending and compression of the field lines in the Lagrangian, Eq. (2-20), are the parallel derivative:

$$(\vec{B} \cdot \nabla)\vec{\xi} = B \frac{\partial \vec{\xi}}{\partial \ell_{||}} = \left(\frac{B_x}{h_x} \frac{\partial}{\partial x} + \frac{B_\phi}{h_\phi} \frac{\partial}{\partial \phi}\right) \vec{\xi} \qquad (2\text{-}26)$$

and the divergence of the displacement, which appears also in the term that drives the slow sound wave.

Thus, although we allow the derivatives $\partial/\partial x$ and $\partial/\partial \phi$ themselves to be large, in order to bring those terms to the same order of magnitude of the ballooning term, we have first to demand that the combination in Eq. (2.26), that gives the

derivative along the field line, remain of order unity. This suggests a representation for the displacement in eikonal form, 'a la WKB:

$$\vec{\xi}(\psi, \chi, \phi) = \hat{\vec{\xi}}(\psi, \chi)\, e^{i\alpha} \tag{2-27}$$

with

$$\alpha = N\left(\phi - \int^{\chi} q_{\ell}(\psi,\chi)d\chi\right) \tag{2-28}$$

The phase factor is constant along the field lines (since $\vec{B}\cdot\nabla\alpha = 0$), while changing rapidly in the perpendicular direction ($\nabla_{\perp}\alpha \sim N$). Slow variations along the parallel direction, of the same order as the variations of the equilibrium fields, are still present in the mode, though the (comparatively) weak dependence of the amplitude on χ:

$$\frac{\nabla_{\parallel}\hat{\xi}}{\hat{\xi}} \sim \frac{1}{L} \ll |\nabla_{\perp}\alpha| \tag{2-29}$$

where L is a length characteristic of the equilibrium, such as the connection length.

With this representation, we automatically eliminate the predominance of large parallel derivatives. The next step to suppress large stabilizing terms is to order the divergence of the displacement:

$$\nabla\cdot\vec{\xi} = i\, e^{i\alpha}\, \nabla\cdot\hat{\vec{\xi}} + i\, e^{i\alpha}\, \hat{\vec{\xi}}\cdot\nabla\alpha \tag{2-30}$$

as small, relative to the transverse variations of the perturbed quantities. Specifically, we require that

$$\frac{\nabla \cdot \hat{\vec{\xi}}}{|\vec{\xi}|} \sim \frac{\hat{\vec{\xi}} \cdot \nabla a}{|\vec{\xi}|} \sim \frac{1}{L} \ll |\nabla_\perp a| \qquad (2\text{-}31)$$

We will see that these assumptions are sufficient for the derivation of the mode equations.

The Ballooning Representation

The eikonal representation, to which we were naturally led by a consideration of the general features that we want tc ascribe to the mode, entails, however, a difficulty. Since the magnetic surfaces are nested tori, the mode should exhibit a periodic dependence on the poloidal variable with the same period of the equilibrium quantities. Of course, periodicity in the toroidal angle is also a requirement, but in axisymmetric systems, we may analyse the azimuthal dependence of any perturbation in Fourier components, and treat each of them separately. The amplitude of each component does not depend on the ϕ-coordinate, and a representation like Eq. (2-27) corresponds to a "mode" in the proper sense, that satisfies automatically the requirement of periodicity in ϕ. With regard to the poloidal coordinate, however, the situation is different. The eikonal representation, both by the poloidal dependence of the "amplitude" and the form of the phase factor, is not a

Fourier-mode in χ (it is usually called a "quasi-mode", from the fact that the dominant dependence on χ is still given by the phase). The condition that the perturbation is periodic in the poloidal angle implies that

$$\hat{\xi}\,(\psi,\ \chi+2\pi) \;=\; \hat{\xi}\,(\psi,\chi)\ e^{i2\pi Nq} \qquad (2\text{-}32)$$

and, unless we are precisely on a rational surface, where $q = M/N$, the amplitude itself is not a periodic quantity. Moreover, since the phase factor in Eq. (2-27) varies rapidly with χ, and in general it is not periodic with the equilibrium quantities, the requirement of periodicity of the entire perturbation can be satisfied only if the "amplitude" compensates the lack of periodicity of the phase, and for this it has to contain a dependence on χ of the same order as that of the phase itself. Then, it appears that the eikonal representation, that separates neatly the slow and the fast dependencies of the perturbations on the poloidal angle, is inherently incompatible with the physical requirement of periodicity, except for a particular set of flux surfaces — the rational surfaces.

The most satisfactory way to solve this difficulty is probably by means of the so-called "ballooning transformation." It was published originally by Connor, Hastie and Taylor,[16] although Pegoraro and Schep,[15] Lee and VanDam[13] and Glasser[14] have discovered independently this transformation at about the same time (1978) and reported it earlier. We shall give here a brief account of the reasoning developed by Lee and

VanDam to arrive at this ingenious solution of the problem of representation of the ballooning modes, that accomodates the eikonal form with the periodicity constraint in a sheared magnetic field[33].

The central idea associated to a representation of the form $\xi = \hat{\xi}(\psi,\chi)e^{-iNq\chi}$ is that, for $N >> 1$ (and q a number of order unity), the strong dependence on the poloidal variable comes from the exponential factor, as we have repeatedly emphasized. Then, if we turn around the torus the short way, at any meridian plane, the number of oscillations that we will count will be approximately $M \sim Nq$. In other words, if we analyse the mode in its periodic components in χ:

$$\xi\ (\psi,\chi,\phi) \;=\; e^{iN\phi} \sum_{m=-\infty}^{+\infty} \xi_m(\psi)e^{-im\chi} \qquad (2\text{-}33)$$

the dominant component on a rational surface, where Nq equals M, an integer, will be $\xi_M e^{-iM\chi}$. Other components will exist, since the χ dependence of the mode is not only contained in the factor $e^{-iNq\chi}$, but with a much smaller amplitude. On the other hand, for large N, the rational surfaces are closely packed together. If we approximate the variation of q over a small range of flux surfaces by a linear relation as $q(\psi) = q(\psi_o) + (\psi-\psi_o)(dq/d\psi)$, then we may see that the radial distance between two rational surfaces $q = (M-1)/N$ and $q = M/N$ is of the order

$$\Delta r_s \;=\; \frac{1}{N\, dq/d\psi} \;. \qquad (2\text{-}34)$$

On this scale, we may assume that the equilibrium quantities are nearly constant. As we move from a rational surface to the next neighbor surface, however, the poloidal spectrum of the mode has shifted from a localization around the M-component to the M-1 component, with just a slight variation in the relative amplitude of the harmonics, introduced by the change in the equilibrium conditions. Then we are led to recognize two scales in the radial dependence of the mode: a large, given by the scale of variation of the equilibrium quantities, and a short scale, of the order of the separation between adjacent rational surfaces, on which there is local translational invariance among the dominant Fourier components. This fact can be stated as:

$$\xi_M(\psi,Nq) = e^{i\hat{\alpha}}\,\xi_{M-1}(\psi,\ Nq-1) = \ldots = e^{iM\hat{\alpha}}\,\xi_o(\psi,\ Nq-M) \qquad (2\text{-}35)$$

The factor $e^{i\hat{\alpha}}$ allows for a change in phase between adjacent rational surfaces, and $\hat{\alpha}$ should be, rigorously, a function of Nq, and not a constant, as implied by the above relation. A generalization is possible, as done in the original work( ), but we shall not pursue this matter here. We shall postpone to a later section of this chapter the discussion of the significance of this phase factor, only noting now that it is essential for a global analysis of the modes, and it can be made to appear naturally at this level of the argument. For our present purposes, however, it may be ignored all together, without doing any harm to the substance of our conclusions. For simplicity, then, we put $\hat{\alpha} = 0$ in Eq. (2-35), as it is

sufficient for a local analysis. Using the translational property of the Fourier coefficients, the expansion can be rewritten as:

$$\xi(\Psi,S;\chi,\phi) = e^{iN\phi} \sum_{m=-\infty}^{+\infty} \xi_o(\Psi, S-m)e^{-im\chi} \qquad (2\text{-}36)$$

where we have used the notation $S = Nq$.

We now express the amplitude $\xi_o(\Psi,S)$ by a Fourier integral:

$$\xi_o(\Psi, S) = \frac{1}{2\pi} \int_{-\infty}^{+\infty} \hat{\xi}(\Psi,y)e^{-iSy}\, dy. \qquad (2\text{-}37)$$

and the summation becomes:

$$\xi(\Psi,S;\chi,\phi) = e^{iN\phi} \sum_{m=-\infty}^{+\infty} \frac{1}{2\pi} e^{-im\chi} \int_{-\infty}^{+\infty} \hat{\xi}(\Psi,y)e^{-i(S-m)y}\, dy \qquad (2\text{-}38)$$

Assuming that the order of integration and summation can be interchanged, we have:

$$\xi(\Psi,S;\chi,\phi) = e^{iN\phi} \int_{-\infty}^{+\infty} dy\, e^{-iSy}\, \hat{\xi}(\Psi,y)\, \frac{1}{2\pi} \sum_{m=-\infty}^{+\infty} e^{-i(S-m)y} \qquad (2\text{-}39)$$

But, by the completeness relation of the circular functions, the summation on the right hand side is[34]

$$\frac{1}{2\pi}\sum_{m=-\infty}^{+\infty} e^{im(y-\chi)} = \sum_{n=-\infty}^{+\infty} \delta(y-\chi-2\pi n) \qquad (2\text{-}40)$$

where the δ's are the Dirac's impulsive functions. Using well-known properties of these functions, we can carry out formally the integration in Eq. (2-39) and obtain:

$$\xi(\Psi,S;\chi,\phi) = e^{iN\phi}\sum_{n=-\infty}^{+\infty} e^{-iS(\chi+2\pi n)}\,\hat{\xi}(\Psi,\chi+2\pi n). \qquad (2\text{-}41)$$

This is no more than the Poisson summation of Eq. (2-35)[34], and is completely equivalent to Eq. (2-38), the form originally proposed by Connor, Hastie and Taylor.

A series like this can be viewed, more broadly, as a receipt as to how to construct a periodic function from a function that is not periodic. For $e^{iS\chi}\,\hat{\xi}(\Psi,\chi)$, in general, may not exhibit any periodical property as the argument χ ranges from $-\infty$ to $+\infty$, but when it is summed according to the rule specified by Eq. (2-41), it generates a function that is, by force, periodic in χ with period 2π. Also, there is no reason why we cannot assign large variations with χ to the exponential factor, while demanding that the derivative of ξ with respect to χ remains small. Then, here, we have the key to the problem of reconciliation of the eikonal representation with the periodicity of the mode. Instead of working with the perturbation ξ, we work with:

$$\tilde{\xi}(\Psi,\chi,\phi) = e^{iN(\phi - \int^{\chi} q_s \, d\chi)} \hat{\xi}(\Psi,\chi) \quad ,$$

where $\hat{\xi}(\Psi,\chi)$ varies slowly with χ, but is no longer to be regarded as the amplitude of the physical perturbation, and, therefore, does not have to satisfy any periodicity requirements. This leads to a formulation of the problem in terms of the quantity $\hat{\xi}(\Psi,\chi,\phi)$, defined in the infinite domain $-\infty < \chi < +\infty$. Once the mode equations are solved, the physical perturbation can be constructed from the solution by means of either of the equivalent versions of the periodic representations:

$$\xi = \sum_{n=-\infty}^{+\infty} \tilde{\xi}(\Psi, \chi+2\pi n, \phi) = e^{iN(\phi - \int^{\chi} q_s \, d\chi)} \sum_{n=-\infty}^{+\infty} e^{-i2\pi nS} \hat{\xi}(\Psi, \chi+2\pi n) \tag{2-42}$$

$$\xi = \frac{1}{2\pi} e^{iN(\phi - \int^{\chi} q_s \, d\chi)} \sum_{n=-\infty}^{+\infty} e^{i(S-n)\chi} \int_{-\infty}^{+\infty} \hat{\xi}(\Psi,y) \, e^{-i(S-n)y} \, dy \tag{2-43}$$

where

$$S = \frac{N}{2\pi} \int_{-\pi}^{\pi} q_s \, d\chi = Nq \quad .$$

All that is required is the convergence of these series, and for this, $\hat{\xi}(\Psi,y)$ has to decay sufficiently fast as y goes to infinity. The constraint of periodicity is then ultimately replaced by a condition on the asymptotic behavior.

It is also very gratifying to find that this "ballooning transformation" preserves the form of the mode equations. These can be represented in a concise way as

$$L\,\xi = 0 \qquad (2\text{-}44)$$

where L is a linear operator that involves derivatives with respect to χ and with coefficient functions that depend only periodically on the poloidal angle. But to differentiate $\xi(\chi)$ with respect to χ is tantamount to differentiating $\hat{\xi}(y)$ with respect to y. For, using the representation of Eq. (2-43), and omitting the unnecessary factor $(1/2\pi)\, e^{iN\phi}$, we have:

$$\frac{\partial}{\partial\chi}\,\xi = \frac{\partial}{\partial\chi}\sum_{m=-\infty}^{+\infty} e^{-im\chi}\int_{-\infty}^{+\infty} e^{imy}\,\hat{\xi}(y)\,dy = -\sum_{m=-\infty}^{+\infty} im\, e^{-im\chi}\int_{-\infty}^{+\infty} e^{imy}\,\hat{\xi}(y)$$

$$= -\sum_{m=-\infty}^{+\infty} e^{-im\chi}\int_{-\infty}^{+\infty}\hat{\xi}(y)\,\frac{d}{dy}\,e^{imy}dy = \sum_{m=-\infty}^{+\infty} e^{-im\chi}\int_{-\infty}^{+\infty} e^{imy}\,\frac{\partial}{\partial y}\,\hat{\xi}(y)\,dy \qquad (2\text{-}45)$$

where, in the last step, a partial integration was performed and it was assumed that $\hat{\xi}(y)$ vanishes at infinity. Using this same representation, it is straightforward to show that, as we multiply $\xi(\chi)$ by a periodic function of the form $e^{\pm ik\chi}$ (k an integer), the function $\hat{\xi}(y)$ is also multiplied by $e^{\pm iky}$. It follows that, if $\hat{\xi}(y)$ satisfies the equation $L(y)\,\hat{\xi}(y) = 0$, in the infinite domain of the variable y, then $\xi(\chi)$ satisfies automatically $L(\chi)\,\xi(\chi) = 0$. The equations are the same, the eigenvalue problem differs by the boundary conditions imposed on ξ and $\hat{\xi}$.

The form of Eq. (2-42), while providing a more immediately obvious way of generating periodic functions, is less convenient

than the representation of Eq. (2-43). From this last one, we can see that the relation between the perturbation ξ and the "amplitude" of the quasi-mode $\hat{\xi}$ is analogous to the relation between a function and its Fourier transform, and that the relation between the "physical" poloidal angle χ and the "extended" one y is similar to the relation between a free variable and its Fourier conjugate. To be rigorous, in the future work, we should keep a distinct notation for one and the other, but we shall frequently ignore it, and use χ to refer to both variables, as it is the usual practice.

The reasoning developed by Pegoraro and Schep[15] has several points of contact with the previous derivation of the "ballooning transformation," but is, nonetheless, instructive to examine it briefly. The motivation, for them, was the symmetries in the structure of the mode that are revealed by the mode equations in the local approximation.

As a simple example of the form taken by these equations, let's consider an equilibrium configuration in which the flux surfaces are described by circular concentric surfaces of radius r. On each flux surface, the field lines wind at a constant, uniform rate, independent of the poloidal angle. We assume, however, that $q = q(r)$, so that the model allows for a non-vanishing shear, defined as $\hat{s} = (r/q)\,(dq/dr)$. For the displacement, we assume the form of Eq. (2-27). Then, because of the constraint on the amplitude given by Eq. (2-32), we may recognize as before the existence of two radial scales. Neglecting the dependence of $\hat{\xi}$ on the large scale distance, we

are led to the following partial differential equation for the mode amplitude at marginal stability ($\omega^2 = 0$):

$$\frac{\partial}{\partial \chi}\left[1 + \hat{s}^2\left(\chi + i\frac{\partial}{\partial S}\right)^2\right]\frac{\partial}{\partial \chi}\hat{\xi}(S,\chi) + G\left[\cos\chi + \hat{s}\sin\chi\left(\chi + i\frac{\partial}{\partial S}\right)\right]\hat{\xi}(S,\chi) = 0 \tag{2-46}$$

The quantity G is proportional to the pressure gradient, and will be defined later; for the time being it does not have to concern us, being enough to keep in mind that, as an equilibrium quantity, it does not change on the scale Δr_s, and so, can be assumed here to be a fixed parameter. This same comment applies to $\hat{s}$. The periodic terms that appear above are introduced by the curvature, respectively the normal component ($\propto \cos\chi$) and the geodesic component ($\propto \sin\chi$). It is the existence of these terms that makes difficult the analysis of the poloidal dependence of the mode. For, if we write $\hat{\xi} = \xi\, e^{iS\chi}$, and expand ξ in its periodicity in χ as a Fourier series

$$\sum_{m=-\infty}^{+\infty} \xi_m\, e^{im\chi} \quad ,$$

then the equation for the component ξ_m will be coupled through the curvature terms to the equations for $\xi_{m\pm1}$. In a general equilibrium, the coefficient functions in Eq. (2-46) would contain harmonies of higher order, with the result that the coupling would involve an indefinite number of poloidal components of the perturbation. The coefficient functions, however, do not involve any dependence on S. This suggests that

rather than a decomposition in poloidal components, we may try to find a representation of the mode as a superposition of plane waves in the radial direction. We look, then, for the solutions of the form $\sim e^{+iKs}$ such that:

$$\hat{\xi}\ (S + \Delta S,\ \chi) \ = \ \hat{\xi}\ (S,\ \chi)^{*} \quad . \tag{2-47}$$

But the periodicity constraint on the entire perturbation by Eq. (2-32) requires that

$$\hat{\xi}\ (S,\ \chi + 2\pi) \ = \ \hat{\xi}\ (S,\ \chi)\ e^{+2\pi i S} \tag{2-48}$$

and the combination of these two conditions gives:

$$\hat{\xi}(S+\Delta S,\ \chi+2\pi) = \hat{\xi}(S+\Delta S,\chi)\ e^{+2\pi i(S+\Delta S)} \ = \ \hat{\xi}(S,\chi+2\pi)\ e^{+2\pi i \Delta S} \tag{2-49}$$

It follows that ΔS is restricted to integer values, that is, $K = \pm 2\pi n$ $(n = 0,1,2...)$. We propose then a representation periodic in S:

$$\hat{\xi}(S,\chi) \ = \sum_{m=-\infty}^{+\infty} \ \hat{\xi}\ (\chi)\ e^{-2\pi i m S} \tag{2-50}$$

---

*Or, more generally, $\hat{\xi}(S + \Delta S,\chi) = e^{i\alpha\Delta S}\ \hat{\xi}(S,\chi)$, where the phase change that goes along with the translation ΔS permits us to bridge the local radial analysis with the global one, and is analogous to the phase change in Eq. (2-35). For our present purposes, we may take $\hat{\alpha} = 0$, as we did before.

with period equal to the distance that separates two consecutive mode rational surfaces, $\Delta S = 1$. In order to satisfy the condition expressed by Eq. (2-48) we must have:

$$\hat{\xi}(S,\chi-2\pi n) = \sum_{m=-\infty}^{+\infty} \hat{\xi}\ (\chi-2\pi n)\ e^{-2\pi imS} = e^{-2\pi imS}\ \hat{\xi}(S,\chi), \tag{2-51}$$

showing that

$$\hat{\xi}(S,\chi) = \sum_{m=-\infty}^{+\infty} \hat{\xi}_m(\chi-2\pi n)\ e^{-2\pi i(m-n)S} = \sum_{m'=-\infty}^{+\infty} \hat{\xi}_{m'+n}(\chi-2\pi n)^{-2\pi im'S} \tag{2-52}$$

Comparing this last expression for $\hat{\xi}$ with Eq. (2-50), we find again that the coefficients must obey a translational property

$$\hat{\xi}_{m+n}\ (\chi - 2\pi n) = \hat{\xi}_m(\chi)\ , \tag{2-53}$$

which, by successive shifts of the argument, can be rewritten as:

$$\hat{\xi}_m(\chi) = \hat{\xi}_o(\chi + 2\pi m) \tag{2-54}$$

The series for the amplitude becomes:

$$\hat{\xi}(S,\chi) = \sum_{m=-\infty}^{+\infty} \hat{\xi}_o(\chi + 2\pi m)\ e^{-2\pi imS} \tag{2-55}$$

and we are back to the representation of Eq. (2-42), etc. etc.

This is the heart of the argument of Pegoraro and Schep. A more thorough discussion can be found in Ref. (35), where an analysis of the symmetries of the mode structure is fully developed. These symmetries can be summarized as follows:

1) The partial differential equation for the mode amplitude, as exemplified by Eq. (2-46), is invariant under the transformation $\chi \to -\chi$, $S \to -S$. It is then possible to choose solutions that are either even or odd under the above transformation, and, in each respective case, they can be obtained from an even or odd function $\hat{\xi}_o(\chi)$ in χ in the infinite series representation of Eq. (2-55). The solutions of greater physical interest, however, are the even ones, since they lead to the highest growth rates for unstable modes and give the strictest conditions for marginal stability.

2) For even $\hat{\xi}_o(\chi)$, the amplitude vanishes at half-rational surfaces, where $S = \pm 1/2, \pm 3/2, \ldots$, when χ is equal to $\pm\pi$, $\pm 3\pi \ldots$. For we have, at $S = 1/2$ and $\chi = \pi$:

$$\hat{\xi}\left(\frac{1}{2}, \pi\right) = \sum_{m=-\infty}^{+\infty} (-1)^m \hat{\xi}_o(\pi+2\pi m) = \sum_{m=-\infty}^{+\infty} (-1)^m \hat{\xi}_o(\pi-2\pi m) \quad (2\text{-}56)$$

changing the dummy variable m by -m. But since $\hat{\xi}_o(\chi)$ is even, this is equal to

$$\hat{\xi}\left(\frac{1}{2}, \pi\right) = \sum_{m=-\infty}^{+\infty} (-1)^m \hat{\xi}_o(-\pi+2\pi m) = \sum_{m=-\infty}^{+\infty} (-1)^{m-1} \hat{\xi}_o(\pi+2\pi m) \quad (2\text{-}57)$$

where, in the last summation, we have replaced m by m-1. From this expression and the first summation in Eq. (2-56), we

conclude that $\hat{\xi}(1/2, \pi)$ is zero. It is straightforward to show that this property repeats itself periodically with periods $\Delta S=1$, $\Delta\chi=2\pi$.

Then the functions $\hat{\xi}(S,\chi)$ and $\xi(S,\chi)$ have a lattice structure in the two-dimensional space (S,χ), the unit cell given by the domain $-1/2 \leq S \leq 1/2$, $-\pi \leq \chi \leq \pi$. At the corners of this cell, both functions vanish, while translation by steps equal to the sides of the fundamental unity are accompanied by the transformations:

$$\hat{\xi}(S+1,\chi) = \hat{\xi}(S,\chi) , \quad \xi(S+1,\chi) = e^{-i\chi}\, \xi(S,\chi) \tag{2-58a}$$

$$\hat{\xi}(S,\chi+2\pi) = e^{2\pi i S}\, \hat{\xi}(S,\chi) , \quad \xi(S,\chi+2\pi) = \xi(S,\chi) \tag{2-58b}$$

We now return to the partial differential equation, Eq. (2-46) that provided the initial motivation for the construction of the infinite series. When Eq. (2-55) is substituted back in this equation, we obtain a summation in m over the equations:

$$\frac{d}{d\chi}\left[1 + \hat{s}^2(\chi + 2\pi m)^2 \right] \frac{d}{d\chi}\, \hat{\xi}_o(\chi + 2\pi m) +$$

$$+ G\left[\cos(\chi+2\pi M) + s\, \hat{\sin}(\chi + 2\pi m) \right] \xi\, \hat{(}\chi+2\pi m) = 0 \tag{2-59}$$

With the substitution $\chi + 2\pi m \rightarrow \chi$, which leaves the periodic functions unchanged, we rewrite the above equation as

$$\frac{d}{d\chi}\left(1 + \hat{s}^2\chi^2\right)\frac{d\hat{\xi}_o}{d\chi} + G\left(\cos\chi + \hat{s}\chi\sin\chi\right)\hat{\xi}_o(\chi) = 0 \qquad (2\text{-}60)$$

a differential equation in the poloidal variable alone. Obviously, if $\hat{\xi}_o$ satisfies this equation in the infinite domain $-\infty < \chi < +\infty$, the original differential equation for $\hat{\xi}$ is automatically satisfied, and all periodicity constraints for $\hat{\xi}$ (or ξ) are guaranteed by the representation of Eq. (2-55) [or Eq. (2-42)]. Observe that the extension of the range of the variable from $-\pi$ to π to infinity is actually possible because of the choice $K = \pm 2\pi n$ in the basis functions e^{iKS} and this provides another justification of Eq. (2-47).

Noting that, for the model considered here, the element of length of the field lines is given by $d\ell = Rq\,d\chi$, we may substitute the variable χ in Eq. (2-60) by ℓ. Then, by use of the ballooning transformation, we were able to reduce the local problem to a single ordinary differential equation that describes the structure of the mode along the field lines. We are going to see in the next section that this is generally true, regardless of the equilibrium considered. The fine structure of the mode along the radial direction, because of the crowding of the rational surfaces in the large N limit, can be described by translational symmetries that are ultimately contained in Eq. (2-58) and decouples from the analysis of the poloidal dependence. It remains only to determine the global radial structure. As we shall see still in this chapter, however, the relevant information concerning the global eigenvalue can be determined by a clever exploration of the eikonal

representation in the limit $N \gg 1$, that makes it possible to avoid solving another differential equation in the variable ψ. Because of this, a typical two-dimensional problem can be reduced to the solution of ordinary differential equations in the poloidal-like variable. Thus the theory of ballooning modes can be simplified in more than one way by the assumption of high toroidal mode number.

To conclude this section, a few words about the relation between the localization of the modes in the poloidal and radial directions. Because of the predominance of the Fourier component of order M on the rational surface $Nq = M$, the radial function $\xi_o(S)$ in Eq. (2-36) is highly localized around $S = 0$. The global poloidal dependence of the mode at any rational surface, that is determined by the amount of interference between its domihant component with the dominant components of all other rational surfaces, appears then as the result of the finite width of the radial distribution of the mode. Weak overlap between adjacent rational surfaces means that the mode is extended in the poloidal coordinate, as it is well approximated, at each rational surface, by a few harmonics. On the opposite extreme, we could figure a situation of strong interference, in which all Fourier components would have about the same amplitude on each surface, and $\xi_o(S)$ would be approximately constant. Then, by Eq. (2-36), we would produce a mode peaked around the outer edge of the torus, as an impulsive function $\delta(\chi)$.

A mode sharply defined in the poloidal angle is called a strong ballooning mode, as opposed to the weakly ballooning mode that spreads over the whole interval $-\pi$ to π. Strong ballooning corresponds to solutions of the mode equations in the infinite domain that are themselves peaked around the origin. In this case, because of its fast decay, $\hat{\xi}(\chi)$ becomes negligible at $\pm\pi$, and the summation that represents the periodic mode, Eq. (2-42), collapses to one single term:

$$\xi(\chi) = e^{iN(\phi - q\chi)} \hat{\xi}(\chi)$$

This corresponds to the "disconnected mode approximation" of Coppi[11], the name "disconnected" coming from the fact that the modes appear as if they were acting independently or periodically spaced, successive regions along a given magnetic field line. In this model, $\hat{\xi}$ is regarded as the true amplitude of the mode, and the mode equations are solved in the finite domain $-\pi < \chi < \pi$ with boundary conditions $\hat{\xi}(\pm\pi) = 0$.

As we have learned from the discussion on the interplay between radial and poloidal profiles, strong ballooning is associated to modes that are radially extended. The "disconnected mode approximation," therefore, gives more accurate results if the rational surfaces are closely spaced, and, by Eq. (2-34), this condition is better satisfied in configurations with strong shear. Shear, then, appears as the physical agent that causes the disconnection of the modes on the inner side of the torus. Another way of seeing this is by a

straight consideration of the asymptotic behaviour of the eigenmodes, that decay more rapidly as the shear is increased. This is shown in a subsequent section of this chapter.

The representation of the modes proposed by Coppi, that leads to a treatment of the eigenvalue problem in the finite domain $-\infty < \chi < \infty$, in fact, is more general and more sophisticated than the simplified version that we presented here. A detailed exposition of his method can be found in Ref. (35), where the correspondence with the method of the infinite series is also discussed and the "disconnected mode approximation" is formulated in more rigorous terms than above. In this thesis, however, we are mainly concerned with equilibrium configurations that are characterized by weak shear, that cannot be dealt with properly by this approximation.

Derivation of the Mode Equations

At this point, with what we have learned from a consideration of the energy principle, we may start the derivation of the mode equations, using the normal mode method[36]. We assume small perturbations of the equilibrium, that vary harmonically with time ($\sim e^{i\omega t}$) and linearize the equation of ideal MHD. The equation of motion that results from this procedure is:

$$-\rho_m \omega^2 \hat{\xi} = -\nabla P_1 + \hat{J}_1 \times \hat{B} + \hat{J} \times \hat{B}_1 \qquad (2\text{-}61)$$

The perturbed magnetic field $\hat{B}_1$ has already been introduced in Eq. (2-24). This expression results both from Faraday's

induction law and the so-called "frozen-in-law" of ideal magnetohydrodynamics, that ties the motion of the particles to the motion of the field lines. The perturbed current $\vec{J}_1$, for low frequency modes as those that we are considering here, obeys Ampere's law:

$$\vec{J}_1 = \nabla \times \vec{B}_1 \tag{2-62}$$

and the perturbed pressure P_1 follows from the law of adiabatic transformations:

$$P_1 + \vec{\xi} \cdot \nabla P + \gamma_c P \nabla \cdot \vec{\xi} = 0 \ , \tag{2-63}$$

where P is the equilibrium pressure and γ_c the adiabaticity index. We assume that all perturbed quantities have the same eikonal representation as the displacement, namely:

$$\vec{B}_1 = \hat{\vec{B}}_1 e^{i\alpha} \tag{2-64a}$$

$$\vec{J}_1 = \hat{\vec{J}}_1 e^{i\alpha} \tag{2-64b}$$

$$P_1 = \hat{P}_1 e^{i\alpha} \tag{2-64c}$$

with α given by Eq. (2-27). Then

$$\hat{\vec{B}}_1 = \nabla \times (\hat{\vec{\xi}}_\perp \times \vec{B}) - i \vec{B} \hat{\vec{\xi}}_\perp \cdot \nabla\alpha \tag{2-65}$$

$$\hat{\vec{J}}_1 = \nabla \times \hat{\vec{B}}_1 + i \nabla\alpha \times \hat{\vec{B}}_1 \tag{2-66}$$

Vector quantities will be projected locally on three mutually perpendicular directions: along the field line, as specified by the unity vector $\vec{b}$; in the direction of $\nabla\alpha$ (that, although perpendicular to the field line is not necessarily normal to the flux surface at that point) and in the direction of the vector $\nabla\alpha \times \vec{b}$.

Taking the scalar product of the equation of motion with $\vec{B}$, we obtain:

$$-\rho_m \omega^2 \hat{\vec{\xi}} \cdot \vec{B} = -\vec{B} \cdot \nabla \hat{P}_\perp - \hat{\vec{B}}_\perp \cdot \nabla P \quad , \tag{2-67}$$

where use was made of the equilibrium relation, Eq. (2-1).

The component in the direction of $\nabla\alpha$ gives:

$$- \omega^2 \rho_m \hat{\vec{\xi}} \cdot \nabla\alpha = -i|\nabla\alpha|^2 \hat{P}_1 - \nabla\alpha \cdot \nabla \hat{P}_1 - i\,|\nabla\alpha|^2 \hat{\vec{B}}_\perp \cdot \vec{B} +$$

$$+ \quad \nabla\alpha \cdot [(\nabla \times \hat{\vec{B}}_\perp) \times \vec{B}] + \nabla\alpha \cdot (\vec{J} \times \hat{\vec{B}}_\perp) \tag{2-68}$$

The dominant terms in the right-hand side of this equation, of order N^2, scale like $k_\perp{}^2 B^2 \xi_\perp k_\parallel$, while the left-hand side is $\sim \omega^2 \rho_m \xi_\perp k_\parallel$, so that the ratio of the two sides is $\sim k_\perp{}^2 V_A^2/\omega^2$. We now make more precise the range of frequencies of the phenomena we are studying. We are interested in low frequency modes, with ω on the order of Alfvén and sound frequencies. By ordering $\omega^2 \lesssim k_\parallel^2 V_A^2 \sim O(1)$, the dominant balance in the above equation is simply:

$$\hat{P}_1 + \vec{B} \cdot \hat{\vec{B}}_1 = 0 \qquad (2\text{-}69)$$

and fast magnetosonic modes, for which $\omega^2 \sim k_\perp^2 V_A^2 \sim O(N^2)$, are therefore excluded from our equations.

We take next the scalar product of the equation of motion with the vector $\nabla\alpha \times \vec{B}$, and after some algebra, we obtain the third component:

$$-\rho_m \omega^2 \nabla\alpha \cdot (\vec{B} \times \hat{\vec{\xi}}) = \nabla\alpha \cdot [\nabla \times (\hat{P}_1 \vec{B}) + B^2 \nabla \times \hat{\vec{B}}_1] +$$

$$+ \quad \nabla\alpha \cdot [\vec{B} \times (\vec{J} \times \vec{B})] - \hat{P} \ \nabla\alpha \cdot (\nabla \times \vec{B}) \qquad (2\text{-}70)$$

The first of the three terms on the right hand side can also be written as:

$$\nabla \cdot [(\hat{P}_1 \vec{B} + B^2 \hat{\vec{B}}_1) \times \nabla\alpha] - \nabla\alpha \cdot (\nabla B^2 \times \hat{\vec{B}}_1) \qquad (2\text{-}71)$$

and, since

$$\hat{P}_1 \vec{B} + B^2 \hat{\vec{B}}_1 = B^2 \hat{\vec{B}}_1 - \vec{B} \cdot \hat{\vec{B}}_1 \vec{B} = \vec{B} \times (\hat{\vec{B}}_1 \times \vec{B}) \qquad (2\text{-}72)$$

by Eq. (2-69), we can recast Eq. (2-70) in the following form:

$$-\rho_m \omega^2 \nabla\alpha \cdot (\vec{B} \times \hat{\vec{\xi}}) = \nabla \cdot \{[\vec{B} \times (\hat{\vec{B}}_1 \times \vec{B})] \times \nabla\alpha - \nabla\alpha \cdot (\nabla B^2 \times \hat{\vec{B}}_1)$$

$$- 2 \hat{P} \ \nabla\alpha \cdot \vec{J} \qquad (2\text{-}73)$$

If we now express the displacement as

$$\hat{\vec{\xi}} = X \nabla\alpha \times \vec{b} + Y \nabla\alpha + Z\vec{b} \quad , \tag{2-74}$$

from the requirement that $\nabla\cdot\vec{\xi} \sim \vec{\xi}_{\perp}\cdot \nabla\alpha \sim O(1)$, it follows that $Y \sim X/L|\nabla\alpha| \sim (k_{\parallel}/k_{\perp})\, X$, i.e., Y is a quantity of order 1/N as compared to X. This implies that, to lowest order, the perturbed magnetic field can be represented as:

$$\hat{\vec{B}}_1 = \nabla\alpha \times \nabla(BX) - i\,|\nabla\alpha|^2\, Y\, \vec{B} \tag{2-75}$$

and that $\nabla\alpha \cdot \vec{B}_1 = 0$. Using this fact, we transform the third term on the right hand side of Eq. (2-73) as follows

$$-2\,\hat{P}_1\, \nabla\alpha \cdot \vec{J} = 2\,\nabla\alpha \cdot (\hat{\vec{B}}_1 \times \nabla P) \quad , \tag{2-76}$$

recalling Eqs. (2-69) and (2-1). Introducing the expression for $\hat{\vec{B}}_1$ also in the term of the divergence, the scalar equation for transverse motions takes the form:

$$-\rho_m\omega^2|\nabla\alpha|^2(BX) = \nabla\cdot[|\nabla\alpha|^2\, \vec{B}\,\vec{B}\cdot\nabla(BX)] + \hat{\vec{B}}_1\cdot[\nabla(2P+B^2)\times\nabla\alpha] \tag{2-77}$$

To reduce further this equation, we note that $\hat{\vec{B}}_1$ can be trivially written as:

$$\hat{\vec{B}}_1 = \frac{\vec{B} \times (\hat{\vec{B}}_1 \times \vec{B})}{B^2} + \frac{\vec{B} \cdot \hat{\vec{B}}_1}{B^2} \vec{B} \quad , \tag{2-78}$$

and, replacing in the cross product in the right hand side $\vec{B}_1$ again, as given by Eq. (2-65), we obtain:

$$\hat{\vec{B}}_\perp = \frac{\vec{B} \cdot \vec{B}_1}{B^2} \vec{B} - \frac{\vec{B} \cdot \nabla(BX)}{B^2} \vec{B} \times \nabla\alpha \tag{2-79}$$

This permits us to rewrite the last term on the right hand side of Eq. (2-77) as:

$$\hat{\vec{B}}_\perp \cdot [\nabla(2P+B^2) \times \nabla\alpha] = K_T \frac{\vec{B} \cdot \hat{\vec{B}}_1}{B^2} - \frac{\vec{B} \cdot \nabla(BX)}{B^2} (\vec{B} \cdot \nabla B^2) \, |\nabla\alpha|^2 \tag{2-80}$$

where K_T is the curvature-related quantity:

$$K_T = 2 \frac{\vec{B}}{B^2} \cdot [\nabla(P + \frac{B^2}{2}) \times \nabla\alpha] = 2 \nabla\alpha \cdot (\vec{B} \times \vec{\kappa}) \tag{2-81}$$

The first term can be expanded as

$$\nabla \cdot [|\nabla\alpha|^2 \vec{B} \; \vec{B} \cdot \nabla(BX)] = B^2 \vec{B} \cdot \nabla \left[|\nabla\alpha|^2 \frac{\vec{B} \cdot \nabla(BX)}{B^2}\right] +$$

$$+ \frac{\vec{B} \cdot \nabla(BX)}{B^2} (\vec{B} \cdot \nabla B^2) \, |\nabla\alpha|^2 \tag{2-82}$$

and, substituting Eqs. (2-80) and (2-82) into Eq. (2-77), we obtain:

$$-\rho_{m_i}\omega^2 \frac{|\nabla\alpha|^2}{B^2}(BX) = \vec{B}\cdot\nabla\left[|\nabla\alpha|^2 \frac{\vec{B}\cdot\nabla(BX)}{B^2}\right] + K_T \frac{\hat{\vec{B}}_1\cdot\vec{B}}{B^2} \qquad (2\text{-}83)$$

We now turn our attention to the scalar equation for the parallel motion, Eq. (2-67). With the expressions for $\hat{P}_1$ and $\vec{B}_1$ given by Eqs. (2-69) and (2-75), this equation becomes:

$$-\rho_{m_i}\omega^2 \hat{\vec{\xi}}\cdot\vec{B} = \vec{B}\cdot\nabla(\vec{B}\ \hat{\vec{B}}_1) + \frac{(\vec{B}\times\nabla\alpha)\cdot\nabla P}{B^2}\ \vec{B}\cdot\nabla(BX) \qquad (2\text{-}84)$$

In the Appendix 2A, we show that, for α given by Eq. (2-27),

$$\vec{B}\cdot\nabla\left[\frac{(\vec{B}\times\nabla\alpha)\cdot\nabla P}{B^2}\right] = 0\ , \qquad (2\text{-}85)$$

and this permits us to write the above equation as

$$-\rho_{m_i}\omega^2 \hat{\vec{\xi}}\cdot\vec{B} = \vec{B}\cdot\nabla\left[\vec{B}\cdot\hat{\vec{B}}_1 + (BX)\frac{(\vec{B}\times\nabla\alpha)\cdot\nabla P}{B^2}\right] \qquad (2\text{-}86)$$

The couple of equations, Eq. (2-83) and (2-86), as it is, still contain the three components of the displacement vector, X, Y and Z, the transverse component y being implied by the expression for $\vec{B}_1$ (Eq. (2-75)). The missing relation is supplied by the law of adiabatic transformation, that can be used to eliminate Y and Z in benefit of the divergence. The linearized form for small perturbations, Eq. (2-63) is equivalent to:

$$\hat{B}_1 \cdot \vec{B} = \hat{\xi} \cdot \nabla P + \gamma_c P \, (\nabla \cdot \hat{\xi} + i \, \hat{\xi} \cdot \nabla \alpha) \qquad (2\text{-}87)$$

The mathematical tranformations of this expression, although straightforward, are quite tedious. In the Appendix 2B, we give the details of the calculation and show that, by neglecting quantities down by 1/N, the divergence of the parallel displacement can be obtained as:

$$\nabla \cdot \left[\left(\frac{\hat{\xi} \cdot \vec{B}}{B^2} \right) \vec{B} \right] = W \left(\frac{1}{\gamma_c P} + \frac{1}{B^2} \right) + \frac{BX}{B^2} K \qquad (2\text{-}88)$$

where W, defined by

$$W = \vec{B} \cdot \hat{B}_1 + (BX) \, \frac{(\vec{B} \times \nabla \alpha) \cdot \nabla P}{B^2} \qquad (2\text{-}89)$$

is the same quantity that appears on the right hand side of Eq. (2-86).

We now eliminate $\vec{B}_1 \cdot \vec{B}$ in favor of W in Eq. (2-83) and insert $\vec{\xi} \cdot \vec{B}$, given by Eq. (2-86), into the expression for the divergence we have just obtained. The result is:

$$-\rho_m \omega^2 \frac{|\nabla \alpha|^2}{B^2} (BX) - \vec{B} \cdot \nabla \left[|\nabla \alpha|^2 \frac{\vec{B} \cdot \nabla (BX)}{B^2} \right] - \frac{K_T K_P}{B^2} (BX) = \frac{K_T W}{B^2} \qquad (2\text{-}90a)$$

$$- \frac{1}{\omega^2} \vec{B} \cdot \nabla \left(\frac{B \cdot \nabla W}{\rho_m B^2} \right) - \left(\frac{1}{\gamma_c P} + \frac{1}{B^2} \right) W = \frac{K_T (BX)}{B^2} \qquad (2\text{-}90b)$$

where we defined the pressure-gradient related quantity:

$$K_P = \frac{\vec{B} \cdot (\nabla P \times \nabla \alpha)}{B^2} \tag{2-91}$$

Note that, if the displacement vector in Eq. (2-74) is represented in terms of flux-coordinates (and the expressions given in Appendix 2A can be useful for this), we find that the quantity BX is essentially $RB_\chi \xi_\psi$, where ξ_ψ is the component normal to the flux surface. Thus, Eq. (2-90a) is essentially an equation for the normal displacement.

To see the meaning of the quantity W, we observe first that Eq. (2-89) is equivalent to

$$W e^{i\alpha} = \vec{B}_1 \cdot \vec{B} - \vec{\xi}_\perp \cdot \nabla P \tag{2-92}$$

where $\vec{\xi}_\perp$ denotes the perpendicular displacement vector. Then $|W|/B^2$ reproduces the first term in the expresssion for the Lagrangian, and can be interpreted as the potential energy associated to the compression of the field lines. Remember, however, that by the minimization process that was effectively carried out, fast magnetosonic modes have been eliminated from our equations. Indeed, an alternative form for W, that we shall give now, shows that this quantity can also be related to the term in the Lagrangian usually associated with slow sound waves.

Eq. (2-92) can be rewritten as

$$W e^{i\alpha} = -B^2 (\nabla \cdot \vec{\xi}_\perp + 2\vec{\xi}_\perp \cdot \vec{\kappa}) , \qquad (2\text{-}93)$$

(see Appendix 2C for the details of this transformation) and, Eq. (2-88) is the same as

$$\nabla \cdot \vec{\xi}_{\parallel} = W e^{i\alpha} \left(\frac{1}{\gamma_c P} + \frac{1}{B^2}\right) + 2\vec{\xi}_\perp \cdot \vec{\kappa} \qquad (2\text{-}94)$$

Combining these two results, we can derive an expression for the divergence of the displacement, which shows that

$$W e^{i\alpha} = \gamma_c P \nabla \cdot \vec{\xi} , \qquad (2\text{-}95)$$

and therefore $|W|^2/\gamma_c P$ is the potential energy associated with the expansion or compression of the fluid. The ratio of the compressional magnetic energy to the energy of the compressional fluid is $\gamma_c P/B^2 \sim \beta$. We see that Eq. (2-90b) is essentially an equation for the fluid compressibility.

To summarize, we have derived two equations for low-frequency, short perpendicular wavelength, electromagnetic modes in an inhomogeneous plasma. The differential operators in both equations involve only the parallel derivative $\vec{B} \cdot \nabla$, and consequently they describe the structure of the mode along the field lines. The dependence on the radial coordinate ψ, through the various quantities P, B^2, etc., appears only parametrically. This permits us to treat the stability analysis as a separate problem for each magnetic surface.

In the equation for the perturbations normal to the flux surfaces, the term that contains the interaction of the curvature and the pressure gradient, as represented by the quantities K_T and K_P, is responsible for the ballooning instability, while the term involving the parallel derivative clearly represents the (stabilizing) effect of the bending of the field lines. If we decouple the pair of equations, by assuming that $K_T \sim 0$, then a simple scaling shows that the first describes transverse modes that propagate down the field lines with frequencies of the order of the shear Alfvén waves, while the second gives modes with typical sound frequencies. High frequency waves, as we could expect, are absent. Note that in this limit of vanishingly small curvature, the quantity W becomes

$$W \approx -\left(\frac{1}{B^2} + \frac{1}{\gamma_c P}\right)^{-1} \nabla \cdot \vec{\xi}_{\parallel} \qquad (2\text{-}96)$$

and the slow waves are mainly polarized in the longitudinal direction[37].

The equations decouple also at marginal stability ($\omega^2 \to 0$), since this limit, by the second equation, requires that $W = 0$. Then, by Eqs. (2-95) and (2-92), we have $\nabla \cdot \vec{\xi} = 0$ and $\vec{B} \cdot \vec{B}_1 - \vec{\xi}_{\perp} \cdot \nabla P = 0$, and the terms arising from the field compression and fluid compression in the energy integral vanish. This corresponds to the most dangerous condition for the onset of the instability, in which stabilizing effects were reduced to a minimum, leaving only the unavoidable bending of the field

lines. Once the instability starts to grow, the subsequent motion of the field lines, due to the finite parallel wavelength of the perturbation, introduces longitudinal oscillations and excites sound waves, in addition to shear-Alfvén waves, bringing the effect of the other stabilizing terms that our minimization process had suppressed at neutral equilibrium. In other words, finite values of W tend to slow down the growth of the mode.

To obtain a simple scaling law for the critical conditions of equilibrium, we note that $K_p \sim -(k_\perp/B)(dP/dr)$, and $K_T \sim 2(k_\perp B/R)$, where $dP/dr \sim -(P/r_p)$ measures the pressure gradient along the radial coordinate r, with a typical scale length r_p. The balance between the Shear-Alfvén term and the curvature term in the ballooning equation then gives:

$$k_{\parallel}^2 \sim -\frac{2}{B^2 R}\frac{dP}{dr} \qquad (2\text{-}97)$$

and taking $k_{\parallel} = 1/L \sim 1/Rq$, where L is the connection length, we obtain that marginal conditions are reached when

$$G \equiv -\frac{2Rq^2(dP/dr)}{B^2} \sim 1 \qquad (2\text{-}98)$$

or $\beta_{crit} \sim r_p/Rq^2$. Numerical studies[38] show that the increase of the critical value of beta with the inverse aspect ratio follows indeed an approximate linear relation. The dimensionless pressure-gradient dependent parameter on the left-hand side of Eq. (2-98) — that we shall call G — is an important

quantity in the theory of ballooning modes and appears repeatedly in the formulation of stability criteria.

It is useful also to examine how finite values of W affect the growth rates of unstable modes. We consider two cases. In the first, we assume that the equilibrium conditions are highly unstable, and that the growth of the mode is large, in the sense that $-\omega^2 \sim k \ V_A^2 >> k^2 V_s^2$. Then, in Eq. (2-90b), the initial term can be dropped, and W is approximated by:

$$W \sim - K_T \frac{(BX)}{B^2} \left(\frac{1}{\gamma_c P} + \frac{1}{B^2}\right)^{-1} \qquad (2\text{-}99)$$

Inserting this in the first equation, Eq. (2-90a) the term that couples the two equations is subtracted from the curvature-pressure gradient term, and we can see that the instability is now effectively driven by a term proportional to

$$G \left(1 - \frac{(2\gamma_c P)/R}{dP/dr}\right) \sim G \left(1 - 2\gamma_c \frac{r_p}{R}\right) \qquad (2\text{-}100)$$

where we have assumed, for simplicity, that $\beta \sim \gamma_c P/B^2 << 1$. The net effect of the compressibility, in this case, is to reduce the pressure gradient, thus an evaluation of the growth rate squared that neglects the coupling between the two mode equations will be in error by a factor of the order of Gr_p/R.

For slightly unstable equilibria, the stabilizing effect of W appears in a different way. If we assume that the growth rates are small, i.e., $-\omega^2 << k_{\|}^2 V_s^2$, the second term on the left hand side of Eq. (2-90b) becomes negligible and we have

$$W \sim K_T \left(\frac{BX}{B^2}\right) \frac{\omega^2 \rho_m}{k^2} , \qquad (2\text{-}101)$$

replacing the differential operator $\vec{B} \cdot \nabla$ by $B\, k_{\parallel}$.

Substituting this estimate for W in Eq. (2-90a), we see that the coupling term now adds to the first term on the left hand side of this equation. Then, the stabilization introduced by W appears as an enhanced inertia of the fluid, rather than as a diminished pressure gradient. Note that compressibility effects, as represented by terms involving $\gamma_c P$, were eliminated from the mode equation by our ordering of the growth-rates, and that the role of W here is only to add the parallel displacement to the transverse motion of the fluid. The slowing down of the growth of the instability by this effective parallel inertia is measured by the ratio of the coupling term to the (transverse) inertial term in the ballooning equation:

$$\frac{K_T\, W/B^2}{\rho_m \omega^2 |\nabla\alpha|^2 (BX/B^2)} \sim \frac{(K_T^2/B^2)\rho_m(\omega^2/k_{\parallel}^2)}{\rho_m \omega^2 k_{\perp}^2} \sim \frac{4}{R^2 k_{\parallel}^2} \sim 4q^2 , \qquad (2\text{-}102)$$

showing that the fluid looks "heavier" by a factor $1 + O(q^2)$.

To conclude this discussion, we remind the reader that, at the beginning of this section, we had stated that the term in the energy functional that drives the kink mode is negligible in the limit of high-toroidal number modes. That this is so, it is apparent from our final equations, which contain, as source

of instabilities, only the pressure gradient-curvature term. We can also verify our previous assertion by a direct evaluation of the kink term. Using Eq. (2-79) for $\vec{B}_1$, we have

$$\frac{J_{\parallel}}{B} (\vec{B} \times \vec{B}_1) \cdot \vec{\xi} = \frac{J_{\parallel}}{B} \vec{B} \cdot \nabla(BX) \nabla S \cdot \hat{\vec{\xi}}_{\perp} \qquad (2\text{-}103)$$

Since, by our ordering, $\nabla S \ \vec{\xi}_{\perp}$ remains of order unity and $BX = \vec{B} \cdot (\vec{\xi}_{\perp} \times \nabla S)/|\nabla S|^2 \sim O(1/N^2)$, the kink term is less than the others by 1/N, and becomes vanishingly small as N tends to infinity.

In subsequent chapters, Eqs. (2-90a) and (2-90b) will find a number of applications, as the formulation of stability criteria, the determination of the growth-rates of unstable modes, and the study of the propagation of stable disturbances, under specific equilibrium conditions.

The Boundary Conditions

A thorough and clear discussion of the boundary conditions to be applied to the mode equations and of the asymptotic behavior of the eigensolutions is given in Ref. (17). In this section we summarize the main results, omitting the details of the derivations and the delicate arguments that are involved. Many of these results will be recovered later, when we will solve the mode equations for specific equilibrium conditions, and the general statements that follow will appear self-evident.

The most interesting case corresponds to the condition $\omega^2 = 0$. Performing an asymptotic analysis that makes use of two-scales, Connor, Hastie and Taylor showed that, for $|x| \to \infty$ the solutions behave as

$$T \sim \frac{1}{\ell^{2\gamma}} \qquad (2\text{-}105)$$

where ℓ is a variable defined as

$$\ell = \int^{\chi} \frac{\partial q_\ell}{\partial \Psi} dx \quad , \qquad (2\text{-}106)$$

depending both on the transformed variable χ and the shear.

The exponent γ is given as the roots of a second degree equation with coefficients specified in terms of field line averages of the equilibrium quantities. The two values of γ are

$$\gamma_{1,2} = \frac{1}{4} \pm \frac{1}{2} \sqrt{\frac{1}{4} - D} \quad , \qquad (2\text{-}107)$$

where the quantity D is the same which appears in the Mercier stability criterion when this is expressed in the form $1/4 - D > 0$.

We see that, for $D > 1/4$, the two roots are complex and the mode equation admits two solutions that are oscillatory for large χ. To show that the system in this case is indeed unstable and recover the Mercier criterion, Connor, Hastie and Taylor invoke a general theorem due to Newcomb[39], which can be stated concisely as follows. If a solution of the Euler equation of a variational form δW vanishes at two points x_1 and x_2, then a function can always be constructed such that $f(x_1) = f(x_2) = 0$ and make the potential energy variation δW negative. Oscillatory solutions, therefore, imply necessarily the existence of instabilities.

Rewriting Eq. (2-105) as

$$T \sim \frac{1}{\sqrt{\ell}} \left[\cos\left(\sqrt{D - \frac{1}{4}}\, \ell n\, \ell\right) \pm i \sin\left(\sqrt{D - \frac{1}{4}}\, \ell n\, \ell\right)\right] \quad (2\text{-}108)$$

we may see that, in the transformed space of the variable, the solutions oscillate infinitely rapidly as ℓ tends to infinity and are asymptotically singular. In the physical space, however, they give rise to modes that are in general well behaved, except for a particular set of surfaces. When a function with an asymptotic behavior like the one in Eq. (2-108) is inserted in the ballooning infinite series, given by Eq. (2-43), the exponential kernel $e^{i(S-n)y}$ for $S \neq n$ guarantees the convergence of the Fourier integrals. At the surfaces specified by $S = n$ ($n = 0, \pm 1, \pm 2, \ldots$), however, the singular character of the solutions manifests as divergent integrals. Thus the radial profile of the mode is dominated by isolated singularities localized around the rational surfaces, where they take the form of increasingly fast oscillations modulated by an unbounded growth of the mode amplitude. This structure is not surprising, given the characteristics of the instabilities covered by the Mercier criterion. As we have seen in another section of this chapter, modes highly peaked around the rational surfaces are associated with a broad distribution in the poloidal angle, another typical feature of the so-called flutes. From this discussion, it also becomes clear that, by carrying out the asymptotic analysis ($\ell \to \infty$), we are effectively testing the behavior of the system to short wavelength oscillations ($k_\perp \to \infty$).

When $D < 1/4$, the exponents in Eq. (2-105) are real and unequal. We wil find, in subsequent chapters, that one of the solutions decays asymptotically and is acceptable, while the other diverges asymptotically and must be rejected. The physically acceptable solution gives rise to well behaved ballooning modes in the physical space that are radially extended and localized in the angular variable, distinguishing them from the pure flutes.

In the unstable case ($\omega^2 < 0$), the asymptotic behavior of the solutions is dominantly exponential, and we retain only the decaying one. Because of the fast decay of the eigensolution in the transformed space of the variable, growing modes are more localized in the poloidal angle than the ones that are marginally stable. Since the variable ℓ is proportional to the shear, we may see that the angular definition of the mode becomes sharper with the increase of shear.

The case $\omega^2 > 0$ gives again oscillating solutions at large ℓ but with a uniform wavelength, and they are both acceptable. Singularities appear in the physical space that are related to the structure of the continuum, and will be discussed in detail in Chapter V.

The Global Eigenvalue

In a previous section, we called attention to the fact that the lowest order equations in an expansion in powers of 1/N describe the mode structure along the lines of force, and that the oscillations on each flux coordinate surface are decoupled.

These equations, therefore, contain no information about the radial structure of the mode. This simplifies considerably the problem of the stability analysis, which is then reduced to the solution of a single ordinary differential equation in the poloidal variable, whose coefficient functions depend only parametrically on the radial coordinate ψ. In more general terms, by solving the system of two ordinary differential equations, for any specified equilibrium profile, we obtain a local eigenvalue for each flux surface, $\omega_\ell^2(\psi)$. On physical grounds, however, we expect that a global normal mode exists, so that the instability grows at the same rate over the bulk of the unstable flux surfaces, ω^2 = constant. Then, the theory developed until now, with all its advantages, is still incomplete, in the sense that it does not determine the radial structure of the mode and cannot provide the relation between the local eigenvalue $\omega_\ell^2(\psi)$ and the global eigenvalue ω^2 for a given value of N.

These two problems, which are intimately related, have received two different approaches. The original one, which was given by Taylor and coworkers, relies on a higher order expansion in powers of 1/N of the minimizing equations of the energy functional, and is expounded in detail in Ref. (17). We shall give here just a summary account.

The eikonal of the perturbation is represented as $\alpha = N(\phi - \int_{\chi_o}^{\chi} q_\ell(\psi,\chi')d\chi')$, where χ_o, the "origin" of the quasi-mode, is a function of the flux-coordinate ψ. To obtain the explicit dependence of χ_o on ψ, and the equation governing the radial

structure of the mode, two scales are introduced along the direction normal to the flux surfaces, one of them given by the scale of variation of the equilibrium quantities, and another, faster, as $x = N^{1/2} \Psi$, in between the equilibrium and the eikonal scales. The radial dependence of the mode on the slow scale is given by the parametric dependence on Ψ as obtained from the lowest order equations, but we introduce further a "modulation", that describes the variation of the amplitude on the intermediate scale x, and will complete the characterization of the mode. That is, we write $\xi = A(x)\, T(\Psi, \chi_o, \chi) e^{i\alpha}$. With this, two additional equations can be derived by an appropriate expansion procedure in powers of $N^{-1/2}$, that will provide the information missing in the lowest-order theory regarding $\chi_o(\Psi)$ and $A(x)$.

We have seen in the previous section, that, in the case of growing modes, one of the two solutions of the mode equations is acceptable and the other is not. The equation of order $N^{-1/2}$ that comes next in the hierarchy of the expansions, then shows that, if the undesirable solution is indeed to be eliminated, the origin of the quasi-mode is unambiguously determined. Specifically, an integrability condition on T demands that, on each magnetic surface, χ_o has to be located at an extrenum of the local eigenvalue:

$$\frac{\partial^2 \omega_I}{\partial \chi_o} (\Psi, \chi_o) = 0 \qquad (2\text{-}109)$$

The next order equation, of order N^{-1}, under a similar requirement of integrability of the solution, fixes the radial function A(x), at the same time that gives the global eigenvalue in terms of the local eigenvalue evaluated at the most unstable surface. Under certain circumstances, that we shall specify shortly, the equation for A(x) has the same form as the equation for a quantum-mechanical harmonic oscillation, and the solution which corresponds to the highest growth rate is a Gaussian function centered about the flux coordinate $x_o = N^{1/2} \psi_o$ where $\partial \omega_\ell^2 / \partial \psi = 0$. The eigenvalue condition, in this case, shows that the global eigenvalue ω^2 differs from the local one $\omega_\ell^2(\psi_o)$ at the surface ψ_o by a factor inversely proportional to N.

From this analysis, the radial structure of the mode can be pictured as fast oscillations, with a scale of variation of order 1/N given by the separation of the mode rational surfaces, modulated by a broad profile, with a width of order $1/\sqrt{N}$.

We give now a derivation of the formula for the global eigenvalue using the second approach that we mentioned. This one has in its favor a greater simplicity and permits us to find the global eigenvalue with no further information than the one contained in the lowest order theory. It is based on the concept of the phase-integral, and is therefore, a natural unfolding of the asymptotic theory of ballooning modes (large N) and the eikonal representation.

This method has been extensively used by the Princeton group in the investigation of the N-dependence of ballooning instabilities[18,40,41]. A more general formulation, that

extends its use to non-axisymmetric systems, is given in Ref. 18. Here, rather than aiming at a rigorous discussion, we shall illustrate its use by deriving the "1/N correction formula" for the growth-rate ω^2, under the same assumptions made by Connor, Hastie and Taylor.[17]

The most general form of writing the eikonal, that preserves the property that $\vec{B} \cdot \nabla\alpha = 0$, is

$$\alpha = N \left[\phi - \int_0^\chi q_\ell(\psi,\chi')d\chi' + \hat{\alpha}(\psi)\right] \qquad (2\text{-}110)$$

The function $\hat{\alpha}$, that depends on the flux coordinate only plays here a role analogous to the "origin" of the quasi-mode, in the formulation described previously. Note that $\hat{\alpha}$, as much as the piece that gives the pitch of the mode, is multiplied by N, and enters the lowest-order equations for the perturbations through its gradient:

$$\nabla\alpha = N[\nabla\phi - q_\ell(\psi,\chi)\nabla\chi - \nabla\psi \int_0^\chi \frac{\partial q_\ell}{\partial\psi}(\psi,\chi')d\chi' + \hat{\alpha}_\psi \nabla\psi], \qquad (2\text{-}111)$$

where $\hat{\alpha}_\psi \equiv d\hat{\alpha}/d\psi$.

Treating the mode equations as an eigenvalue problem, we obtain in general $\omega^2 = \omega^2(\psi, \hat{\alpha}_\psi)$. For a fixed value of ω^2, this dispersion relation can be represented by a curve in the $(\psi, \hat{\alpha}_\psi)$ plane, that specifies the functional dependence of $\hat{\alpha}_\psi$ on ψ. Notice that, for configurations with up-down symmetry (id est, invariant under a transformation $\chi \to -\chi$), these contours of

extends its use to non-axisymmetric systems, is given in Ref. 18. Here, rather than aiming at a rigorous discussion, we shall illustrate its use by deriving the "1/N correction formula" for the growth-rate ω^2, under the same assumptions made by Connor, Hastie and Taylor.[17]

The most general form of writing the eikonal, that preserves the property that $\vec{B} \cdot \nabla\alpha = 0$, is

$$\alpha = N \left[\phi - \int_0^\chi q_\ell(\psi,\chi')d\chi' + \hat{\alpha}(\psi)\right] \qquad (2\text{-}110)$$

The function $\hat{\alpha}$, that depends on the flux coordinate only plays here a role analogous to the "origin" of the quasi-mode, in the formulation described previously. Note that $\hat{\alpha}$, as much as the piece that gives the pitch of the mode, is multiplied by N, and enters the lowest-order equations for the perturbations through its gradient:

$$\nabla\alpha = N\left[\nabla\phi - q_\ell(\psi,\chi)\nabla\chi - \nabla\psi \int_0^\chi \frac{\partial q_\ell}{\partial\psi}(\psi,\chi')d\chi' + \hat{\alpha}_\psi \nabla\psi\right], \qquad (2\text{-}111)$$

where $\hat{\alpha}_\psi \equiv d\hat{\alpha}/d\psi$.

Treating the mode equations as an eigenvalue problem, we obtain in general $\omega^2 = \omega^2(\psi, \hat{\alpha}_\psi)$. For a fixed value of ω^2, this dispersion relation can be represented by a curve in the $(\psi, \hat{\alpha}_\psi)$ plane, that specifies the functional dependence of $\hat{\alpha}_\psi$ on ψ. Notice that, for configurations with up-down symmetry (id est, invariant under a transformation $\chi \to -\chi$), these contours of

constant ω^2 are symmetric with respect to the axis $\hat{\alpha}_\psi = 0$, or, in other words, ω^2 is an even function of $\hat{\alpha}_\psi$. An example of such possible contours is given in Fig. 2.1. The curve corresonds to $\omega^2 = 0$, as it intercepts the axis $\hat{\alpha}_\psi = 0$, determines the two marginally stable surfaces Ψ_1 and Ψ_2, while the curve for $\omega^2 = \omega^2_{min}$ degenerates into a point that locates the position of the most unstable surface, Ψ_o, somewhere in between Ψ_1 and Ψ_2.

The first step to construct $\hat{\alpha}_\psi$ is to impose the condition that the local eigenvalue ω^2_ℓ is a constant, independent of Ψ and $\hat{\alpha}_\psi$. If, in general, we describe a curve in the "phase space" $(\Psi, \hat{\alpha}_\psi)$ as

$$\Psi = \Psi(\tau) \tag{2-112a}$$

$$\hat{\alpha}_\psi = \hat{\alpha}_\psi(\tau) \tag{2-112b}$$

then the trajectories along which ω^2_ℓ remains constant are defined by the equations[42,27]:

$$\frac{d\hat{\alpha}_\psi}{d\tau} = -\frac{\partial \omega_\ell}{\partial \Psi} \tag{2-113a}$$

$$\frac{d\psi}{d\tau} = \frac{\partial \omega^2_\ell}{\partial \alpha_\psi} \tag{2-113b}$$

since this makes

$$\frac{d\omega_\ell^2}{d\tau} = \frac{\partial\omega_\ell^2}{\partial\Psi}\frac{d\Psi}{d\tau} + \frac{\partial\omega_\ell^2}{\partial\hat{\alpha}_\psi}\frac{d\hat{\alpha}_\psi}{d\tau} \qquad (2\text{-}114)$$

vanish. The parameter τ has no direct significance.

To make a specific use of these equations, let us expand ω_P^2 in Taylor series about the point P in Figure 2.1, where $\Psi = \Psi_o$, $\hat{\alpha}_\psi = 0$. Since it defines a local minimum of ω_ℓ^2, the first order derivatives are zero:

$$\left(\frac{\partial\omega_\ell^2}{\partial\Psi}\right)_P = 0 \qquad (2\text{-}115a)$$

$$\left(\frac{\partial\omega_\ell^2}{\partial\hat{\alpha}_\psi}\right)_P = 0 \qquad (2\text{-}115b)$$

and, up to second order powers, the expansion is:

$$\omega_\ell^2 = \omega_{min}^2 + \frac{1}{2}\left(\frac{\partial^2\omega_\ell^2}{\partial\Psi^2}\right)_P(\Psi - \Psi_o)^2 + \frac{1}{2}\left(\frac{\partial^2\omega_\ell^2}{\partial\hat{\alpha}_\psi^2}\right)_P\hat{\alpha}_\psi^2 \qquad (2\text{-}116)$$

where $(\partial^2\omega_\ell^2/\partial\Psi^2)_P$ and $(\partial^2\omega_\ell^2/\partial\hat{\alpha}_\psi^2)_P$ are positive quantities.

The trajectories of constant ω_ℓ are given by:

$$\frac{d\hat{\alpha}_\psi}{d\tau} = -\left(\frac{\partial^2\omega_\ell^2}{d\Psi^2}\right)_P(\Psi - \Psi_o) \qquad (2\text{-}117a)$$

$$\frac{d\Psi}{d\tau} = \left(\frac{\partial^2 \omega_\ell^2}{\partial \hat{\alpha}_\psi^2}\right)_P \alpha_\psi \qquad (2\text{-}117b)$$

Taking the derivative of the first equation with respect to t, and using the second equation to eliminate $d\Psi/d\tau$, we obtain:

$$\frac{d^2 \hat{\alpha}_\psi}{d\tau^2} = -\nu^2 \hat{\alpha}_\psi \qquad (2\text{-}118)$$

where

$$\nu^2 = \left(\frac{\partial^2 \omega_\ell^2}{\partial \Psi^2}\right)_P \left(\frac{\partial^2 \omega_\ell^2}{\partial \hat{\alpha}_\psi^2}\right)_P \qquad (2\text{-}119)$$

This equation is solved by

$$\hat{\alpha}_\psi = C \cos \nu(\tau - \tau_o) \qquad (2\text{-}120)$$

and the solution for Ψ, obtained from Eq. (2-117b), is

$$\Psi - \Psi_o = C \sqrt{\frac{(\partial^2 \omega_\ell^2 / \partial \hat{\alpha}_\psi^2)_P}{(\partial^2 \omega^2 / \partial \Psi^2)_P}} \; \text{sinc}\, \nu(\tau - \tau_o) \qquad (2\text{-}121)$$

The parameter τ_o, that defines some "starting point" on the trajectory, can be arbitrarily chosen; to simplify matters, we may take it to be zero. By changing the integration constant C, we generate a family of contours in the $(\Psi, \hat{\alpha}_\psi)$ plen, each of them corresponding to a different value of ω_ℓ^2. Substituting

Eqs. (2-120) and (2-121) into the expansion for ω_ℓ^2, Eq. (2-116), we can obtain an expression for C in terms of the local eigenvalue:

$$C = \sqrt{\frac{2(\omega_\ell^2 - \omega_{min}^2)}{(\partial^2\omega^2/\partial\hat{\alpha}_\psi^2)_P}} \qquad (2\text{-}122)$$

Eliminating the auxiliary variable τ from Eqs. (2-120) and (2-121), the equation for the trajectories reduces to the form:

$$\hat{\alpha}_\psi^2 + \frac{\left(\frac{\partial^2\omega_\ell^2}{\partial\Psi^2}\right)_P}{\left(\frac{\partial^2\omega_\ell^2}{\partial\hat{\alpha}_\psi^2}\right)_P}(\Psi - \Psi_o)^2 = \frac{2(\omega_\ell^2 - \omega_{min}^2)}{(\partial^2\omega_\ell^2/\partial\hat{\alpha}_\psi^2)_P} \qquad (2\text{-}123)$$

which describes an ellipse in the $(\Psi, \hat{\alpha}_\psi)$ plane, as represented in Fig. 2.1.

The next task is to find the value of ω_ℓ^2 that makes it a true eigenvalue of the global problem. In the high-N limit, this condition can be approximated by the familiar "quantization-rule" of the phase-integral:

$$N \oint \hat{\alpha}_\psi \, d\Psi = 2\pi\,(n + \tfrac{1}{2}) \qquad (2\text{-}124)$$

Figure 2.1: Contours of ω_ℓ^2 = constant in the Phase Plane (Ψ, $\hat{\alpha}_\Psi$).

The outermost contour, corresponding to $\omega_\ell^2 = 0$, intercepts the axis $\hat{\alpha}_\Psi = 0$ at the two marginally stable surfaces Ψ_1 and Ψ_2. The most unstable surface is Ψ_o. The dashed-line contour is similar to the ones reported in Ref. (41), while the elliptic contour results from a Taylor expansion of ω_ℓ^2 in the vicinity of Ψ_o.

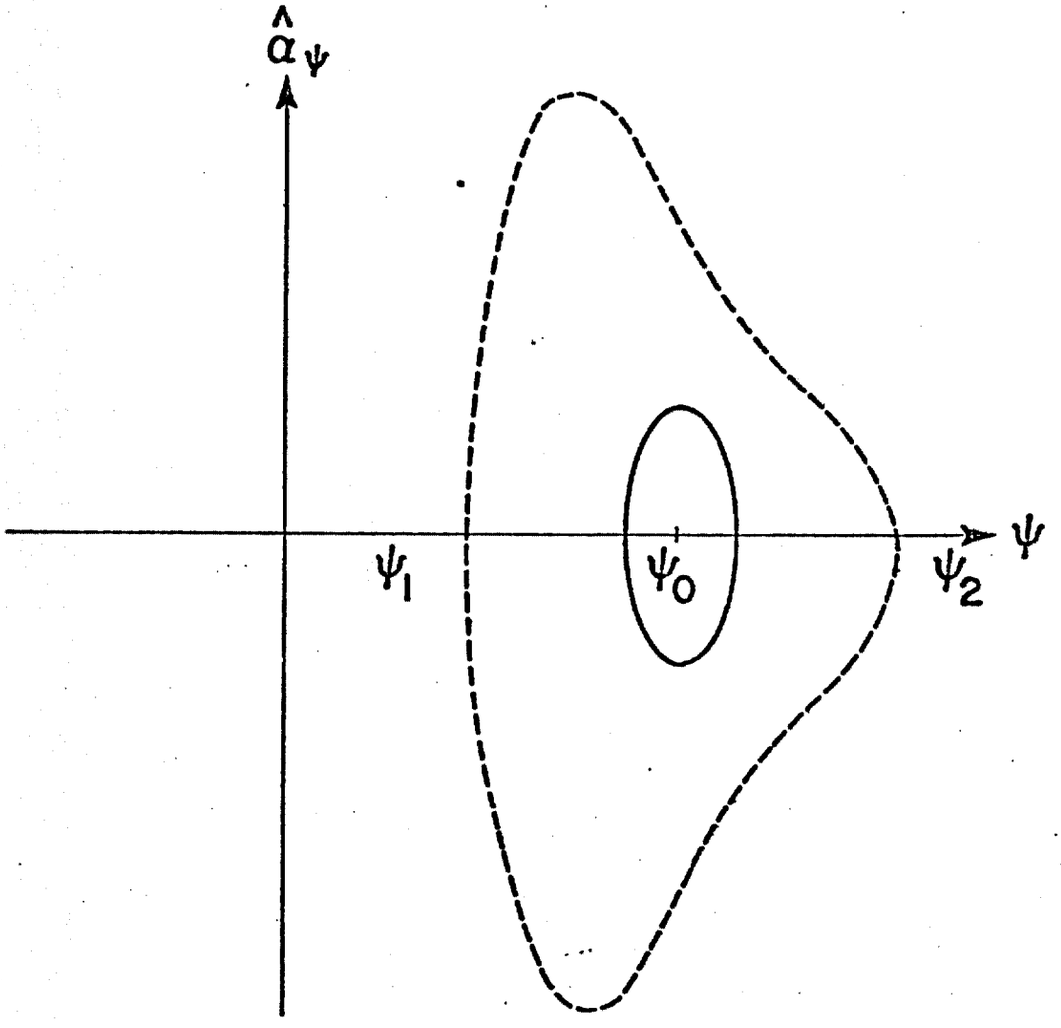

Figure 2.1: Contours of ω^2 = constant in the Phase Plane $(\psi, \hat{\alpha}_\psi)$.

where n = 0, 1, 2, is a non-negative integer, and the path of integration is a closed contour in the $(\psi, \hat{\alpha}_\psi)$ plane. As it is well known from the WKB theory[43], this formula results from the asymptotic matching of two one-turning point solutions. For an overlap region to exist, and make possible the matching, the two turning points of $\hat{\alpha}_\psi$, which define the critically stable flux surfaces (for a given value of N) must be well separated. According to Ref. (41), the validity of the WKB approximation requires the band of unstable surfaces $\Delta\psi_{unst}$ to be much greater than $\sim\psi_o/N^{1/2}$. In addition, we should require the integer n to be large, at least of the same order of N. There are many cases, however, that the quantization formula still gives good accuracy for low numbers, as for a parabolic potential. We assume, then, that this restriction can be relaxed and that Eq. (2-124) remains valid for n = 0, which corresponds to the mode of highest growth rate.

In the approximation of elliptic contours, the phase integral over a cycle can be evaluated to be:

$$N \int_{\nu\tau=-\pi}^{\nu\tau=+\pi} \hat{\alpha}_\psi \frac{d\psi}{d\tau}\, d\tau = \frac{2\pi N}{\nu}\left(\omega^2 - \omega_{min}^2\right), \qquad (2\text{-}125)$$

using Eqs. (2-117b), (2-120) and (2-122). The lowest eigenvalue (n=0) is given by:

$$-\omega^2 = -\omega_{min}^2 - \frac{1}{2N}\sqrt{\left(\frac{\partial^2\omega_\ell^2}{\partial\psi^2}\right)_P \left(\frac{\partial^2\omega_\ell^2}{\partial\hat{\alpha}_c^2}\right)_P} \qquad (2\text{-}126)$$

This is the "1/N-correction formula", originally presented in Ref. (17). Note that the correction decreases the growth rate, and that the most unstable modes occur for $N \to \infty$. Viewed in another way, if a region in the plasma is found to be locally unstable for some value of N, then it remains unstable for all values of N greater than this. Conversely, there is a minimum value N_{min} of the toroidal number, below which the most unstable flux surface in the configuration becomes stable, and no instability is found over all the plasma volume. This lower bound on N is determined, in general, by[41]

$$N_{min} = \frac{\pi}{\oint_{\omega_\ell^2=0} \hat{\alpha}_\psi \, d\psi} \tag{2-127}$$

where the integral represents the area enclosed by the outermost contour in the plane $(\psi, \hat{\alpha}_\psi)$, corresponding to $\omega_\ell^2 = 0$, and covers, therefore, the domain of all surfaces ψ that can become unstable, as N ranges from N_{min} to ∞.

If, for all values of ω_ℓ^2 comprised between ω_{min}^2 and 0, the trajectories of constant ω_ℓ^2 can be well approximated by ellipses, then, putting $\omega^2 = 0$ in Eq. (2-126), we obtain

$$N_{min} = \frac{1}{2|\omega_{min}^2|} \sqrt{\left(\frac{\partial^2 \omega_\ell^2}{\partial \psi^2}\right)_P \left(\frac{\partial^2 \omega_\ell^2}{\partial \hat{\alpha}_\psi^2}\right)_P} \tag{2-128}$$

The boundaries of the instability region (the least unstable flux surfaces) in this model, are given by:

$$\Psi_{1,2} = \Psi_o \pm \frac{2|\omega^2_{min}|}{(\partial^2\omega^2_\ell/\partial\Psi^2)_P} \qquad (2\text{-}129)$$

In practice, the assumption of elliptic contours is not really well verified. Numerical solutions for the dispersion relation $\omega^2_\ell = \omega^2_\ell(\Psi, \hat{\alpha}_\psi)$ sequences of equilibria generated numerically, show considerable distortion of these trajectories, that become more pronounced as the plasma average beta increases. In Ref. (41), where these studies are reported, for an equilibrium with beta as high as 10%, the numerical evaluation of the integral

$$\oint_{\omega^2_\ell=0} \hat{\alpha}_\psi \, d\Psi \qquad *$$

gives $N_{min} \sim 18$, while Eq. (2-128) gives $N_{min} \sim 26$. This discrepancy (~30%), however, will look more acceptable if we

---

*Not quite this one, in fact. The Princeton group uses a somewhat different formulation, in which the "radial" coordinate is the inverse rotational transform q, rather than Ψ. The other difference is the use of Hamada coordinates instead of the orthogonal flux coordinates that we have been using.

remember that this is a particularly unfavorable case for comparison. Anyway, there is little gain in the use of the 1/N formula in concrete computations of N_{min}, since the coefficients $(\partial^2\omega_\ell^2/\partial\psi^2)_P$ and $(\partial^2\omega_\ell^2/\partial\hat{\alpha}_\psi^2)_P$ have always to be determined numerically. The merit of the theory based on an expansion of ω_ℓ^2, as in Eq. (2-116), is to illustrate the use of the WKB formalism by means of a simple example, and to help us to understand the qualitative aspects of the dependency of the ballooning instabilities on the toroidal mode number.

Appendix 2A

Proof that $\vec{B} \cdot \nabla \left[\frac{\nabla\alpha \cdot (\nabla P \times \vec{B})}{B^2} \right] = 0$

Too prove this identity, we write the vector quantities explicitly in flux coordinates:

$$\vec{B} = B_\chi \vec{e}_\chi + B_\phi \vec{e}_\phi \tag{2A-1}$$

$$\nabla P = \frac{1}{h_\psi} \frac{dP}{d\psi} \vec{e}_\psi \tag{2A-2}$$

$$\nabla\alpha = -\frac{1}{h_\psi} \int^{\chi} \frac{\partial q_\ell}{\partial \psi} d\chi \, \vec{e}_\psi - \frac{1}{h_\chi} q_\ell \vec{e}_\chi + \frac{1}{h_\phi} \vec{e}_\phi \tag{2A-3}$$

Using the expressions (2-5) and (2-12) in Chapter II for h_ψ and q_ℓ, we obtain for the triple product:

$$\frac{\nabla\alpha \cdot (\nabla P \times \vec{B})}{B^2} = \frac{dP}{d\psi} \tag{2A-4}$$

which is a flux quantity. Then, its gradient is normal to the flux surface, and the projection on $\vec{B}$ is identically zero.

Appendix 2B

Derivation of the Expression for the Divergence of the Parallel Displacement

To lowest order, the terms related to fluid compression in Eq. (2-87) combine to produce:

$$\nabla \cdot \hat{\vec{\xi}} + i\,\hat{\vec{\xi}} \cdot \nabla\alpha = \nabla \cdot \left[\left(\frac{\nabla\alpha \times \vec{B}}{B^2}\right)(BX)\right] + \nabla \cdot \left[\left(\frac{\xi \cdot B}{B^2}\right)\vec{B}\right]$$

$$+ i\,|\nabla\alpha|^2\, Y \qquad (2B\text{-}1)$$

Taking the scalar product of Eq. (2-75) with $\vec{B}$, we obtain an expression for $\vec{B} \cdot \vec{B}_1$:

$$\vec{B} \cdot \vec{B}_1 = \vec{B} \cdot [\nabla\alpha \times \nabla(BX)] - i\,|\nabla\alpha|^2\, B^2\, Y, \qquad (2B\text{-}2)$$

which can be used to eliminate Y. If we also expand the first divergence on the right-hand side of Eq. (2B-1), that expression simplifies to:

$$\nabla \cdot \hat{\vec{\xi}} + i\,\hat{\vec{\xi}} \cdot \nabla\alpha = \nabla \cdot \left[\left(\frac{\vec{\xi} \cdot \vec{B}}{B^2}\right)\vec{B}\right] + (BX)\,\nabla \cdot \left(\frac{\nabla\alpha \times \vec{B}}{B^2}\right) - \frac{\vec{B} \cdot \vec{B}_1}{B^2} \qquad (2B\text{-}3)$$

Now,

$$\nabla \cdot \left(\frac{\nabla\alpha \times \vec{B}}{B^2}\right) = -\frac{\nabla\alpha \cdot (\nabla \times \vec{B})}{B^2} + (\nabla\alpha \times \vec{B}) \cdot \nabla\left(\frac{1}{B^2}\right) \qquad (2B\text{-}4)$$

and remembering that

$$(\nabla \times \vec{B})_{\perp} = \frac{\vec{B} \times \nabla P}{B^2} , \tag{2B-5}$$

we obtain:

$$\nabla \left(\frac{\nabla\alpha \times \vec{B}}{B^2}\right) = -\frac{1}{B^4} \nabla\alpha \left[\vec{B} \times \nabla(P + B^2)\right] . \tag{2B-6}$$

The other term that appears in Eq. (2-87) is

$$\hat{\vec{\xi}} \cdot \nabla P = (BX) \left(\frac{\nabla\alpha \times \vec{B}}{B^2}\right) \cdot \nabla P , \tag{2B-7}$$

neglecting higher order terms. If we substitute Eqs. (2B-3), (2B-6) and (2B-7) into Eq. (2-87) in Chapter II, we arrive at the following expression for $\vec{B} \cdot \vec{B}_1$:

$$\left(1 + \frac{\gamma_c P}{B^2}\right) \vec{B} \cdot \hat{B}_1 = -(BX) \frac{(\vec{B} \times \nabla\alpha) \cdot \nabla P}{B^2} + \gamma_c P \nabla \cdot \left[\left(\frac{\hat{\vec{\xi}} \cdot \vec{B}}{B^2}\right)\vec{B} -\right.$$

$$\left. - \frac{BX}{B^4} \nabla\alpha \cdot \left[\vec{B} \times \nabla(P + B^2)\right]\right] \tag{2B-8}$$

The equation for the divergence of the parallel displacement, Eq. (2-88), can then be immediately obtained from this result and the definition of W, given by Eq. (2-89).

Appendix 2C

Derivation of Eq. (2-93)

The identity:

$$\vec{B} \cdot \vec{B}_1 - \vec{\xi}_\perp \cdot \nabla P = - B^2(\nabla \cdot \vec{\xi}_\perp + 2\, \vec{\xi}_\perp \cdot \vec{\kappa}) \qquad (2C\text{-}1)$$

is frequently used in the methematics of MHD, and if we reproduce here the derivation, it is only to facilitate the work of the meticulous reader.

Expanding $\vec{B}_1$ as in Eq. (2-24), we have

$$\vec{B} \cdot \vec{B}_1 = \vec{B}\,(\vec{B} \cdot \nabla)\vec{\xi}_\perp - \vec{B} \cdot (\vec{\xi} \cdot \nabla)\vec{B} - B^2\, \nabla \cdot \vec{\xi}_\perp \qquad (2C\text{-}2)$$

Since $\vec{\xi}_\perp \cdot \vec{B} = 0$, the first term on the right can be rewritten $-\vec{\xi}_\perp \cdot (\vec{B} \cdot \nabla)\vec{B}$, or, remembering the expression for the curvature, as

$$\vec{B} \cdot (\vec{B} \cdot \nabla)\vec{\xi}_\perp = - \vec{\xi}_\perp \cdot \nabla\left(P + B^2/2\right) \qquad (2C\text{-}3)$$

With this result and also

$$\vec{B} \cdot (\vec{\xi}_\perp \cdot \nabla)\vec{B} = \vec{\xi}_\perp \cdot \nabla\, (B^2/2)\ , \qquad (2C\text{-}4)$$

Eq. (2-93) can be immediately obtained.

Chapter III

THE EQUILIBRIUM SOLUTION

This chapter is devoted to a derivation of a solution of the equilbirium equation and its subsequent use in the determination of the equilibrium quantities of interest for the analysis of the mode equations.

Within the framework of MHD theory, the driving terms of equilibrium, namely, the pressure $P(\Psi)$ and the poloidal current stream function $T(\Psi)$ are arbitrarily specified as functions of Ψ. The solution of the Grad-Shafranov equation then, under very general conditions, is uniquely determined by the boundary conditions applied to Ψ. It is well known, however, that, except for very particular choices of the equilibrium profiles, no closed form solutions can be obtained. The most extensively used of these exact analytic solutions is the so-called Solovev solution[44] which assumes that the source functions $dP/d\Psi$ and $T(dT/d\Psi)$ are constant over the plasma volume. This equilibrium model has been used by more than one author in the investigation of the stability of small aspect ratio tokamaks. When the source functions $dP/d\Psi$ and $T(dT/d\Psi)$ are linear in Ψ, the boundary-value problem is still amenable to an analytic treatment, and a solution can be obtained by an expansion procedure about the corresponding cylindrical configurations[45]. Derivation of the terms of the expansion, however, rapidly increase in complexity, severely restricting its attractiveness for analysis in which high-order terms are

required. Clearly, if one chooses for the gradients of the pressure profile and poloidal current stream function a dependence on ψ that includes powers higher than one, the magnetic equation becomes non-linear, and a solution uniformaly valid over the plasma cross-section is no longer available. In this case, we have to content ourselves with an expansion that gives for the magnetic surfaces a mathematical description restricted to the vicinity of the magnetic axis.

The following method is due to Shafranov and Solovev[46], and permits us to reduce the partial differential equation to a set of ordinary differential equations in the poloidal-like variable, each of them corresponding to a different order in the expansion.

The toroidal plasma is assumed to have rotational symmetry around the major axis of the torus. The magnetic surfaces are nested tori, with only one magnetic axis, located at distance R_o from the major axis. On the plasma cross section, the distance from a point to the magnetic axis is denoted by r. The poloidal coordinate, indicated by the symbol θ, is taken to be the angle of rotation about the magnetic axis. The zero of θ lies on the equatorial plane passing through the magnetic axis. In this coordinate system, ilustrated in Fig. 3.1, the distance of a point to the major axis of the torus is given by

$$R = R_o + r \cos \theta \qquad (3\text{-}1)$$

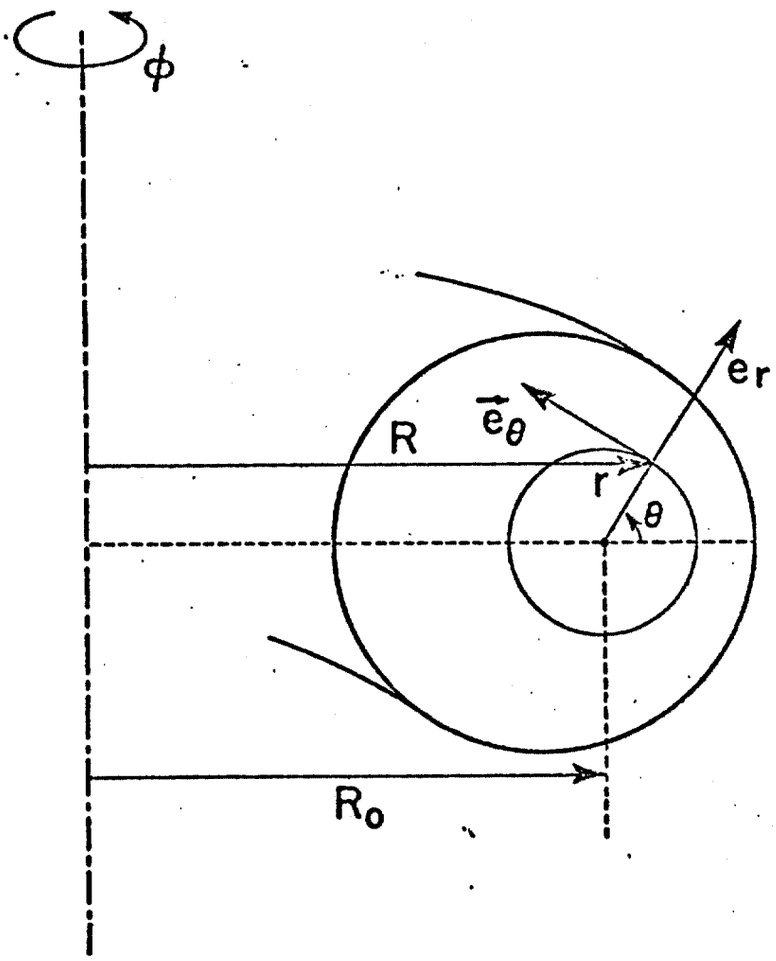

Figure 3.1: Coordinate System for an Axisymmetric Toroid.

The equilibrium equation can be written as:

$$\frac{\partial^2 \Psi}{\partial r^2} + \left(\frac{1}{r} - \frac{\cos\theta}{R}\right) \frac{\partial \Psi}{\partial r} + \frac{1}{rR} \sin\theta \frac{\partial \Psi}{\partial \theta} + \frac{1}{r^2} \frac{\partial^2 \Psi}{\partial \theta^2} =$$

$$- R^2 \frac{dP}{d\Psi} - \frac{1}{2} \frac{d}{d\Psi} T^2 \qquad (3\text{-}2)$$

The left hand side of this equation, which represents the explicit form of the Grad-Shafranov operator $\Delta^* \psi$ in the coordinate system, as discussed previously, is related to the toroidal current density J_T by

$$\Delta^* \psi = R J_T \qquad (3\text{-}3)$$

We normalize the quantities entering Eq. (3-2) as follows:

$$\Psi = \psi^* \psi \qquad (3\text{-}4a)$$

$$r = R_o x \qquad (3\text{-}4b)$$

$$P(\Psi) = \frac{B_o \psi^*}{R_o^2} p(\psi) \qquad (3\text{-}4c)$$

$$T^2(\Psi) = B_o \psi^* f^2(\psi) \qquad (3\text{-}4d)$$

where the normalization flux is defined as:

$$\psi^* = (R_o^3 / J_{To})/4 \qquad (3\text{-}5)$$

J_{To} is the toroidal current at the axis, and B_o is the toroidal magnetic field along the magnetic axis. With this, the equilibrium equation can be conveniently re-written in dimensionless form:

$$\frac{\partial^2\psi}{\partial x^2} + \frac{1}{x(1+x\cos\theta)}\left(\frac{\partial\psi}{\partial x} + \sin\theta\,\frac{\partial\psi}{\partial\theta}\right) + \frac{1}{x^2}\frac{\partial^2\psi}{\partial\theta^2} =$$

$$= -\frac{B_o R_o^2}{\psi^*}\left[(1 + x\cos\theta)^2\frac{dp}{d\psi} + \frac{1}{2}\frac{d}{d\psi}f^2\right] \qquad (3\text{-}6)$$

With regard to the source functions $dp/d\psi$ and $(1/2)(d/d\psi)f^2$, we assume only that they can be expanded as Taylor series in powers of ψ about the magnetic axis, which is defined by $\psi=0$. Thus we have:

$$-\frac{dp}{d\psi} = p_o + p_1\psi + p_2\psi^2 + \ldots. \qquad (3\text{-}7)$$

$$-\frac{1}{2}\frac{d}{d\psi}f^2 = f_o + f_1\psi + f_2\psi^2 + \ldots. \qquad (3\text{-}8)$$

where the coefficients p_o, p_1 ..., f_o, f_1, ... remain arbitrary.

Note that the toroidal current at the axis is

$$J_{To} = \frac{B_o}{R_o}(p_o + f_o) \qquad (3\text{-}9)$$

and the normalization flux is then

$$\psi^* = \frac{B_o R_o^2}{4}(p_o + f_o) \qquad (3\text{-}10)$$

We shall find it useful to define the local poloidal beta as the ratio

$$\beta_p = - \frac{2R^2(dP/d\psi)}{J_T R} \qquad (3\text{-}11)$$

which, at the magnetic axis, can be expressed as:

$$\beta_p = \frac{2p_o}{p_o + f_o} \qquad (3\text{-}12)$$

and we will verify shortly that it corresponds to the familiar idea of poloidal beta as the ratio of the plasma energy density to the poloidal field energy density.

We now proceed to derive a solution to Eq. (3-2). Following the method of Solovev and Shafranov, we represent the magnetic surfaces as a series of powers of the distance to the magnetic axis:

$$\psi = \psi_2(\theta)\, x^2 + \psi_3(\theta) x^3 + \psi_4(\theta)\, x^4 + \psi_5(\theta)\, x^5 + \ldots, \qquad (3\text{-}12)$$

where the coefficients ψ_2, ψ_3, ... are dimensionless functions depending only on the poloidal variable.

To simplify the expansion procedure, we first multiply Eq. (3-2) by $1 + x\cos\theta$, and, upon substitution of the expansions given by Eqs. (3-7), (3-8) and (3-12), we obtain to lowest order in x:

$$\psi_2'' + 4\psi_2 = 4 \qquad (3\text{-}13)$$

with primes denoting derivatives with respect to θ. The general solution of this second order differential equation is

$$\psi_2(\theta) = 1 + \lambda \cos 2\theta, \tag{3-14}$$

where λ is an arbitrary integration constant. Then, very close to the origin, the flux surfaces are described by

$$r(\psi,\theta) = \frac{R_o}{\sqrt{1 + \lambda \cos 2\theta}} \left(\frac{\psi}{\psi}\right)^{1/2} \tag{3-15}$$

which represents, for $|\lambda| < 1$, an ellipse centered at the magnetic axis.

The usual definition of the macroscopic poloidal beta is

$$\bar{\beta}_p = 2 \frac{\langle P \rangle - P(\psi_o)}{\langle B_p^2 \rangle} \tag{3-16}$$

where $P(\psi_o)$ is the pressure at any flux surface ψ_o, $\langle P \rangle$ means the surface average of the plasma pressure distribution over the cross-sectional area delimited by ψ_o.

$$\langle P \rangle = \frac{\int_s P \, dS}{\int_s dS} \tag{3-17}$$

and $\langle B_p^2 \rangle$ is similarly defined. In the Appendix 3A we derived an integral equlibrium relation that can be used to evaluate this

latter quantity. On a small area about the magnetic axis, both the toroidal current density and the distance to the major axis of the torus are approximately constant, and Eq. (3A-5) furnishes

$$\langle B_p^2 \rangle \approx \frac{J_{To}}{R_o} (\Psi_o - \langle \Psi \rangle) \tag{3-18}$$

In this limit, the flux surfaces are represented by Eq. (3-15), and the area element is

$$dS = \frac{R_o^2}{2\Psi^*} \frac{d\theta}{1 + \lambda \cos 2\theta} d\Psi \tag{3-19}$$

so that the above average can be calculated to be

$$\langle B_p^2 \rangle = \frac{J_{To} \Psi_o}{2R_o} \tag{3-20}$$

The pressure distribution can be approximated by a linear relation:

$$P = P_o + \left(\frac{dP}{d\Psi}\right)_o \Psi \tag{3-21}$$

where P_o is the value at the magnetic axis. Performing the area average, we obtain

$$\langle P \rangle = P_o + \left(\frac{dP}{d\Psi}\right)_o \frac{\Psi_o}{2} \tag{3-22}$$

and, upon substitution of the expressions for the averages, the quantity defined by Eq. (3-16) becomes:

$$\bar{\beta}_p = -2 \frac{(dP/d\psi)_o \, (\psi_o/2)}{(J_{To}/\psi_o)/2R_o} = 2 \left(\frac{p_o}{p_o + f_o}\right) \qquad (3\text{-}23)$$

which is the same as the "local poloidal beta" previously introduced.

The limiting value of the rotational transform as we approach the magnetic axis can be evaluated as

$$q_o = \frac{1}{2\pi} \left(\frac{d\phi}{d\psi}\right)_{axis} \qquad (3\text{-}24)$$

The toroidal field in this limit is constant and equal to B_o, so that the element of toroidal flux across a small strip encircling the axis is

$$d\phi = \int B_T \, dS = \frac{B_o R_o^2}{2\psi^*} \oint \frac{d\theta}{1 + \lambda \cos 2\theta} \, d\psi \,, \qquad (3\text{-}25)$$

Performing the integration along the poloidal contour, we obtain for q_o:

$$q_o = \frac{\nu R_o B_o}{2\psi^* \sqrt{1-\lambda^2}} = \frac{2B_o}{R_o J_{To}} \frac{1}{\sqrt{1-\lambda^2}} = \left(\frac{2}{p_o + f_o}\right) \frac{1}{\sqrt{1-\lambda^2}} \qquad (3\text{-}26a)$$

or

$$q_o = \frac{\beta_p}{p_o \sqrt{1-\lambda^2}} \qquad (3\text{-}26b)$$

Having established the meaning of the parameter β_p, we return now to the derivation of higher order terms of the expansion of ψ. To first order in x, we have:

$$\psi_3'' + 9\psi_3 + \psi_2'' \cos\theta + \psi_2' \sin\theta + 2\psi_2\cos\theta = \frac{R_o^2 B_o}{\psi^*}(3p_o+f_o)\cos\theta$$

$$= 4(1 + \beta_p)\cos\theta \qquad (3\text{-}27)$$

Substituting the solution for $\psi_2(\theta)$ as given by Eq. (3-14), we obtain the differential equation for ψ_3:

$$\psi_3'' + 9\psi_3 = 2(1 + 2\beta_p + \lambda)\cos\theta \qquad (3\text{-}28)$$

and the general solution is

$$\psi_3(\theta) = \frac{1}{4}(1 + 2\beta_p+\lambda)\cos\theta + \mu_3 \cos 3\theta. \qquad (3\text{-}29)$$

The term in $\cos 3\theta$, depending on the free integration constant μ_3, introduces a triangular deformation in the shape of the flux surfaces. The effect of the term proportional to $\cos\theta$ is to displace the geometric center of the flux surfaces inwards with respect to the magnetic axis. This displacement, known in the literature as the "Shafranov shift", has important implications on the stability of both interchange and ballooning modes. We note that, if the free shape factor λ is set equal to

zero, the shift of the flux surfaces is not accompanied by any distortion in the lowest order circular shape.

The balance between second order terms in x in the expanded equilibrium equation gives:

$$\psi_4'' + 16\,\psi_4 + (\psi_3'' + 6\psi_3)\cos\theta + \psi_3' \sin\theta =$$

$$= \frac{B_o R_o^2}{\psi^*} [\psi_2(p_1 + f_1) + \frac{3}{2} p_o (1 + \cos 2\theta) \qquad (3\text{-}30)$$

We introduce another parameter by

$$\alpha = \frac{B_o R_o^2}{4\psi^*} (p_1 + f_1) = \frac{p_1 + f_1}{p_o + f_o} \qquad (3\text{-}31)$$

and, upon substitution of the known solutions for $\psi_2(\theta)$ and $\psi_3(\theta)$, we obtain:

$$\psi_4'' + 16\psi_4 = \frac{1}{2} [4\beta_p + 8\alpha - (\lambda+1)]$$

$$+ [\frac{3}{2} \beta_p + 3\mu_3 - \frac{3}{4} (\lambda+1) + 4\alpha\lambda]\cos 2\theta \qquad (3\text{-}32)$$

The general solution of this equation is:

$$\psi_4(\theta) = \frac{\beta_p}{8} + \frac{\alpha}{4} - \frac{1}{32} (\lambda+1) + [\frac{\beta_p}{8} + \frac{\mu_3}{4} - \frac{1}{16} (\lambda+1) + \frac{\alpha\lambda}{3}]\cos 2\theta$$

$$+ \mu_4 \cos 4\theta \qquad (3\text{-}33)$$

where the quadrangularity μ_4 is another arbitrary constant.

Equating third order powers of x in the equilibrium equation, we obtain:

$$\psi_5'' + 25\,\psi_5 + (\psi_4'' + 12\,\psi_4)\cos\theta + \psi_4' \sin\theta =$$

$$= \frac{B_o R_o^2}{\psi^*} [(p_1+f_1)\,\psi_3 + (3p_1+f_1)\,\psi_2\cos\theta + p_o \cos^3\theta] \quad (3\text{-}34)$$

and, proceeding in a similar way to the previous steps, we find the solution to be:

$$\psi_5(\theta) = \frac{1}{24} [2\alpha + 2h(\lambda+2) - \frac{3}{8}]\beta_p + (2\alpha + \frac{9}{16})(\lambda+1) - \frac{3}{4}\,\mu_3 \cos\theta$$

$$+ \frac{1}{16} [\beta_p(-\frac{1}{8} + 2h\lambda) + \alpha(\frac{\lambda}{3} + 4\mu_3) + \frac{5}{16}(\lambda+1) - \frac{5}{4}\,\mu_3 + 4\mu_4]\cos 3\theta$$

$$+ \mu_5 \cos 5\theta \,. \quad (3\text{-}35)$$

The constant h is

$$h = \frac{p_1}{p_o} \quad (3\text{-}36)$$

and μ_5 is a pentagonality free shape factor.

The Equilibrium Quantities in the Neighborhood of the Axis

The equilibrium solution derived in the previous section contain all information that is required to calculate the equlibrium fields and the coefficient functions entering the mode equation, to the order necessary for the determination of the stability limits in the vicinity of the axis. The coordinate variable, adopting this representation, are the normalized radial distance x and the polar angle θ. For our

purposes however, it is convenient to express the equilibrium quantities in terms of the normalized flux ψ rather than x. The calculation will be facilitated if we start by inverting the series given by Eq. (3-12), obtaining for x the explicit representation[47]:

$$x = Z_1(\theta)\rho + Z_2(\theta)\rho^2 + Z_3(\theta)\rho^3 + Z_4(\theta)\rho^4 + ... \qquad (3\text{-}37)$$

where $\rho = \psi^{1/2}$. Substituting the above series in Eq. (3-12) and equating powers of ρ, the coefficients Z_1, Z_2, ..., can be determined as combinations of the angular functions ψ_2, ψ_3, ψ_4 and ψ_5. We present here the results for the simplest equilibrium, that will be the object of a detailed analysis, in which the shape factors λ, μ_3, μ_4 and μ_5 are set equal to zero. This choice, in particular, corresponds to flux surfaces that tend to circles in the vicinity of the axis and effects of boundary conditions are ignored. Then we have:

$$Z_1 = 1 \qquad (3\text{-}38a)$$

$$Z_2 = -\frac{1}{4}\left(\beta_p + \frac{1}{2}\right)\cos\theta \qquad (3\text{-}38b)$$

$$Z_3 = \frac{5}{64}\left(\beta_p^2 + \frac{\beta_p}{5} - \frac{8\alpha}{5} + \frac{9}{20}\right) + \frac{5}{64}\left(\beta_p^2 + \frac{1}{5}\beta_p + \frac{13}{20}\right)\cos 2\theta \qquad (3\text{-}38c)$$

$$Z_4 = -\frac{3}{32}\left[\beta_p^3 + \frac{5}{12}\beta_p + \frac{1}{2} - \frac{\alpha}{9}(14\beta_p + 5) + \frac{8}{9}h\beta_p\right]\cos\theta - \frac{1}{32}\left(\beta_p^3 + \frac{5}{6}\beta_p + \frac{13}{16}\right)\cos 3\theta \qquad (3\text{-}38d)$$

The poloidal current stream function, defined by Eq. (3-4d), can be obtained by integrating the expansion of f^2, as given by Eq. (3-8). The result is

$$R^2B_T^2 = R_o^2B_o^2 - B_o\psi^*(2f_o\,\psi + f_1\,\psi^2) \qquad (3\text{-}39)$$

where the integration constant was chosen as to reproduce the magnetic field at the axis. This expression can also be written as

$$\frac{R^2B_T^2}{R_o^2B_o^2} = 1 - \frac{2}{q_o^2}\left(1 - \frac{\beta_p}{2}\right)\rho^2 - \frac{1}{q_o^2}\left(\alpha + \frac{h\beta_p}{2}\right)\rho^4 \qquad (3\text{-}40)$$

upon convenient substitution of parameters, and furnishes:

$$\frac{RB_T}{R_oB_o} = 1 - \frac{1}{q_o^2}\left(1 - \frac{\beta_p}{2}\right)\rho^2 - \frac{1}{2q_o^4}\left[\left(1 - \frac{\beta_p}{2}\right) + q_o^2\left(\alpha + \frac{h\beta_p}{2}\right)\right]\rho^4 \qquad (3\text{-}41)$$

Expressing R as a power series in ρ, by means of Eqs. (3-1) and (3-37), we obtain for the toroidal field:

$$\frac{B_T}{B_o} = 1 - \rho\cos\theta + \rho^2\left[\frac{1}{16}(2\beta_p + 9)(1 + \cos2\theta) + \frac{1}{q_o^2}\left(\frac{\beta_p}{2} - 1\right)\right]$$

$$+ \rho^3\left\{ - \frac{1}{512}\left[4\beta_p\,(5\beta_p + 17)\,(3\cos\theta + \cos3\theta) + 173\cos3\theta\right.\right.$$

$$+ (511-64\alpha)\cos\theta] + \frac{1}{q_o^2}\left(1 - \frac{\beta_p}{2}\right)\cos\theta \Bigg\} \qquad (3\text{-}42)$$

To derive a representation for the poloidal field, we take the gradient of $r = r(\psi, \theta)$:

$$\nabla r = \left(\frac{\partial r}{\partial \psi}\right)_\theta \nabla\psi + \left(\frac{\partial r}{\partial \theta}\right)_\psi \nabla\theta \qquad (3\text{-}43)$$

which gives:

$$\nabla\psi = \frac{1}{(\partial r/\partial\psi)_\theta}\left[\hat{e}_r - \frac{1}{r}\left(\frac{\partial r}{\partial\theta}\right)_\psi \hat{e}_\theta\right] \qquad (3\text{-}44)$$

Then

$$RB_p = |\nabla\psi| = \frac{1}{(\partial r/\partial\psi)_\theta}\sqrt{1 + \frac{1}{r^2}\left(\frac{\partial r}{\partial\theta}\right)_\psi^2} \qquad (3\text{-}45)$$

or, in terms of normalized quantities,

$$\frac{RB_p}{(R\,B/q_o)} = \frac{\rho}{(\partial x/\partial\rho)_\theta}\sqrt{1 + \frac{1}{x^2}\left(\frac{\partial x}{\partial\theta}\right)_\rho^2} \qquad (3\text{-}46)$$

Introducing the expansion for x, Eq. (3-37), we obtain:

$$\frac{q_o B_p}{B} = \rho + \rho^2\left(\frac{\beta_p}{2} - \frac{3}{4}\right)\cos\theta - \frac{\rho^3}{128}\left[(16\cos 2\theta + 12)\beta_p^2 + \right.$$

$$\left. + (8\cos 2\theta + 4)\beta_p - 40\cos 2\theta - 48\alpha - 47\right] + \frac{\rho^4}{6144}$$

$$(312\cos 3\theta + 648\cos\theta)\beta_p^3 + (132\cos 3\theta + 156\cos\theta)\beta_p^2$$

$$+ \quad [90\cos 3\theta + (2048\,h - 1280\,\alpha - 330)\cos\theta]\beta_p$$

$$- \quad (1664\,\alpha + 3387)\cos\theta - 813\cos 3\theta \Big\} \tag{3-47}$$

The total magnetic field is

$$B = \sqrt{B_T^2 + B_p^2} \tag{3-48}$$

and can be evaluated by use of Eqs. (3-42) and (3-47).

We next find the expression for the Jacobian in the coordinate system (Ψ, θ, ϕ):

$$J = \frac{1}{|\nabla\Psi \cdot (\nabla\theta \times \nabla\phi)|} = rR\left(\frac{\partial r}{\partial \Psi}\right)_\theta , \tag{3-49}$$

using Eq. (3-44) for $\nabla\Psi$.

In terms of previously defined quantities, this can be rewritten as:

$$\hat{J} \equiv \frac{J}{2/J_{To}} = (1 + x\cos\theta)\frac{x}{\rho}\left(\frac{\partial x}{\partial \rho}\right)_\theta \tag{3-50}$$

where $\hat{J}$ is a normalized Jacobian, such that the volume element is $dV = \hat{J}\, R_o^3\, \rho d\rho d\theta d\phi$. Introducing the expanded solution, we have

$$\hat{J} = 1 - \rho\left(\frac{3}{4}\beta_p - \frac{5}{8}\right)\cos\theta + \frac{\rho^2}{32}\left[12\,\beta_p(\beta_p - 1)(1+\cos 2\theta)\right.$$

$$\left. - (3 + 16\alpha + \cos 2\theta)\right] - \frac{\rho^3}{12288}\Big\{\beta_p^2\,(2520\beta_p - 2940)(\cos 3\theta + 3\cos\theta)$$

$$+ \left[210\cos 3\theta + (5120h - 10880\alpha - 810)\cos\theta\right]\beta_p$$

$$- \left.(45\cos 3\theta - 3520\alpha\cos\theta + 1095\cos\theta)\right]\Big\} \qquad (3\text{-}51)$$

The degree of twist of the field lines is measured by the local quantity

$$q_\ell = \left(\frac{\partial\phi}{d\theta}\right)_{\text{along a field line}} \qquad (3\text{-}52)$$

and can be obtained from the equation of the field lines:

$$d\vec{\ell} \times \vec{B} = 0 \qquad (3\text{-}53)$$

In the coordinate system (r,θ,ϕ), the element of arc is

$$d\vec{\ell} = B_r\,\vec{e_r} + B_\theta\,\vec{e_\theta} + B_T\,\vec{e_\phi} \qquad (3\text{-}54)$$

Then, Eq. (3-53) resolves in two independent equations, the first one giving

$$q_\ell = \frac{r}{R}\frac{B_\phi}{B_\theta} \qquad (3\text{-}55)$$

and the second

$$\frac{dr}{d\theta} = \left(\frac{\partial r}{\partial\theta}\right)_\psi = \frac{rB_r}{B_\theta}\ , \qquad (3\text{-}56)$$

which corresponds to the statement that field lines lie on flux surfaces. Since $B_p = \sqrt{B_r^2 + B_\theta^2}$, this latter relation gives

$$B_\theta = \frac{B_p}{\sqrt{1 + \frac{1}{r^2}\left(\frac{\partial r}{\partial \theta}\right)^2_\psi}} = \frac{1}{R\left(\frac{\partial r}{\partial \psi}\right)_\theta}, \tag{3-57}$$

the second equality coming from Eq. (3-45) for the poloidal field. It follows that

$$q_\ell = r B_T \left(\frac{\partial r}{\partial \psi}\right)_\theta \tag{3-58}$$

or

$$\frac{q_\ell}{q_o} = \frac{B_T}{B_o}\frac{x}{\rho}\left(\frac{\partial x}{\partial \rho}\right)_\theta \tag{3-59}$$

The series expansion about the axis can be immediately obtained as

$$\frac{q_\ell}{q_o} = 1 - \frac{\rho}{\delta}(11+6\beta_p)\cos\theta + \frac{\rho^2}{32}\left\{4\beta_p(3\beta_p+5)(1+\cos 2\theta) - 18\alpha + \right.$$

$$\left. + 29 + 31\cos 2\theta - \frac{1}{q_o^2}\left(1 - \frac{\beta_p}{2}\right)\right\} + \frac{\rho^3}{12288}\left\{2520\,\beta_p^3(\cos 3\theta + 3\cos\theta)\right.$$

$$+ 3780\,\beta_p^2(\cos 3\theta + 3\cos\theta) + \beta_p[(5120h - 10880\alpha + 19350)\cos\theta$$

$$+ 6930\cos 3\theta]$$

$$\left. + \quad 6547\cos 3\theta + (22761 - 11840\alpha)\cos\theta + \frac{768}{q_o^2}(6\beta_p^2 - \beta_p - 22)\cos\theta\right\}$$

(3-60)

The average value of q_ℓ over the poloidal angle is the reciprocal of the rotational transform:

$$q = \frac{1}{2\pi} \oint q_\ell(\rho,\theta)d\theta \tag{3-61}$$

and is given by:

$$\frac{q}{q_o} = 1 + \rho^2[\frac{1}{32}(12\beta_p^2 + 20\beta_p - 16\alpha + 29) - \frac{1}{q_o^2}(1 - \frac{\beta_p}{2})] \tag{3-62}$$

Another important equilibrium quantity is the shear of the magnetic field lines, which is a measure of the variation of the pitch of the field lines with the flux surfaces. We define the shear as

$$\hat{s} = \frac{\rho}{q_o}\frac{dq}{d\rho} \tag{3-63}$$

and, to lowest order in ρ, it is

$$\hat{s} = s_o \rho^2 \tag{3-64}$$

where

$$s_o = \frac{3}{4}\beta_p^2 + \frac{9}{4}\beta_p - \frac{3}{16} - \alpha + 2(1 - \frac{\beta_p}{2})(1 - \frac{1}{q_o^2}) \tag{3-65}$$

This definition provides a relation between the shear and the parameter α, and, in subsequent analysis, we shall frequently discard α in favor of the more interesting parameter s_o.

The Expressions for the Curvature

Before deriving explicit representations for the normal and geodesic curvatures of the field lines, we shall give an alternative form of the equilibrium equation, in which r appears as the unknown function and Ψ as the coordinate variable. In other words, we shall replace the elliptical operation $\Delta^*_{(r,\theta)}$ which operates on Ψ, by another operator, that we shall denote by $\mathcal{G}_{(\Psi,\theta)}$, which acts upon r, in this way interchanging the former role of Ψ and r.

This transformation can be achieved by noting first that the general expression for the divergence of a vector function (V_r, V_θ), in our coordinate system is

$$\nabla \cdot \vec{V} = \frac{1}{r}\frac{\partial}{\partial r}(rV_r) + \frac{V_r}{R}\cos\theta - \frac{V_\theta}{R}\sin\theta + \frac{1}{r}\frac{\partial V_\theta}{\partial \theta}$$

and then substituting for $\vec{V}$ the vector $(1/R^2)\nabla\Psi$, whose components can be obtained from Eq. (3-44). To convert the partial derivatives that appear in the divergence from the (r,θ) representation to the (Ψ,θ) one, we observe that the gradient of a general scalar function $u(\Psi,\theta)$ can be written as:

$$\nabla u = \left(\frac{\partial u}{\partial \Psi}\right)_\theta \nabla\Psi + \left(\frac{\partial u}{\partial \theta}\right)_\Psi \nabla\theta = \left(\frac{\partial u}{\partial r}\right)_\theta \nabla r + \left(\frac{\partial r}{\partial \theta}\right)_r \nabla\theta \qquad (3\text{-}66)$$

Taking the dot products with ∇r and $\nabla\theta$, and using again Eq. (3-44) for $\nabla\Psi$, we obtain the desired connections:

$$\left(\frac{\partial u}{\partial r}\right)_\theta = \frac{1}{(\partial r/\partial \psi)_\theta}\left(\frac{\partial u}{\partial \psi}\right)_\theta \tag{3-67}$$

$$\left(\frac{\partial u}{\partial \theta}\right)_r = \left(\frac{\partial u}{\partial \theta}\right)_\psi - \frac{(\partial r/\partial \theta)_\psi}{(\partial r/\partial \psi)_\theta}\left(\frac{\partial u}{\partial \psi}\right)_\theta \tag{3-68}$$

This procedure gives for the right hand side of the equilibrium equation:

$$\mathcal{G}_{r(\psi,\theta)} = R^2\,\nabla\cdot\left(\frac{1}{R^2}\nabla\psi\right)$$

$$= \frac{R^2}{r}\frac{1}{(\partial r/\partial\psi)_\theta}\left\{\frac{\partial}{\partial\psi}\left[\frac{r}{R^2(\partial r/\partial\psi)_\theta}\right]_\theta + \left(\frac{\partial r}{\partial\theta}\right)_\psi\frac{\partial}{\partial\psi}\left[\frac{1}{R^2 r}\frac{(\partial r/\partial\theta)_\psi}{(\partial r/\partial\psi)_\theta}\right]_\theta\right\}$$

$$- \frac{R^2}{r}\frac{\partial}{\partial\theta}\left[\frac{1}{R^2 r}\frac{(\partial r/\partial\theta)_\psi}{(\partial r/\partial\psi)_\theta}\right]_\psi + \frac{1}{R}\frac{1}{(\partial r/\partial\psi)_\theta}\left[\cos\theta + \frac{1}{r}\left(\frac{\partial r}{\partial\theta}\right)_\psi \sin\theta\right] \tag{3-69}$$

which can be trivially manipulated to be expressed in terms of the variables x and ρ that we have been using throughout. Note that the "inversion" of the Grad-Shafranov operator permits us to obtain directly a local solution of the form of Eq. (3-37). The expansion of the equilibrium equation in powers of ρ then provides, for every order n, an ordinary differential equation in the poloidal variable, which is solved by the corresponding angular function $Z_n(\theta)$ (n = 1,2,...). This method was, in fact, used in Ref. (48) to discuss analytically the evolution of the equilibrium states in a tokamak heated through flux conservation. Its advantage with respect to the method that we

adopted here is that it provides directly a representation of x in terms of ρ, avoiding the need of inverting the series. The price to be paid is that the algebraic manipulations required to arrive at the final set of ordinary differential equations are much more involved.

With the choice that we have made to work with the coordinates ρ and θ, however, the "inverted" form of the equilibrium equation can be used for the derivation of the expansions for the curvatures. The normal curvature was found in Chapter II to be:

$$\kappa_n = \frac{1}{B^2} \frac{1}{h_\psi} \frac{\partial}{\partial \Psi} \left(P + \frac{B^2}{2}\right)_\chi \tag{3-70}$$

in orthogonal flux coordinates. Eliminating $dP/d\Psi$ by means of the equilibrium equation, we have

$$\kappa_n = + \frac{1}{B^2} \frac{1}{h_\psi} \left[-\nabla \cdot \left(\frac{1}{R^2} \nabla \Psi\right) - \frac{1}{2R^2} \frac{d}{d\Psi} \left(R^2 B_T^2\right) + \frac{1}{2} \left(\frac{\partial}{\partial \Psi} B^2\right)_\chi\right] \tag{3-71}$$

which can be recast as

$$\kappa_n = \frac{RB_p}{B^2} \left[\frac{1}{R^2} \mathcal{G} r(\Psi,\theta) + \frac{1}{2R^2} \frac{\partial}{\partial \Psi} \left(R^2 B_p^2\right)_\chi - \frac{B^2}{R} \left(\frac{\partial R}{\partial \Psi}\right)_\chi\right] \tag{3-72}$$

To translate this expression into the coordinate system (Ψ,θ) we note first that the gradient of a scalar function $u(\Psi,\chi)$ can be written as:

$$\nabla u = \left(\frac{\partial u}{\partial \Psi}\right)_{\chi} \nabla\Psi + \left(\frac{\partial u}{\partial \chi}\right)_{\Psi} \nabla\chi = \left(\frac{\partial u}{\partial \Psi}\right)_{\theta} \nabla\Psi + \left(\frac{\partial u}{\partial \theta}\right)_{\Psi} \nabla\theta \qquad (3\text{-}73)$$

Taking next the dot product with $\nabla\Psi$, given by Eq. (3-14), we obtain the relation between partial derivatives.

$$\left(\frac{\partial u}{\partial \Psi}\right)_{\chi} = \left(\frac{\partial u}{\partial \Psi}\right)_{\theta} - \frac{(1/r^2)(\partial r/\partial\theta)_{\Psi}(\partial r/\partial\Psi)_{\theta}}{1+(1/r^2)(\partial r/\partial\theta)^2_{\Psi}} \left(\frac{\partial u}{\partial \theta}\right)_{\Psi} \qquad (3\text{-}74)$$

With this transformation rule, and the use of Eqs. (3-1), (3-42) and (3-47), after a tedious calculation, we obtain the expansion in powers of ρ for the normal curvature:

$$R_o\kappa_n = -\cos\theta + \rho \frac{1}{16}[2(\cos\theta-1)\beta_p + 9\cos 2\theta + 7] - \frac{1}{q_o^2}$$

$$- \rho^2 \frac{1}{512}[36(\cos 3\theta - \cos\theta)\beta_p^2 + 4(17\cos 3\theta + 15\cos\theta)\beta_p +$$

$$+ 185\cos 3\theta + 391\cos\theta] - \frac{1}{q_o^2}(\beta_p - \tfrac{1}{2}) \cos\theta +$$

$$+ \frac{\rho^3}{6144}(264\cos 4\theta - 24\cos 2\theta - 240)\beta_p^3 + (372\cos 4\theta + 444\cos 2\theta$$

$$+ 144)\beta_p^2 + [834\cos 4\theta + (256h - 352\alpha + 1568)\cos 2\theta - 256h + 352\alpha$$

$$+ 864]\beta_p + 1521\cos 4\theta + (1-496\alpha + 4017)\cos 2\theta - 272\alpha + 2670$$

$$\frac{1}{q_o^2}\left[(-384\cos 2\theta + 960)\beta_p^2 + (768\cos 2\theta + 2112)\beta_p - 1440\cos 2\theta\right.$$

$$\left. - \quad 5376\alpha - 240\right] + \frac{6144}{q_o^4}(\beta_p - 1) \qquad (3\text{-}75)$$

The geodesic curvature, in orthogonal curvilinear coordinates, was found in Chapter II to be

$$\kappa_s = \frac{1}{B^2 B_p}\frac{1}{J_o}\left[\frac{\partial}{\partial \chi}\left(\frac{B^2}{2}\right)\right]_\Psi \qquad (3\text{-}76)$$

where J_o is the Jacobian in the orthogonal system. Since

$$\frac{1}{J_o}\left(\frac{\partial u}{\partial \chi}\right)_\Psi = \frac{1}{J}\left(\frac{\partial u}{\partial \theta}\right)_\Psi \qquad (3\text{-}77)$$

where J is the Jacobian in the system (Ψ,θ,ϕ), we have

$$\kappa_s = \frac{1}{B^2 B_p}\frac{1}{J}\left[\frac{\partial}{\partial \theta}\left(\frac{B^2}{2}\right)\right]_\Psi \qquad (3\text{-}78)$$

Introducing the expansions already derived for the quantities entering the above expression, we obtain:

$$R_o \kappa_s = \sin\theta - \frac{\rho}{16}(2\beta_p + 9)\sin 2\theta +$$

$$+ \quad \frac{\rho^2}{512}\left[(36\sin 3\theta + 20\sin\theta)\beta_p^2 + (68\sin 3\theta + 52\sin\theta)\beta_p + \right.$$

$$+ \quad 185\sin 3\theta + 181\sin\theta - \frac{1}{q_o^2}\left(\frac{\beta_p}{2} - \frac{1}{r}\right)\sin\theta]$$

$$- \quad \frac{p^3}{6144}\,(264\sin^4\theta + 312\sin^2\theta)\beta_p^3 + (372\sin^4\theta + 516\sin^2\theta)\beta_p^2$$

$$+ [834\sin^4\theta + (256h - 352\alpha + 1362)\sin^2\theta]\beta_p + (-496\alpha + 2811)\sin^2\theta$$

$$+ \quad \frac{1}{q_o^2}\,(-384\,\beta_p^2 + 1920\,\beta_p - 1248)\,\sin^2\theta \qquad (3\text{-}79)$$

This completes the characterization of the field structure.

Before leaving this chapter, we rewrite the general mode equations in dimensionless form in the coordinate system (ρ,θ), making them ready for future work:

$$r^2\left(\frac{J}{\hat{J}}\right)^2 M T - \frac{d}{d\theta}\left(M\,\frac{dT}{d\theta}\right) - 2\beta_p N T = 2q_o\,\frac{N\Xi}{1+h\rho^2} \qquad (3\text{-}80a)$$

$$r^2\left[\hat{J}\,B_o^2\left(\frac{1}{\gamma_c P} + \frac{1}{B^2}\right)\Xi + 2q_o\,\frac{N}{\rho^2}\,\frac{T}{1+h_\rho^2}\right] =$$

$$= \quad \frac{d}{d\theta}\left(\frac{1}{\hat{J}}\,\frac{B_o}{B^2}\,\frac{d\Xi}{d\theta}\right), \qquad (3\text{-}80b)$$

where we have replaced the function W, appearing in the original set, by

$$\Xi = \frac{R_o^2}{B_o}\,W\,. \qquad (3\text{-}81)$$

and Γ^2, that we shall call the growth-rate squared parameter, is defined as

$$\Gamma^2 = - \frac{\omega^2 R_o^2 q_o^2}{V_{Ao}^2} \tag{3-82}$$

where V_{Ao} is the Alfvén speed evaluated at the magnetic axis. The coefficient functions M and N, respectively, are:

$$M = \rho^2 \left(\frac{\hat{J}}{J}\right) \left(\frac{R_o B_o / q_o}{R B_p}\right) \quad (1 + \Sigma^2) \tag{3-83a}$$

$$N = - \rho^2 \left(\frac{\hat{J}}{J}\right) \left(\frac{R_o B_o / q_o}{R B_p}\right) \quad (1 + h_\rho^2)(R_o \kappa_n - R_o \kappa_s \frac{B_T}{B_o} \Sigma) \tag{3-83b}$$

where Σ is the shear-related quantity:

$$\Sigma = \frac{R^2 B_p^2}{F} \frac{\partial}{\partial \Psi} \int^{\chi} q_1 (\Psi, \chi) \, d\chi \tag{3-84}$$

Note that we have already replaced the pressure gradient by the expansion:

$$\frac{dP}{d\Psi} = - \frac{B_o p_o}{R_o^2} (1 + h_\rho^2) \quad , \tag{3-85}$$

since higher-order terms will not be needed anyway.

Appendix 3A

An Equlibrium Integral Relation

Developing the divergence of the Grad-Shafranov operator in Eq. (2-11), and recalling that the toroidal current density is given by Eq. (2-12), the equilibrium equation can be written as

$$\nabla \cdot \left(\frac{\Psi}{R^2} \nabla\Psi\right) - \frac{1}{R^2} |\nabla\Psi|^2 = \frac{\Psi J_T}{R} . \qquad (3A\text{-}1)$$

Integrating this relation over the volume comprised by a magnetic surface Ψ_o, all the way around the torus, we obtain

$$\int_A \frac{\Psi}{R^2} \nabla\Psi \, d\vec{A} - \int_v \frac{1}{R^2} |\nabla\Psi|^2 \, dV = \int_v \frac{\Psi J_T}{R} \, dV, \qquad (3A\text{-}2)$$

where $d\vec{A} = Rd\phi \, d\ell \, \vec{e}_\psi$ is the normal surface element on the boundary, $d\ell$ being the element of arc along the poloidal contour.

Since the poloidal magnetic field is $B_p = |\nabla\Psi|/R$, we may rewrite Eq. (3A-2) as

$$2\pi \Psi_o \oint B_p \, d\ell - \int_v B_p^2 \, dV = \int_v \frac{J_T}{R} \Psi \, dV \qquad (3A\text{-}3)$$

Observing that the volume elementt is $dV = Rd\phi dS$, where dS represents the cross sectional element of area between two

neighboring magnetic surfaces, and that the toroidal current flowing inside the volume delimited by Ψ_o is

$$I = \oint B_p \, d\ell = \int_S J_T \, dS \quad , \tag{3A-4}$$

we finally obtain

$$\int_S J_T \, (\Psi_o - \Psi) \, dS = \frac{1}{2\pi} \int_V B_p^2 \, dV \tag{3A-5}$$

Chapter IV

THE SPECTRUM OF UNSTABLE MODES

The "Distilled" Equation

In Chapter II, we have seen that the poloidal dependence of the coefficient functions of the mode equations includes both periodic terms, arising from the periodicity of the equilibrium quantities, and secular, non periodic terms as well, introduced by the magnetic shear. In general, this mixed behavior will be reflected in the form of the eigensolutions, as rapid oscillations superimposed on a slower, secular decay. At marginal stability, in particular, the eigensolutions vanish asymptotically with some power of $1/s\theta$, and the secular decay can be quite slow. As we approach the magnetic axis and the shear decreases, the numerical solution of the mode equations becomes increasingly difficult, requiring a large domain of integration to take into account the proper behavior of the eigensolution at "infinity". If we point out this difficulty, it is just to mention, that, by contrast, it can be turned into an advantage, when the problem is envisaged from an analytical point of view.

The fact that the independent variable appears under two guises, the first as the argument of periodic functions with the period of the equilibrium, and the second, consistently as a secular term proportional to the shear, permits us to introduce a formalism that decouples the short-scale, rapidly oscillating

part of the solution from the long scale, slowly varying part. This method, for example, has been used in the asymptotic analysis of the mode equations for general equilibria[17]. The same technique can be used in a perturbative analysis of the mode equations to obtain analytically a solution in the vicinity of the magnetic axis in the form of a power series that is uniformly valid over the infinite range of the poloidal-like variable.

Since the secular terms in the coefficient functions always appear through the combination $\hat{s}\theta$, it is natural to recognize this as the "long" variable for the problem, and we introduce

$$\xi = \hat{s}\theta \tag{4-1}$$

while keeping the same old notation (θ) for the "short" variable. The origin of the secular term is the shear-related quantity Σ, here reproduced:

$$\Sigma = \frac{R^2 B_p^2}{B} \left[\frac{\partial}{\partial \Psi} \int^{\chi} q_{\xi}(\Psi,\chi)\, d\chi\right]_{\chi} \tag{4-2}$$

and, as a first step in the perturbative treatment of the mode equation, we obtain an expansion of Σ in powers of ρ using the expressions derived in Chapter III. In doing so, we keep in mind that the variable ξ itself is assumed to be of "order unity", although $\hat{s}$, specified by Eq. (3-64), is of order ρ^2. Here lies precisely the merit of the multiple scaling, that makes possible to treat the limits $\hat{s} \to 0$, $\theta \to \infty$ simultaneously.

Switching from χ to θ coordinate, with the help of the general transformation relation given by Eq. (3-74), we have

$$\Sigma = \frac{R^2 B_p^2}{B} \left[\left(\frac{\partial}{\partial \Psi} \int^{\theta} q_\ell(\Psi,\theta) d\theta \right)_\theta - \frac{\left[(1/r^2)(\partial r/\partial \theta)_\Psi \ (\partial r/\partial \Psi)_\theta \right]}{1 + (1/r^2)(\partial r/\partial \theta)_\theta^2} q_\ell \right] \tag{4-3}$$

where q_ℓ, now, is the same as in Eq. (3-60). The expansions of all quantities appearing in this expression are already known, and can be substituted to give:

$$\Sigma = \ell + \rho \left(\beta_p + \frac{3}{2} \right) (\ell \cos\theta - \sin\theta) + ... \tag{4-4}$$

Higher order terms, that are needed to obtain the solution to lowest order, are given in the Appendix 4A.

The strategy of solution of the mode equations can now be stated in more precise terms. With the introduction of two distinct scale-lengths, the differential operator $d/d\theta$ is split in two pieces:

$$\frac{d}{d\theta} = \frac{\partial}{\partial \theta} + \hat{s} \frac{\partial}{\partial \ell} \tag{4-4}$$

the first applying only to the periodic components of the coefficient functions and the solution, and the second to the secular part. All functions entering the couple of mode equations, in the representation of Eqs. (3-80a) and (3-80b), are then expanded in powers of ρ:

$$M = M_0(\ell,\theta) + \rho M_1(\ell;\theta) + \rho^2 M_2(\ell,\theta) + \ldots \qquad (4\text{-}5a)$$

$$N = \rho N_1(\ell,\theta) + \rho^2 N_2(\ell,\theta) + \rho^2 N_3(\ell,\theta) + \rho^4 N_4(\ell,\theta) + \ldots \qquad (4\text{-}5b)$$

$$T = T_0(\ell,\theta) + \rho T_1(\ell,\theta) + \rho^2 T_2(\ell,\theta) + \rho^3 T_3(\ell,\theta) + \rho^4 T_4(\ell,\theta) + \ldots \qquad (4\text{-}5c)$$

etc. The explicit form of the coefficient functions M and N is given in the Appendix 4B. The parameter r^2 is also expanded in a similar way. Collecting powers of ρ of the expanded equations, we generate a sequence of partial differential equations in the variables ℓ and θ. The solution of each of these equations in the θ-variable, in general, would involve secular terms in θ, which are in conflict with the requirement that dependencies on the fast scale are periodic. Taking advantage of the flexibility afforded by an extra variable, we demand at every step of the calculation that the coefficients of secular terms vanish. This procedure, which, in general, introduces restrictions on the values of the equilibrium parameters, will lead also to a condition on the ℓ-dependence of the solution, ultimately an ordinary differential equation in the "stretched" variable ℓ only. Together with appropriate boundary conditions, this equation is an eigenvalue problem, which can be solved to furnish the growth rates and the critical parameters of the equilibrium for marginal stability.

For clarity of exposition, let us consider first this latter case, which corresponds to $r^2 = 0$. As we have seen in Chapter II, in this limit the pair of mode equations decouple, and the analysis can be restricted to

$$(\frac{\partial}{\partial\theta} + s_o\rho^2 \frac{\partial}{\partial\ell}) [M(\frac{\partial T}{\partial\theta} + s_o\rho^2 \frac{\partial T}{\partial\ell})] + 2\beta_p N T = 0 \qquad (4\text{-}6)$$

The expansion of this equation in powers of ρ gives to lowest order:

$$\frac{\partial}{\partial\theta} (M_o \frac{\partial T_o}{\partial\theta}) = 0 \qquad (4\text{-}7)$$

where

$$M_o = 1 + \ell^2 \qquad (4\text{-}8)$$

Thus, in order to avoid secularities in θ, T_o has to be a function only of the long variable, $T_o = T_o(\ell)$. To first order in ρ, we find:

$$\frac{\partial}{\partial\theta} (M_o \frac{\partial T_1}{\partial\theta}) + 2\beta_p N_1 T_o = 0 \qquad (4\text{-}9)$$

where N_1 is the function

$$N_1 = \cos\theta + \ell \sin\theta \quad , \qquad (4\text{-}10)$$

which introduces the lowest order contribution of the curvatures. The dependencies on θ are solved by

$$T_1 = 2\beta_p \left(\frac{\cos\theta + \ell \sin\theta}{1 + \ell^2}\right) T_o + K_1(\ell) \qquad (4\text{-}11)$$

where K_1 comes from the second integration of Eq. (4-9) and depends only on ℓ.

The next order gives:

$$\frac{\partial}{\partial\theta}\left(M_1 \frac{\partial T_1}{\partial\theta} + M \frac{\partial T_2}{\partial\theta}\right) + 2\beta_p (N_1 T_1 + N_2 T_o) = 0 \qquad (4\text{-}12)$$

and the average of the left hand side of this equation is

$$2\beta_p \frac{1}{2\pi} \oint (N_1 T_1 + N_2 T_o) d\theta = 2\beta_p \left[\left(\frac{1}{q_o^2} + \beta_p\right) - (1 + \beta_p)\right] T_o \ , \qquad (4\text{-}13)$$

which is identically zero only for $q_o = 1$. Thus the perturbative treatment that we are giving to the ballooning equation is strictly compatible only with a definite value of the rotational transform at the axis. Although this represents a restriction, it corresponds, in fact, to the most interesting case for analytical investigation, since it separates the analysis of the ballooning modes from that of the flute modes.

With this choice for q_o, the first integral of Eq. (4-12) gives

$$M_o \frac{\partial T_2}{\partial\theta} = K_{21}(\ell) - \frac{\beta_p}{4}\left(7\beta_p + \frac{15}{2}\right)\ell\, T_o + (\text{periodic terms in } \theta) \qquad (4\text{-}14)$$

If T_2 is indeed to be periodic, the integration constant has to be chosen as

$$K_{21}(\ell) = \frac{\beta_p}{4}\left(7\beta_p + \frac{15}{2}\right)\ell\, T_o \qquad (4\text{-}15)$$

A further integration then yields:

$$T_2 = \frac{\beta_p}{4(1+\ell^2)^2}\left[2\beta_p + 3 - (10\beta_p + 9)\ell^2\right]T_o \cos 2\theta +$$

$$+ \frac{\beta_p\,\ell}{4(1+\ell^2)^2}\left[8\beta_p + 9 - (4\beta_p + 3)\ell^2\right]T_o \sin 2\theta +$$

$$+ \frac{2\beta_p}{1+\ell^2}(\cos\theta + \ell\sin\theta)\,K_1(\ell) + K_2(\ell) \qquad (4\text{-}16)$$

where K_2 is a new undetermined function of ℓ.

The third order equation is

$$\frac{\partial}{\partial\theta}\left(M_o\frac{\partial T_3}{\partial\theta} + M_1\frac{\partial T_2}{\partial\theta} + M_2\frac{\partial T_1}{\partial\theta}\right) + s_o\frac{\partial M_1}{\partial\theta}\frac{\partial T_o}{d\ell} +$$

$$+ 2s_o M_o\frac{\partial^2 T_1}{\partial\theta\,\partial\ell} + s\frac{dM_o}{d\ell}\frac{\partial T_1}{\partial\theta} + 2\beta_p(N_1T_2 + N_2T_1 + N_3T_o) = 0\ , \qquad (4\text{-}17)$$

using again $q_o = 1$. Periodicity is automatically satisfied by this equation, without bringing about any additional constraint. The first integral introduces a function $K_{31}(\xi)$ which has to be chosen in such a way as to eliminate secularities in θ, and is given in the Appendix 4C. The solution for T_3, considerably complicated and not particularly illuminating, can also be found in the Appendix 4C.

Finally, the fourth order equation closes the cycle. The average over one period of θ is

$$\frac{\partial}{\partial \xi}\left(M_o \frac{\partial T_o}{\partial \xi}\right) + \frac{1}{s_o}\frac{\partial}{\partial \xi}\left(\frac{1}{2\pi}\oint M_1 \frac{\partial T_1}{\partial \theta}\, d\theta\right) + \frac{2\beta_p}{s_o^2}\left[\frac{1}{2\pi}\oint (N_1 T_3 + \right.$$

$$\left. + \quad N_2 T_2 + N_3 T_1) d\theta \;+\; \frac{1}{2\pi}\oint N_4 T_o \, d\theta\right] \;=\; 0 \qquad (4\text{-}18)$$

The functions K_1, K_2 and K_3 introduced in the previous steps as integration constants do not contribute to the above averages, that are listed in the Appendix 4D, and we are left with a second order ordinary differential equation only for T_o in the variable ξ:

$$\frac{d}{d\xi}\left[(1+\xi^2)\frac{dT_o}{d\xi}\right] + \left(\frac{A}{1+\xi^2} - B\right)T_o \;=\; 0 \qquad (4\text{-}19)$$

where A and B are functions of the equilibrium given by

$$A \;=\; 4g - \frac{3}{2} g^2 \delta_1\left(\frac{1}{\beta_p}\right) \qquad (4\text{-}20a)$$

$$B = \frac{3}{8} g^2 \delta_2 \left(\frac{1}{\beta_p}\right) + \frac{2g}{\beta_p} \qquad (4\text{-}20b)$$

The parameter g is the finite quantity

$$g = \frac{\beta_p^2}{s_o} = \lim_{\psi \to 0} \frac{(G/2)^2}{\hat{s}} \quad , \qquad (4\text{-}21)$$

where G is the dimensionless pressure gradient parameter:

$$G = -8 \left(\frac{\psi}{R_o J_{To}^3}\right)^{1/2} \frac{dP}{d\psi} \quad , \qquad (4\text{-}22)$$

and the functions δ_1 and δ_2 are:

$$\delta_1 \left(\frac{1}{\beta_p}\right) = 1 - \frac{3}{\beta_p} - \frac{3}{2} \frac{1}{\beta_p^2} \qquad (4\text{-}23a)$$

$$\delta_2 \left(\frac{1}{\beta_p}\right) = 1 + \frac{3}{\beta_p} - \frac{1}{4} \frac{1}{\beta_p^2} + \frac{1}{4} \frac{1}{\beta_p^3} \qquad (4\text{-}23b)$$

Stability Limits

We shall refer to Eq. (4-19) as a "distilled" equation since it is an equivalent version of the ballooning equation at the magnetic axis obtained by a process that can be compared to a filtering of the net coupling between the mode and the equilibrium. It was presented simultaneously at the Sherwood Conference of 1979 by the M.I.T. group[49] and D. Lortz and J. NÜhrenberg[50]. The researchers of M.I.T., to reduce the labor

of computation, had considered the particular limit $\beta_p \to \infty$, that gives for the function A and B the form of Eqs. (4-26) to follow, but included the growth rate term, extending its use to the study of unstable equilibria, while Lortz and Nührenberg obtained the equation for marginally stable equilibria for all values of β_p. The work of both groups appeared subsequently in current journals[51,52].

The factor $1+\ell^2$ in Eq. (4-19) arises from the transverse wavenumber of the perturbations and can be understood as follows. Consider, for simplicity, an equilibrium configuration in which the flux surfaces are nearly concentric circles, and the eikonal of the mode can be approximated by

$$S = n^o(\phi - q(r)\theta) \tag{4-24}$$

where we assume q to be a function of the radius in order to retain shear effects. Then, the perpendicular displacement vector is

$$\vec{k}_\perp = \nabla S = \frac{1}{R} e_\phi^+ - \frac{q}{r}(e_\theta^+ + \hat{s}\theta\, e_r^+) \tag{4-25}$$

and $k_\perp^2 \approx [(q^2/r^2)(1+\hat{s}^2\theta^2)]$, for small inverse aspect ratio. The first term on the left hand side of Eq. (4-19) describes the effect of the bending of the field lines in a sheared magnetic configuration caused by the finite longitudinal wavelength of the perturbations, which is represented by the operator $\partial/\partial\ell$. The second term on the left hand side contains the net product

of the averages of the coupling between the mode and the curvature. This term, which drives the instability, exhibits two remarkable features:

1) The functions A and B are specified by two equilibrium quantities, namely, g and β_p, or, alternatively, by the dimensionless pressure gradient parameter G and the shear $\hat{s}$. Note that the parameter h, which is proportional to $d^2P/d\psi^2$ and affects individually the several terms in the coefficients functions, has nonetheless disappeared in the final equation. This does not mean, however, that second order derivatives of the equilibrium profiles (the coefficients p_1 and f_1 in Eq. (3-7) and (3-8)) do not play any role in this derivation; they are built in the shear. In the limit $\beta_p \to \infty$, the functions A and B depend only on the single parameter g:

$$A = 4g - \frac{3}{2} g^2 \qquad (4\text{-}26a)$$

$$B = \frac{3}{8} g^2 \qquad (4\text{-}26b)$$

2) The functions A and B depend both linearly and quadratically on g. The linear part of A results from the first order effects of the pressure gradient on the equilibrium, that produce shifts of the flux surfaces with respect to the magnetic axis without changing the circular shape. The quadratic parts of A and B are determined by distortions of the flux surfaces, that, for the particular equilibrium that we are considering, include poloidal harmonics up to the third order.

The solution of Eq. (4-19) can be immediately found to be:

$$T_o(\ell) = \frac{1}{(1+\ell^2)^{\gamma}} \qquad (4\text{-}27)$$

where the exponent γ and the values of the equilibrium function A and B at marginal stability satisfy the algebraic equations:

$$\gamma = \frac{1}{4}\left[1 \pm \sqrt{1+4B}\,\right] = \sqrt{\frac{A}{4}} \qquad (4\text{-}28)$$

Taking the square, the second equality gives:

$$(A - B)^2 = A \qquad (4\text{-}29)$$

and, substituting A and B by Eqs. (4-26a) and (4-26b), we obtain:

$$ag^3 + bg^2 + cg + d = 0 \qquad (4\text{-}30)$$

where

$$a(\beta_p) = 9\left(20 - \frac{36}{\beta_p} - \frac{25}{\beta_p^2} + \frac{1}{\beta_p^3}\right)^2 \qquad (4\text{-}31a)$$

$$b(\beta_p) = -384\left(20 - \frac{36}{\beta_p} - \frac{25}{\beta_p^2} + \frac{1}{\beta_p^3}\right)\left(2 - \frac{1}{\beta_p}\right) \qquad (4\text{-}31b)$$

$$c(\beta_p) = 256(70 - \frac{82}{\beta_p} + \frac{7}{\beta_p^2}) \qquad (4\text{-}31c)$$

$$d(\beta_p) = -4096 \qquad (4\text{-}31d)$$

This third degree equation in g, in general, may admit two, one, or no acceptable roots, depending on the value of β_p. To be specific, let us consider first the limit $\beta_p >> 1$, in which case the eigenvalue condition reduces to:

$$g^3 - \frac{64}{15} g^2 + \frac{224}{45} g - \frac{256}{225} = 0 \qquad (4\text{-}32)$$

and can be solved exactly. The roots and corresponding values of γ are:

$$g_I = \frac{4}{15}(5 - \sqrt{15}) \approx 0.301 \qquad \gamma_I = \frac{2}{\sqrt{15}} \approx 0.515 \qquad (4\text{-}33a)$$

$$g_{II} = \frac{8}{5} = 1.6 \qquad \gamma_{II} = \frac{4}{5} = 0.8 \qquad (4\text{-}33b)$$

$$g_{III} = \frac{4}{15}(5 + \sqrt{15}) \approx 2.366 \qquad \gamma_{III} = -\frac{2}{\sqrt{15}} \approx -0.516 , \qquad (4\text{-}33c)$$

The third one gives a divergent behavior of the solution at large t, and therefore must be rejected. This shows that we have two points of marginal stability in the parameter space (g, β_p) for large values of β_p.

For finite values of β_p, other possibilities arise. In Fig. 4.1, we represented pictorially the limits of marginal stability for the full range of the parameter β_p, where we can recognize three distinct regions. For $\beta_p < 0.0380$, the configuration is stable for all values of g, or equivalently, of the shear. In the interval $0.0380 < \beta_p < 2.328$, there is only one threshold of instability, and the increase of shear is always stabilizing. For $\beta_p > 2.328$, an upper branch appears, delimiting a "band" of instability, whose boundaries, asymptotically, are given by Eqs. (4-33a) and (4-33b). In this case, the increase of shear can be stabilizing or de-stabilizing, depending on whether the pressure gradient is small and we are in the "first" regime of stability, or whether it is large, and we are in the "second" stable regime. The values of β_p that separate the three regions in this diagram correspond to the positive roots of $a(\beta_p) = 0$. Note that, since $b(\beta_p)$ vanishes at the same time as $a(\beta_p)$, the separation between the regions is very sharp.

To conclude this discussion, we examine the form of the asymptotic solutions of Eq. (4-19), which establishes the connection between ballooning and interchange modes. For large values of ℓ, we have

$$\frac{a}{a\ell}\,(\ell^2 T_o) - B T_o = 0 \qquad (4\text{-}34)$$

Figure 4.1: Instability Boundaries in the (β_p,g) Plane. Logarithmic Scales are Used.

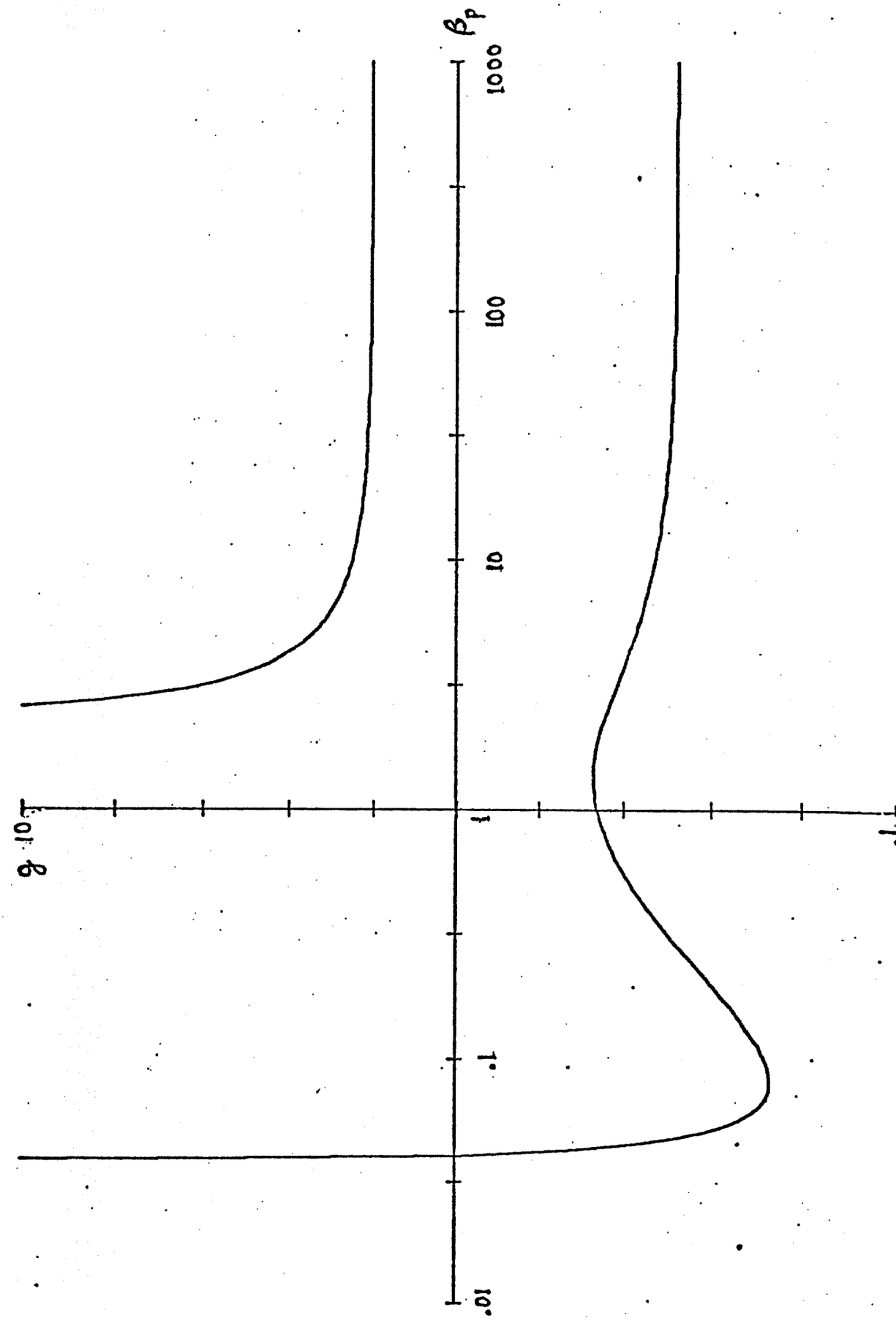
β_p
1000
100
10
1
.1
.01
$g \cdot 10^7$
1
.1

which is satisfied by $T_o = r^{-2\gamma}$, with γ defined by the first of the equalities in Eq. (4-28). We recall from Chapter II that oscillatory solutions at infinity, corresponding here to complex values of the exponent γ, mean that the system is unstable to localized interchanges. For positive values of both g and β_p, however, the discriminant 1 + 4B in Eq. (4-28) is always positive, and this situation never arises. This, of course, stems from the fact that we are taking q = 1 at the axis. On the other hand, if we allow the shear (or g) to be negative, as we have in configurations of the type of the stellarator, this constraint is no longer sufficient to guarantee stability, and flute modes may still be present for low values of β_p [52].

Inclusion of the Growth-Rate Term

A correct treatment of the problem for unstable regimes should include the coupling between the two differential equations that in general describe the modes. In Chapter II, using very general considerations, we showed that this coupling, arising from the curvature, has a stabilizing effect. In this section, extending the method of multiple scales to the full set of mode equations in order to include finite growth-rates, we show that they can be combined to produce a single "distilled" equation, still of second order in the long variable. The stabilizing effect of the coupling then appears as an enhanced inertia of the fluid, slowing down the evolution of the instability.

We refer again to Eqs. (3-80a) and (3-80b), introducing now the expansions:

$$r^2 = r_o^2 + \rho\, r_1^2 + \rho^2\, r_2^2 + \rho^3\, r_3^2 + \rho^4\, r_4^2 + \ldots \tag{4-35}$$

$$\Xi = \Xi_o(\theta,\ell) + \rho\, \Xi_1(\theta,\ell) + \rho^2\, \Xi_2(\theta,\ell) + \rho^3\, \Xi_3(\theta,\ell) + \ldots \tag{4-36}$$

Remembering that the function N is of order ρ, a quick consideration of Eq. (3-80b) shows that the proper balance of powers requires that $r_o^2 = r_1^2 = 0$ and $\Xi_o = 0$, at least. Then, the lowest order meaningful equation is:

$$r^2\, N_1\, T_o = \frac{1}{2q_o}\, \frac{\partial^2}{\partial\theta^2}\, \Xi \tag{4-37}$$

where N_1, we recall, is given by Eq. (4-10). The solution of this equation that satisfies periodicity in θ is:

$$\Xi_1 = -2q_o\, r_2^2\, N_1\, T_o(\ell) + C_1(\ell)\, T_o(\ell)\,, \tag{4-38}$$

where $C_1(\ell)$ is an as undetermined function of ℓ. Introducing this expression in the companion mode equation, we obtain to second order:

$$r_2^2\, M_o T_o - \left[\frac{\partial}{\partial\theta}\left(M_1 \frac{\partial T_1}{\partial\theta} + M_o \frac{\partial T_2}{\partial\theta}\right) + 2\beta_p (N_1 T_1 + N_2 T_o)\right] =$$

$$= -2\, r_2^2\, T_o^2\, N_1^2\, T_o - q_o\, C_1(\ell)\, N_1\, T_o \tag{4-39}$$

Taking the average over one cycle of θ, as before, we find:

$$r_2^2 \, (1+2q_o^2) \, (1+\ell^2) \;=\; 2\,\beta_p\left(\frac{1}{q_o^2} - 1\right) \quad , \tag{4-40}$$

which can be satisfied only if $q_o^2 = 1$, $r_2^2 = 0$. Then Ξ_1 is a function only of ℓ, and will not affect T_o, the same way that the undetermined functions K's disappeared in the final step of averaging the fourth order equation for marginal stability.

An argument on the same lines shows that $r_3^2 = 0$, and $\Xi_2 = \Xi 2(\ell)$ can be ignored. The non-vanishing growth-rate appears only at fourth-order, associated with

$$\Xi_3(\ell,\theta) = -\,2q_o\, r_4^2\, (\cos\theta + \ell \sin\theta)\, T_o(\ell) + C_3(\ell) T_o(\ell). \tag{4-41}$$

With this, following the same steps as in the previous case of marginal stability, we arrive at the new version of the "distilled" equation:

$$\hat{r}^2 \, (1+\ell^2) T_o \;=\; \frac{d}{d\ell}\left[(1+\ell^2)\,\frac{dT_o}{d\ell}\right] \;+\; \left(\frac{A}{1+\ell^2} - B\right) T_o \tag{4-42}$$

where

$$\hat{r}^2 \equiv r_4^2\,(1+2q_o^2) = -\,\frac{\omega^2 R_o^2 q_o^2}{V_{Ao}^2}\;\frac{g^2}{(G/2)^4}\,(1+2q_o^2) \quad , \tag{4-43}$$

remembering the definition of growth-rate squared parameter (Eq. (3-82)).

Thus, as we have anticipated, the effect of the coupling between the two mode equations, represented by the term $2q_o^2$ in the factor that multiplies the growth rate above, can be assimilated to an added inertia to the fluid.

Before going to the discussion of the equation we just derived, two remarks are in order. First, to simplify the exposition, we started the derivation with the assumption that the correct expansion of Ξ is a given by Eq. (4-36), implying that Ξ is, at least, of the same order of τ. There is no reason a priori to be so, and, at first glance, an expansion including inverse powers of ρ would be a valid possibility as well. As a matter of fact, the solution that we found is unique, other alternatives being in conflict with the constraint of periodicity that the solutions must satisfy. Second, the ordering for the growth rate implies that the pressure (rather than the pressure gradient) and the adiabaticity index γ_c do not enter the final equation. By inspecting Eq. (3-80b), we see that the first term on the left hand side is four orders of magnitude higher than the other terms, and therefore gives no contribution to the leading order solution. To first pick up the effects of the finite compressibility of the fluid on the mode, we would have to reach two orders higher in the expansion of the equations. This precise case was discussed in Chapter II, where wee showed that the relative stabilization of barely unstable equilibria is predominantly due to the tangential motion of the fluid, that acts to effectively reduce the rate of growth of the normal displacement. Stabilization effects resulting from

compression and expansion of the fluid are dominant only in frankly unstable regimes. These are the rigorous terms by which the "similarity" frequently pointed out between a "low beta" plasma and an incompressible fluid[32] should be understood.

The contribution of the parallel velocity to the plasma motion is absorbed in the factor $1 + 2q_o^2 = 3$ that multiplies the growth rate squared parameter. In this situation, the coupling between the mode equation introduces no change in the dispersion equation, and there is only a mere renormalization of parameters. It is possible, however, to incorporate heuristically the effects of the fluid compressibility still in a fourth order perturbation equation by treating formally the quantity $1/\gamma_c P + 1/B^2$ in Eq. (3-80b) as of order $1/\rho^4$. This procedure gives again an equation of the form of Eq. (4-42), but with $\hat{\Gamma}^2$ replaced by

$$\Omega^2 = \hat{\Gamma}^2 \left[1 + \frac{2q_o^2}{1+(V_{Ao}^2/V_s^2)\hat{\kappa}^2 \hat{\Gamma}^2}\right] \qquad (4-44)$$

Growth Rates for Slightly Unstable Equilibria

The distilled equation for growing modes, Eq. (4-42), is much nastier than its counterpart for marginal stability. While the latter one can be easily solved, and permits a complete analytical picture of the critical conditions of equilibrium, the former can be solved only numerically, or in approximate ways for particular limiting cases. This equation appears also in the separation of the Laplace equation in spheroidal

coordinates, and defines the so-called radial oblate spheroidal functions, that do not have a simple representation in terms of the more well-known functions[53]. Thus an analytical dispersion relation, which relates the growth of the normal modes to the equilibrium conditions, specified by the functions A and B, cannot be obtained, in full generality, from the differential equation. In the next section, however, we will show how a fitting to the numerically obtained dispersion relation still provides an efficient and compact analytic representation. In this section, we examine the solution for weakly unstable equilibria, for which an analytical approach is possible. As an interesting and useful application, we shall show how the interchange modes, under proper conditions, degenerate into the ballooning instabilities. This derivation is due to T.M. Antonsen, Jr.[54], following a procedure used by Mikhailovsky[55] in the analysis of a similar equation.

We assume that $\hat{r}^2 << 1$, and split the domain of the variable ℓ into two regions. In the first, covering the range $|\ell| \lesssim 1$, which we shall call the "inner region", the differential equation can be approximated by

$$\frac{\partial}{\partial \ell}\left[(1+\ell^2)\frac{\partial T_o}{\partial \ell}\right] + \left(\frac{A}{1+\ell^2} - B\right)T_o = 0 \qquad (4\text{-}45)$$

In the domain $|\ell| >> 1$, called the "outer region", the equation takes the asymptotic form

$$\frac{\partial}{\partial \xi}\left(\xi^2 \frac{\partial T_o}{\partial \xi}\right) - BT_o = \hat{\Gamma}^2 \xi^2 T_o \tag{4-46}$$

Let us consider the inner region first.. Introducing the transformation

$$T_o = (1 + \xi^2)^{-\gamma/2} F \tag{4-47}$$

and subsequently

$$\xi^2 = -z , \tag{4-48}$$

the relevant equation can be converted to:

$$z(1-z) \frac{\partial^2 F}{\partial z^2} + \left[\frac{1}{2} - \left(\frac{1}{2} - \sqrt{A}+1\right) z\right] \frac{\partial F}{\partial z} - \frac{1}{4}(A - \sqrt{A} - B)F = 0 \tag{4-49}$$

which can be recognized as the standard hypergeometric differential equation. The solution is

$$F = {}_1F_2(a_1; b_1; c_1; z) \tag{4-50}$$

where ${}_1F_2$ denotes the hypergeometric function with arguments a_1, b_1, c_1. These are given by:

$$a_1 + b_1 = \frac{1}{2} - \sqrt{A} \tag{4-50a}$$

$$a_1 b_1 = \frac{1}{4}(A - B - \sqrt{A}) \tag{4-50b}$$

$$c_1 = \frac{1}{2} \tag{4-50c}$$

The two first equations above can be solved to give explicit definitions of a and b:

$$a_1 = \frac{1}{2}\left(\frac{1}{2} - \sqrt{A} + \nu\right) \tag{4-51a}$$

$$b_1 = \frac{1}{2}\left(\frac{1}{2} - \sqrt{A} + \nu\right) \quad , \tag{4-51b}$$

where

$$\nu = a_1 - b_1 = \sqrt{B + \frac{1}{4}}$$

The equation for the outer region can be promptly identified with Bessel equation, whose acceptable solution is

$$T_o = \sqrt{\frac{\pi}{2\hat{r}}}\ K_\nu(\hat{r}\ell) \tag{4-52}$$

where K is a modified Bessel function.

The matching of the two solutions will determine the eigenvalue condition. We first stretch the inner solution to infinity, that then takes the asymptotic form[56]:

$$T_o \sim \ell^{-\sqrt{A}}\left[\frac{\Gamma(c_1)\ \Gamma(b_1-a_1)}{\Gamma(b_1)\ \Gamma(c_1-a_1)}\ell^{-2a} + \frac{\Gamma(c_1)\ \Gamma(a_1-b_1)}{\Gamma(a_1)\ \Gamma(c_1-b_1)}\ell^{-2b}\right]$$

$$\sim \frac{\Gamma(c_1)\ \Gamma(b_1-a_1)}{\Gamma(b_1)\ \Gamma(c_1-a_1)}\ell^{-1/2-\nu} + \frac{\Gamma(c_1)\ \Gamma(a_1-b_1)}{\Gamma(a_1)\ \Gamma(c_1-b_1)}\ell^{-1/2+\nu} \tag{4-53}$$

where the Γ's represent gamma-functions. Next, we extend the outer solution to $\xi \to \infty$ [57]:

$$T_o \sim \sqrt{\frac{\pi}{2}} \frac{\pi/2}{\sin \nu\pi} \left[\frac{(\hat{r}\xi/2)^{-\nu-1/2}}{\Gamma(1-\nu)} - \frac{(\hat{r}\xi/2)^{\nu-1/2}}{\Gamma(1+\nu)} \right] \tag{4-54}$$

Matching of both solutions is accomplished by equating the coefficients of equal powers:

$$(\frac{\hat{r}}{2})^{-\nu-1/2} \frac{1}{\Gamma(1-\nu)} \sqrt{\frac{\pi}{2}} \frac{\pi/2}{\sin \nu\pi} = \frac{\Gamma(c)\ \Gamma(b-a)}{\Gamma(b)\ \Gamma(c-a)} \tag{4-55a}$$

$$(\frac{\hat{r}}{2})^{-\nu-1/2} \frac{1}{\Gamma(1+\nu)} \sqrt{\frac{\pi}{2}} \frac{\pi/2}{\sin \nu\pi} = \frac{\Gamma(c)\ \Gamma(a-b)}{\Gamma(a)\ \Gamma(c-b)} \tag{4-55b}$$

or, eliminating the common factor:

$$(\frac{\hat{r}}{2})^{-2\nu} = \frac{\Gamma(b_1)\ \Gamma(c_1-a_1)}{\Gamma(a_1)\ \Gamma(c_1-b_1)} \frac{\Gamma^2(\nu)}{\Gamma^2(-\nu)} . \tag{4-56}$$

where the recurrence relation for gamma-functions, $\Gamma(1+\nu) = \nu\,\Gamma(\nu)$, was used.

This is the desired dispersion relation for $\hat{r}^2 \ll 1$. Given the general behavior of the gamma-functions, this expression vanishes only when the denominator is singular, which happens for values of argument that are negative integers or zero:

$$a_1 = -n \tag{4-57a}$$

$$c_1 - b_1 = -n \ , \tag{4-57b}$$

Of the two conditions, the first is the interesting one, giving:

$$\sqrt{A} = \nu + \frac{1}{2} + 2n = \sqrt{B + \frac{1}{4}} + \frac{1}{2} + 2n \quad (n=0,1,2,\ldots) \tag{4-58}$$

We reproduce, in this way, a generalized version of the criterium of marginal stability previously derived.

The above dispersion relation applies to even modes. A similar analysis can be carried out for odd modes. In this case, starting with

$$T_o = (1+\xi^2)^{-\gamma/2} \ \xi \ F \tag{4-59}$$

for the inner solution, we arrive, by performing exactly the same operations, at the dispersion relation:

$$(\frac{\hat{r}}{2})^{2\nu} = \frac{\Gamma(b_2)\ \Gamma(c_2-a_2)}{\Gamma(a_2)\ \Gamma(c_2-b_2)} \ \frac{\Gamma^2(\nu)}{\Gamma^2(-\nu)} \tag{4-60}$$

where

$$a_2 = \frac{1}{2} (\frac{3}{2} - \sqrt{A} + \nu) \tag{4-61a}$$

$$b_2 = \frac{1}{2} (\frac{3}{2} - \sqrt{A} + \nu) \tag{4-61b}$$

$$c_2 = \frac{3}{2} \qquad (4\text{-}61c)$$

The corresponding criterium for marginal stability is:

$$\sqrt{A} - \sqrt{B + \frac{1}{4}} = \frac{3}{2} \pm 2n \quad (n=0,1,2,\ldots) \qquad (4\text{-}62)$$

In Fig. (4.2) we illustrate a graphical analysis of stability. In the vertical axis, we plot A and in the horizontal, $\nu = B+(1/4)$. The conditioons for excitation of even and odd modes of different order, given by Eqs. (4-58) and (4-62), are represented in this diagram by parallel straight lines that intercept the axis $\nu = 0$ at 1/2, 3/2, 5/2, ... Sequences of equilibria, obtained by varying g with fixed β_p, are described by curves parameterized by g. The trajectory represented in Fig. 4.2 corresponds to the limit $\beta_p \to \infty$, that gives for the functions A and B the form of Eq. (4-26), and intercepts the line n = 0 at $g_I = 0.3$ and $g_{II} = 1.6$. We may expect that, for more general conditions, the trajectories will intercept more than one line, and other modes, with smaller growth rates, will be excited as well.

The equations for small growth rates can be further explored to shed some light on the connections between localized interchanges and ballooning modes. In the previous section we pointed out, partially as a motivation for the analysis that we will undertake now, that our equilibrium does admit interchange

Figure 4.2: Graphical Determination of the Instability Boundaries for Equilibrium Configurations Characterized by Circular Flux Surfaces in the Vicinity of the Axis and $\beta_p = \infty$.

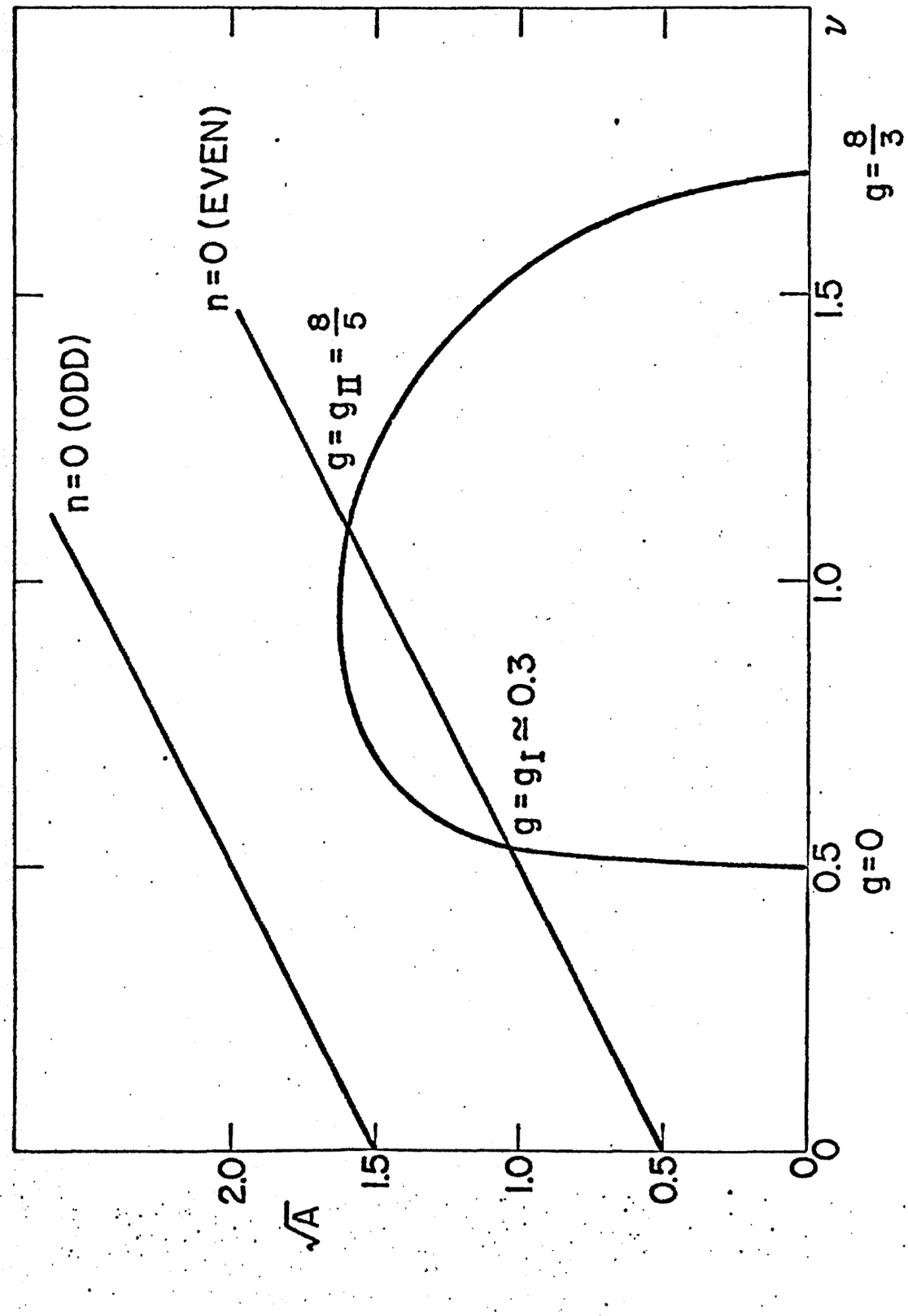
n=0 (ODD)
n=0 (EVEN)
g = g_II = 8/5
g = g_I ≅ 0.3
g=0
g=8/3
ν
√A
0
0.5
1.0
1.5
2.0

modes if we permit $\hat{s}$ to be negative. In general, these modes correspond to imaginary ν, or real

$$\sigma = \sqrt{|B| - \frac{1}{4}} \qquad (4\text{-}63)$$

To describe graphically the transition from the interchange modes to ballooning modes, we may refer to the diagram previously used, plotting values of σ on the continuation of the abscissa axis to the left of the origin, as in Fig. 4.3. Then, points on the half plane on the left of the vertical axis $\nu=0$ are always unstable according to the Mercier criterium, while points on the right-half plane can be either ballooning unstable, if they lie above the line $A - 1/2 = \nu$, or stable, if they lie below. Let us consider a point very close to the threshold for the n=0 ballooning mode, on the left hand side of the boundary between the two domains, as the point P. We show in the Appendix 4A, that the expression derived for the growth rates in this case can be further simplified, and gives:

$$(\frac{\hat{\Gamma}}{4})^{2i\sigma} = (\frac{\epsilon - i\sigma}{\epsilon + i\sigma})\, e^{-2i\gamma_e \sigma} \qquad (4\text{-}64)$$

where ϵ, defined as

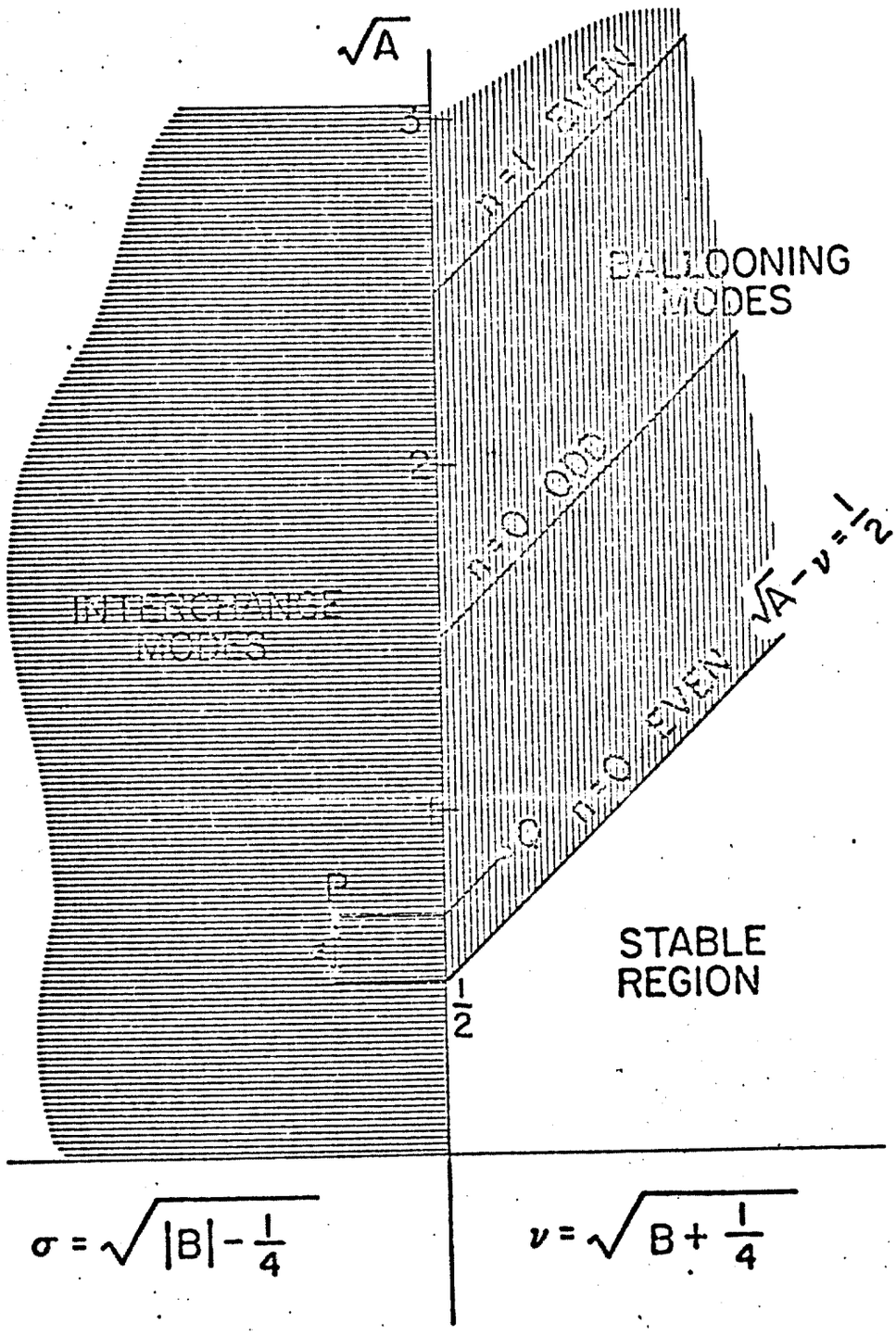

Figure 4.3: Diagram to Interpret the Transition from Interchange Modes to Ballooning Modes.

$$\epsilon = A - 1/2 , \tag{4-65}$$

is a small quantity, and γ_e is the Euler-Mascheroni constant, $\gamma_e = 0.5772 \ldots$ Putting

$$\frac{\epsilon - i\sigma}{\epsilon + i\sigma} = e^{-i\theta} \tag{4-66}$$

with θ defined in the interval $[0, 2\pi]$, the dispersion relation becomes

$$\left(\frac{\hat{\Gamma}}{4}\right)^{2i\sigma} = e^{-i(\theta + 2\gamma_e \sigma)} \tag{4-67}$$

Taking the logarithm of this expression, we obtain

$$\ln\left(\frac{\hat{\Gamma}}{4}\right) = -\left(\frac{\theta + 2\pi m}{2\sigma}\right) - \gamma_e \tag{4-68}$$

where $m = 0, 1, 2, \ldots$. Then there is an infinite sequence of unstable modes whose growth rates accumulate at $\hat{\Gamma} = 0$. The most unstable mode corresponds to $m = 0$. Since $0 < \theta < 2\pi$, the growth rates for all other modes vanish as σ tends to zero and we approach the vertical axis in the diagram. The behavior of the most unstable mode depends on the sign of σ. If $\epsilon < 0$, $\theta \to 2\pi$ as $\sigma \to 0$, the growth rate for the mode $m = 0$ also tends to zero, and we reach the region in the diagram that lies below the line $\epsilon = \nu$, which is absolutely stable. On the other hand, if $\epsilon > 0$, as we cross the vertical axis, we reach the domain unstable

to ballooning modes. For $\sigma << \varepsilon$, the angle θ can be approximated by

$$\theta \simeq \frac{2\sigma}{\varepsilon} \tag{4-69}$$

and the growth-rate, in this limit, becomes:

$$\hat{\Gamma} = 4\varepsilon^{-\gamma_e - (1/\varepsilon)} \quad . \tag{4-70}$$

for the only mode m = 0 that survives as a ballooning instability.

An Approximate Dispersion Relation

If the distilled equation including finite growth-rate is hardly accessible from an analytical point of view, the numerical solution does not offer special difficulty. We have solved Eq. (4-42) numerically by the shooting method for arbitrary values of the equilibrium functions A and B. In particular, specializing these functions to the forms given by Eqs. (4-26a) and (4-26b), which correspond to the limit $\beta_p \to \infty$, we have obtained numerically a table relating the eigenvalue $\hat{\Gamma}^2$ to the equilibrium parameter g. In Fig. 4.4 we display graphically the results of our computations.

This curve shows that, as we reduce the value of g below 1.6 and cross the second threshold of marginal stability, the increase of the growth-rate is much sharper than when we cross the first unstable limit, by increasing g above 0.3. This is

Figure 4.4: The Growth-rate Squared Parameter as a Function of g for Equilibria Characterized by Circular Flux Surfaces in the Vicinity of the Magnetic Axis and $\beta p = \infty$.

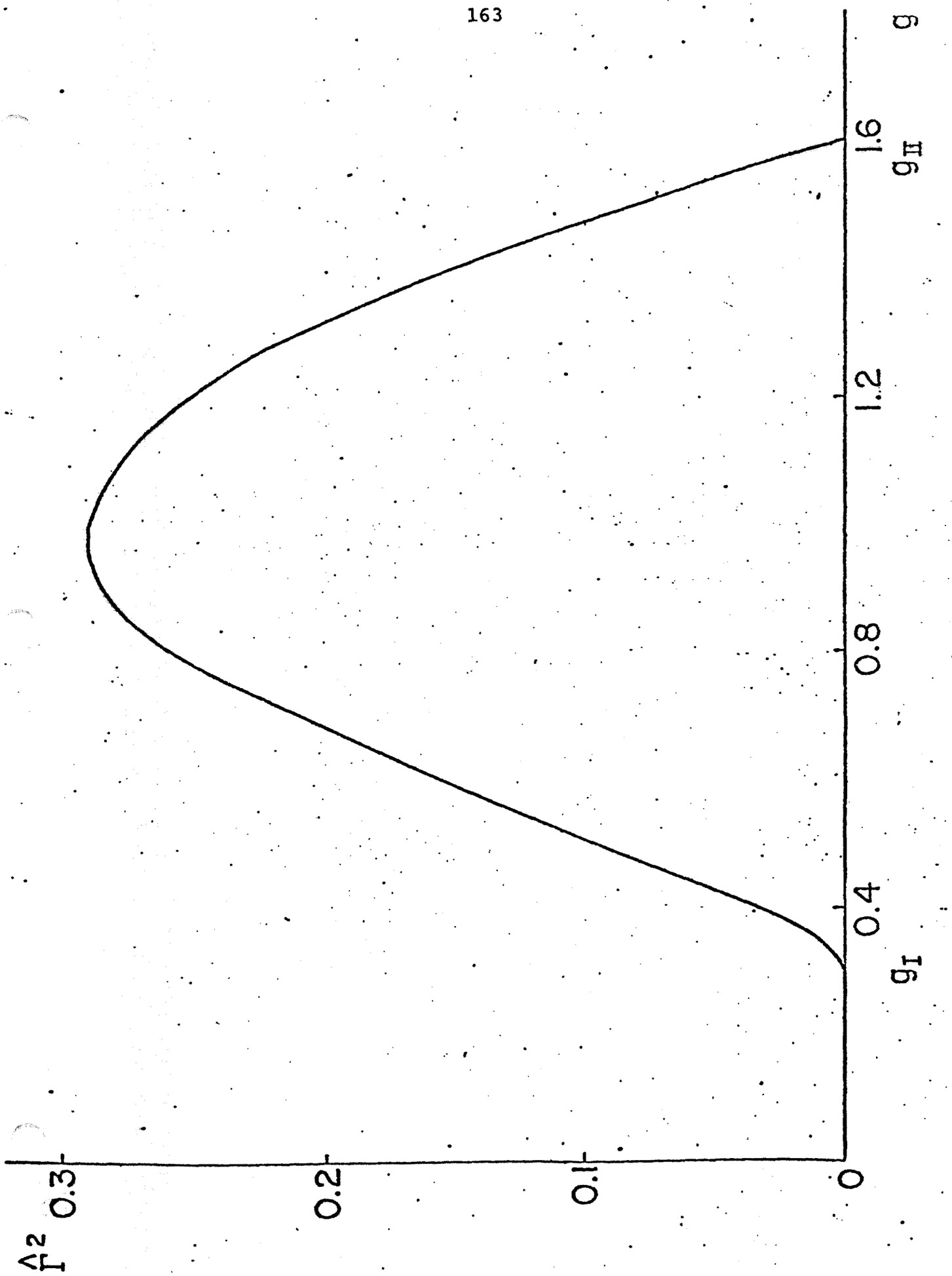
$\Delta\Gamma^2$
0.3
0.2
0.1
0
g_I
0.4
0.8
1.2
1.6
g_{II}
g

because there is a difference in the asymptotic form of the eigensolution at the vicinity of both marginal points, and here a consideration of a quadratic form can be helpful to understand their relative effects on the growth-rates.

We multiply the "distilled" equation by T_o, and integrating over ℓ, we obtain:

$$\hat{\Gamma}^2 \int_{-\infty}^{+\infty} d\ell(1+\ell^2)|T_o|^2 = -\int_{-\infty}^{+\infty} d\ell(1+\ell^2)\left|\frac{dT_o}{d\ell}\right| +$$

$$+ \quad g\int_{-\infty}^{+\infty} d\ell\left[\frac{4-(3/2)g}{1+\ell^2} - \frac{3}{8}g\right]|T_o|^2 \qquad (4\text{-}71)$$

omitting the factors in the curvature term arising from finite β_p. This equation, in the first place, clearly shows the stabilizing effects of the quadratic terms in g, which imply that the growth rate $\hat{\Gamma}^2$ cannot increase indefinitely with g, and will eventually fall back to zero at a second point of marginal stability.

At the first threshold of instability, the eigensolution decays very slowly. In fact, the exponent γ_I (Eq. (4-33a)) is barely above 1/2, which is the limiting value it could take for the integral on the left hand side to converge. On the other hand, the exponent γ_{II} characterizing the eigenfunction at the second marginal point (Eq. (4-33b)) is comfortably above 1/2. Then we may argue, based on the balance of the terms in the quadratic form, that the growth rate must be depressed around the first marginal point g_I with respect to the second, g_{II}.

This suggests that a rational approximation to the dispersion relation in the interval $g_I < g < g_{II}$ could have the form

$$\hat{\Gamma}^2 \propto \left(1 - \frac{g}{g_I}\right)^p \left(\frac{1}{g} - \frac{1}{g_{II}}\right)^q , \qquad (4\text{-}72)$$

where $p > q$ in order to reproduce adequately the different behavior at the two zeros. As a matter of fact, the expression

$$\hat{\Gamma}^2 = \frac{3}{20} g^2 \left(\frac{1}{g} - \frac{10}{3}\right)^2 \left(\frac{1}{g} - \frac{5}{8}\right) \qquad (4\text{-}73a)$$

fits the curve $\hat{\Gamma}^2(g)$ obtained by numerical integration of Eq. (4-42) within errors of less than 5% relative to the maximum value of $\hat{\Gamma}^2$. Remembering Eqs. (4-43) and (4-21), which define $\hat{\Gamma}^2$ and g, it can also be rewritten as:

$$-\omega^2 = \frac{1}{5} \left(\frac{V_{Ao}^2 G^2}{q_o R_o}\right) \left(\frac{\hat{s}}{G^2} - \frac{5}{6}\right)^2 \left(\frac{\hat{s}}{G^2} - \frac{5}{32}\right) \qquad (4\text{-}73b)$$

where we have used $q_o = 1$.

Effects of Ellipticity

As we observed in the previous sections, our analysis of stability applies to those equilibria that are specified only by the profiles of the pressure and the poloidal current stream function, corresponding to flux surfaces that tend to circles as

we approach the magnetic axis. The free integration constants of the equilibrium solution, that represent the effects of the boundary conditions of the equilibrium on the magnetic axis, were chosen to be zero. This particularization, obviously, was dictated by the complexity of our equations, that even in the simplest case that we considered, is almost prohibitive. The inclusion of the ellipticity parameter can be accomplished, in practice, only at the expense of another important equilibrium parameter, β_p, by taking the limit $\beta_p \to \infty$. Not only that, but in order to reduce the integrals to tractable forms, we have to assume that the equilibrium functions are expandable in the smallness of the ellipticity parameter λ.

The equilibrium solution that was adopted is given in Ref. (58). The derivation follows the same steps as before, and we arrive at an eigenvalue equation that has exactly the same structure of Eq. (4-42). The equilibrium functions A and B are modified to

$$A = 4g - \frac{3}{2} g^2 + \lambda \left(\frac{11}{2} g^2 - 7g\right) \qquad (4\text{-}74a)$$

$$B = \frac{3}{8} g^2 - \frac{\lambda}{4} (7g^2 - g) \qquad (4\text{-}74b)$$

The eigenvalue condition, Eq. (4-29), gives the stability limits

$$g_I = 0.301 + 0.543\,\lambda \qquad g_{II} = 1.6 + 3.463\,\lambda\,, \qquad (4\text{-}75)$$

and the corresponding values of the exponents characterizing the eigensolutions, obtained from Eq. (4-28), are:

$$\gamma_I = 0.516 + 0.019\,\lambda \qquad \gamma_{II} = 0.8 + 0.017\,\lambda \qquad (4\text{-}76)$$

These expressions are correct to linear terms on λ. Notice that positive values of λ (i.e., vertically elongated magnetic surfaces) as is the usual case, shift both marginal points towards the right, showing a tendency to make the first stability region wider and the second one narrower.

Reconstruction of the Mode in the Physical Space

In the transformed space of the poloidal variable, to first order in the expansion parameter, the eigensolution at marginal stability is:

$$T = T_o \left[1 + \rho \left(\frac{\cos\theta + \xi \sin\theta}{1+\xi^2}\right)\right] \qquad (4\text{-}77)$$

*

where $T_o = 1/(1+\xi^2)^{\gamma}$.

To return to the physical space, we use the ballooning infinite series of Fourier transforms. Writing $\xi = \hat{s}y$, and performing the integrals in Eq. (2-43), we obtain for the lowest order solution:

---

*We are omitting the integration function $K_1(\xi)$ that appears in Eq. (4-11) for $T_1(\xi)$. By carrying out the expansion of the mode equation to the fifth order, it is possible to show that, in order to satisfy the requirement of periodicity of the solution, K_1 must be a multiple of T_o, that is, $K_1(\xi) = cT_o(\xi)$, where c is an arbitrary constant. Without loss of generality, we may take $c = 0$, since this amounts only to a renormalization of the solution.

$$T_{o_{real}}(s,\theta) = \sum_{n=-\infty}^{\infty} \left|\frac{S-n}{\hat{s}}\right|^{\gamma-1/2} K_{\gamma-1/2}\left(\left|\frac{S-n}{\hat{s}}\right|\right) e^{i(S-n)\theta} \quad (4\text{-}78)$$

omitting normalization factors, where $K_{\gamma-1/2}$ is a modified Bessel function of the second kind. In the limit of weak shear, ($\hat{s} \to 0$), using well known asymptotic expressions for these functions, we obtain at the rational surfaces the representation:

$$T_{o_{real}}(\theta) = 1 + \frac{4\sqrt{\pi}}{2^{\gamma}\Gamma(\gamma-1/2)} \hat{s}^{1-\gamma} e^{-(1/\hat{s})} \cos\theta + \ldots. \quad (4\text{-}79)$$

where Γ is a gamma function. Under the same conditions, the representation of the first order solution is:

$$T_{1\,real}(\theta) = \left(\frac{\gamma-1/2}{\gamma}\right) \cos\theta + \frac{2\sqrt{\pi}}{2^{\gamma}\Gamma(\gamma-1/2)} \hat{s}^{-\gamma} e^{-(1/\hat{s})} \cos 2\theta. \quad (4\text{-}80)$$

Neglecting terms of order $e^{-1/s}$, the combination of Eqs. (4-79) and (4-80) gives the transformation of Eq. (4-77):

$$T_{real}(\theta) = 1 + \rho\, b \cos\theta \quad (4\text{-}81)$$

where we introduced a ballooning coefficient b defined by

$$b = \frac{\gamma - 1/2}{\gamma} \quad (4\text{-}82)$$

At the first threshold of instability $b_I \approx 0.032$ and at the second, $b_{II} \approx 0.375$. Because of the faster secular-decay of the eigensolution at the second threshold, the mode balloons out in the physical space more strongly than at the first threshold. This suggests that, for stable regimes operating close to the second threshold of instability, the level of the fluctuations is higher than for equilibria in the vicinity of the first threshold. We will see in the next chapter that this is indeed true.

Appendix 4A

Expansion of Σ in powers of ρ

$$\Sigma = \ell + \rho(\beta_p + \tfrac{3}{2})(\ell\cos\theta - \sin\theta) -$$

$$- \frac{\rho^2}{32}[(4\beta_p^2-20\beta_p+1)(\ell\cos 2\theta-\sin 2\theta) - (16\beta_p^2+52\beta_p-24s_o+46)\ell$$

$$+ \frac{32}{q_o^2}(1-\tfrac{\beta_p}{4})\ell] - \frac{\rho^3}{3072}\Big\{(120\beta_p^3-468\beta_p^2+210\beta_p+45)(\sin 3\theta$$

$$- \ell\cos 3\theta) + \sin\theta[216\beta_p^3-5348\beta_p^2+(6784s_o+4098h-6118)\beta_p$$

$$+ 5824s_o + 4801] - \ell\cos\theta[72\beta_p^3+500\beta_p^2+(128s_o+2048h+3358)\beta_p$$

$$- 2368s_o + 4091] + \frac{1}{q_o^2}[448\sin\theta(-10\beta_p^2+\beta_p+2) +$$

$$+ 64\ell\cos\theta(26\beta_p^2-5\beta_p+50)]\Big\} \qquad (4A\text{-}1)$$

Appendix 4B

Expansions of the Coefficient Functions in the Vicinity of the Axis

Writing

$$M = M_o + \rho M_1$$

$$N = N_1\rho + N_2\rho^2 + N_3\rho^3 + N_4\rho^4,$$

we have

$$M_o = 1 + \ell^2 \tag{4B-1}$$

$$M_1 = -[1-\ell^2 + \frac{1}{4}(\beta_p + \frac{1}{2})(1-7\ell^2)]\cos\theta - 2(\beta_p + \frac{3}{2})\ell \sin\theta \tag{4B-2}$$

$$N_2 = \cos\theta + \ell \sin\theta \tag{4B-3}$$

$$N_2 = \frac{1}{q_o^2} - 1 - \beta_p - \frac{1}{4}(\beta_p - \frac{3}{2})(\cos 2\theta + \ell \sin 2\theta) \tag{4B-4}$$

$$M_2 = -\frac{1}{2}(\beta_p^2 + \frac{11}{2}\beta_p + 1)\ell \sin 2\theta + \frac{1}{128}[(20\beta_p^2 + 196\beta_p + 13)\ell^2$$

$$- (44\beta_p^2 + 78\beta_p + 51)]\cos 2\theta + \frac{1}{128}[(148\beta_p^2 + 436\beta_p + 133 - 160s_o)\ell^2$$

$$+ \quad (52\beta_p^2 + 148\beta_p + 237 + 32s_o)] \qquad (4B\text{-}5)$$

$$N_3 = \frac{1}{512}(60\beta_p^2 - 84\beta_p - 9)(\cos 3\theta + \ell \sin 3\theta) +$$

$$+ \quad h(\cos\theta + \ell \sin\theta) + \frac{1}{512}[(12\beta_p^2 - 740\beta_p - 133 + 64s_o)\ell \sin\theta +$$

$$+ \quad (420\beta_p^2 - 684\beta_p + 401 + 448s_o)\cos\theta] \qquad (4B\text{-}6)$$

$$N_4 = -\frac{1}{256}(16\beta_p^3 - 24\beta_p^2 + 2\beta_p - 1)(\cos 4\theta + \ell \sin 4\theta)$$

$$- \frac{1}{768}[112(\beta_p - \tfrac{1}{2})s_o + 12\beta_p^3 - 546\beta_p^2 + 256(h + \tfrac{39}{8})\beta_p -$$

$$- \quad 288h + 189]\ell \sin 2\theta - \frac{1}{256}[-96(\beta_p + 3)s_o + 124\beta_p^3 + 110\beta_p^2 +$$

$$+ \quad 516\beta_p - 96h - 15]\cos 2\theta - s_o(\tfrac{19}{8}\beta_p + \tfrac{31}{16}) - 2h\beta_p + 5\beta_p^2$$

$$+ \quad \tfrac{35}{32}\beta_p - \tfrac{3}{64} \qquad (4B\text{-}7)$$

Appendix 4C

Solution of Eq. (4.17)

The first integral of Eq. (4-17) is made periodic in θ by taking

$$K_{31}(\ell) = 2s_o\left[(1+\ell^2)\frac{dK_1}{d\ell} + \ell K_1\right] + \frac{\beta_p}{4}\left(7\beta_p + \frac{15}{2}\right)\ell K_1 \qquad (4C\text{-}1)$$

The solution of Eq. (4-17) is

$$T_3 = \frac{\beta_p}{768(1+\ell^2)^3}\left[(1612\beta_p^2+2236\beta_p+1499)\ell^4 - (1832\beta_p^2+5352\beta_p + \right.$$

$$\left. + 2794)\ell^2 + 140\beta_p^2 + 604\beta_p + 315\right]T_o \cos 3\theta +$$

$$+ \frac{\beta_p}{768(1+\ell^2)^3}\left[(428\beta_p^2+396\beta_p+331)\ell^4 - (2408\beta_p^2+4936\beta_p + \right.$$

$$\left. + 2826)\ell^2 + 748\beta_p^2 + 2860\beta_p + 1451\right]\ell\, T_o \sin 3\theta -$$

$$- \frac{\beta_p}{2(1+\ell^2)^2}\left[(20\beta_p + 9)\ell^2 - (4\beta_p + 3)\right]K_1 \cos 2\theta$$

$$- \frac{\beta_p}{4(1+\ell^2)^2}\left[(4\beta_p + 3)\ell^2 - (8\beta_p + 9)\right]K_1\, \ell \sin 2\theta +$$

$$- \frac{\beta_p}{256(1+\ell^2)^2}\left[(36\beta_p^2+1684\beta_p - 271 - 1088s_o)\ell^2 + 868\beta_p^2 + 1012\beta_p\right.$$

$$\left. + 433 - 1344s_o\right] T_o \cos\theta - \frac{\beta_p}{256(1+\ell^2)^2}\left[(172\beta_p^2+2060\beta_p+331 -\right.$$

$$\left. - 704s_o)\ell^2 + (1004\beta_p^2 + 1388\beta_p + 1035 - 960s_o)\right]\ell\, T_o \sin\theta$$

$$+ \frac{s_o}{8(1+\ell^2)}\left\{16(\beta_p - \tfrac{3}{2})\ell\cos\theta - [(14\beta_p+15)\ell^2 + 30\beta_p - 9]\sin\theta\right\} T_o'$$

$$+ \frac{2\beta_p}{1+\ell^2}(K_2 + h\gamma_o)(\cos\theta + \ell\sin\theta) + K_3(\ell) \qquad (4C\text{-}2)$$

with primes denoting derivatives with respect to ℓ. $K_3(\ell)$ is an undetermined function of ℓ.

Appendix 4D

Integrals for Eq. (4-18)

$$\frac{1}{2\pi}\oint M_1 \frac{\partial T_1}{\partial \theta}\, d\theta = \frac{\beta_p}{8}(15 + 14\beta_p)\ell T_o \qquad (4D\text{-}1)$$

$$\frac{1}{2\pi}\oint (N_1T_3+N_2T_2+N_3T_1)d\theta = -\frac{1}{16}s_o(15+14\beta_p)\ell T_o' + 2\beta_p h T_o$$

$$+ \frac{1}{64(1+\ell^2)}\beta_p[(96s_o-12\beta_p^2-356\beta_p-67)\ell^2 + (224s_o-60\beta_p^2-212\beta_p+5)T_o] \qquad (4D\text{-}2)$$

$$\frac{1}{2\pi}\oint N_4\, d\theta = -s_o\left(\frac{19}{8}\beta_p + \frac{31}{16}\right) - 2h\beta_p + 5\beta_p^2 + \frac{35}{32}\beta_p - \frac{3}{64} \qquad (4D\text{-}3)$$

Appendix 4E

Approximate Expression For Small Growth Rates of Ballooning and Interchange Modes

Introducing the notation $\epsilon = A - 1/2$, Eq. (4-56) can be written as

$$\left(\frac{\hat{\Gamma}}{2}\right)^{2\nu} = \frac{\Gamma[-(\epsilon+\nu)/2]}{\Gamma[-(\epsilon-\nu)/2]} \frac{\Gamma[1/2 + (\epsilon-\nu)/2]}{\Gamma[1/2 + (\epsilon+\nu)/2]} \frac{\Gamma^2(\nu)}{\Gamma^2(-\nu)} \tag{4E-1}$$

Remembering the reflection and duplication formulae for gamma functions:

$$-z\,\Gamma(-z)\,\Gamma(z) = \pi \sin \pi z \tag{4E-2}$$

$$\Gamma(2z) = \frac{1}{\sqrt{2\pi}} \cdot 2^{2z-1/2}\,\Gamma(z)\,\Gamma(z + \tfrac{1}{2}) , \tag{4E-3}$$

this equation can be put in the form:

$$\left(\frac{\hat{\Gamma}}{4}\right)^{2\nu} = [\nu\Gamma(\nu)]^4 \left(\frac{\sin\nu\pi}{\nu\pi}\right)^2 \frac{\sin[(\pi/2)(\epsilon-\nu)]}{\sin[(\pi/2)(\epsilon+\nu)]} \frac{(\epsilon-\nu)\Gamma(\epsilon-\nu)}{(\epsilon+\nu)\Gamma(\epsilon+\nu)} \tag{4E-4}$$

Using the Euler product representation for gamma functions in the limit of small arguments:

$$\Gamma(z) \approx \frac{e^{-\gamma}e^{z}}{z} \tag{4E-5}$$

where γ_e is the Euler number, $\gamma_e = 0.57722 \ldots$, the dispersison relation for weakly unstable ballooning modes finally simplifies to:

$$\left(\frac{\hat{\Gamma}}{4}\right)^{2\nu} = \left(\frac{\epsilon - \nu}{\epsilon + \nu}\right) e^{-2\gamma_e \nu} \quad , \qquad (4E\text{-}6)$$

which gives the growth rates for points slightly above the line $\epsilon = \nu$ and close to the vertical axis in Fig. 4.3.

If ν is imaginary, corresponding to interchange modes, the appropriate extension of Eq. (4E-6) is

$$\left(\frac{\hat{\Gamma}}{4}\right)^{2i\sigma} = \left(\frac{\epsilon - i\sigma}{\epsilon + i\sigma}\right) e^{-2i\gamma_e \sigma} \quad , \qquad (4E\text{-}7)$$

which is the same as Eq. (4-64).

Chapter V

THE CONTINUOUS SPECTRUM

It is well known that, when a normal mode analysis in time is applied to the equations governing the oscillations of a nonhomogeneous plasma, in general singular solutions are found that are associated with a continuous frequency spectrum. The existence of these singularities had been recognized since early investigations on astrophysical plasmas, and were the cause of some bewilderment. The story is told by Barston[59] in a comprehensive paper on the subject published in 1964, where the problem was reexamined and put under proper perspective. In his own words, "it is necessary to realize that behind the normal mode equations, there lies a set of partial differential equations in both space and time variables...one must not let a preoccupation with the normal modes obscure this fact". Normal modes, then, are to be viewed as components of Fourier transforms, from which well-behaved, time-dependent solutions can be constructed by suitable integral superposition. The existence of singularities -- and the consequent lack of convergence of the energy integrals -- should not be a reason to abandon the concept. It is sufficient to require that such singular normal modes be integrable, in order to ensure the existence of the inverse Fourier transform and physically acceptable solutions in time. In fact, a mathematical entity with these characteristics is described by distributions, rather than by functions in the usual sense, and is commonplace in more than one

field of physics. Physically, the occurrence of singularities means that, in an nonhomogeneous medium, no steady-state waves can be found on some particular surfaces that resonate with the frequency of the mode. On the other hand, they lead to the non-exponential growth or decay of convective perturbations[60].

The Plane Stratified Medium

To put these ideas on a concrete basis, let us examine a simple one-dimensional situation that exemplifies the effect of inhomogeneities on Alfvén waves. In the previous chapter, we have seen that, by use of the ballooning transformation, and subsequently, by the introduction of a two-scale analysis, we were able to reduce the equations that describe the oscillations in the vicinity of the axis of a toroidal configuration to a one-dimensional equation that contains all relevant information about the (local) structure of the modes. We will find, not surprisingly, that this equation bears strong resemblance with the equation that describes analogous oscillations in an infinite plasma slab that simulates the equilibrium conditions around the axis (specifically, weak shear). If, in this latter case, we represent the equation governing the modes as

$$\mathcal{L}_T = \omega^2 T \quad , \tag{5-1}$$

where $\mathcal{L}$ is a second-order idfferential operator in the spatial-like variable and γ is the amplitude of the perturbations, then the averaged equation for toroidal geometry can be written as

$$\mathcal{L}_T + V_T = \Omega^2 T \qquad (5\text{-}2)$$

where $\mathcal{L}$ is the same differential operator, and V is a function of the long variable that embodies all the relevant effects induced by the curvatures of the confining magnetic field. Here Ω^2 is the eigenvalue, that in the limit of incompressibility, reduces to ω^2 (Eq. (4-43)), except for normalization factors. We will prove that the properties of the continuum spectrum are determined by the asymptotic limit of this equation, where V vanishes, and therefore all conclusions obtained from the study of Eq. (5-1) can be immediately applied to the toroidal case.

Consider a collisionless plasma, described by the ideal MHD equations in a slab geometry. We assume that the fluid is incompressible and that in equilibrium there is no flow velocity. For simplicity, we assume also that the density is uniform. The field lines of the static magnetic field are contained in the planes x = constant. To introduce the effects of inhomogeneities, we allow this magnetic field to vary in the direction orthogonal to the planes where the field lines lie. Thus:

$$\vec{B}_o(x) = B_{oy}(x)\,\vec{e}_y + B_{oz}(x)\,\vec{e}_z \qquad (5\text{-}3)$$

and we have a plane stratified medium (Fig. 5.1).

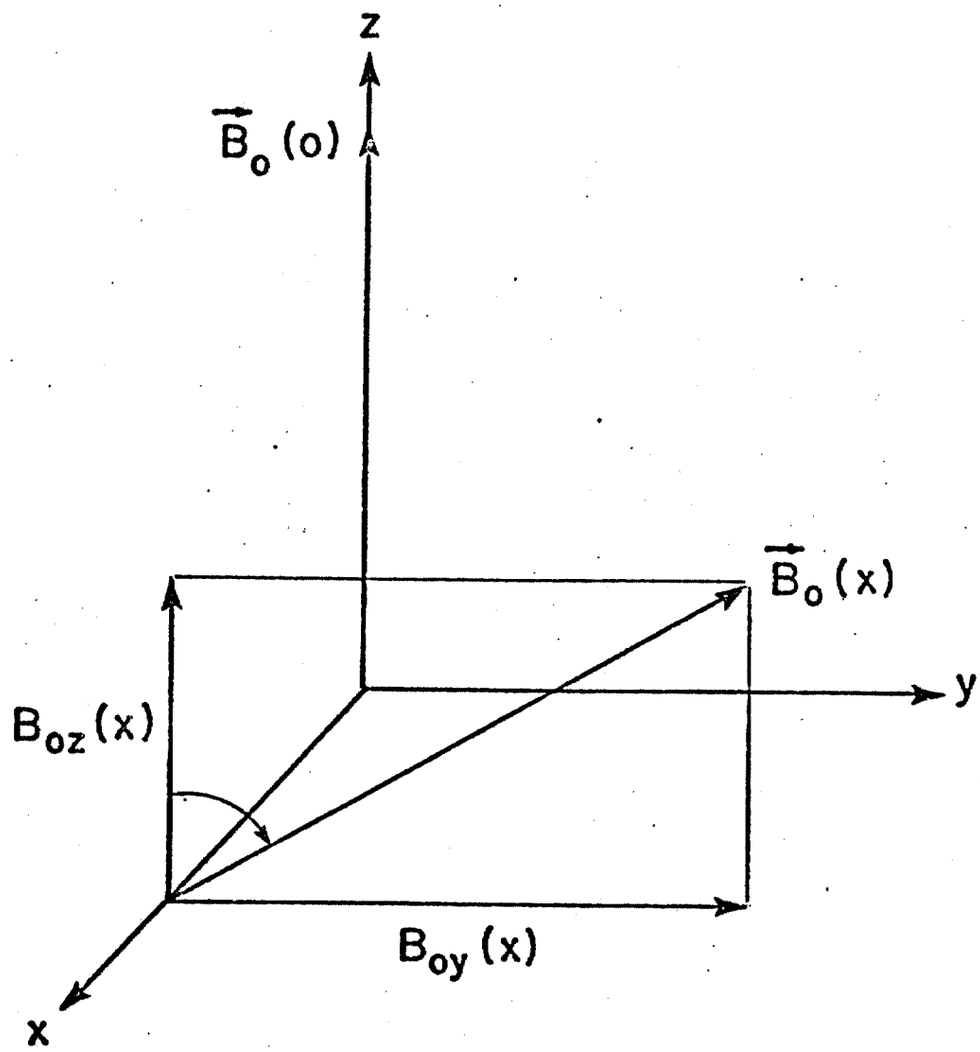

Figure 5.1: The Plane Statified Medium

We consider then the small oscillations on such a configuration. Linearizing the equations of motion, and using the incompressibility condition, we are led to the following equation for the velocity of the displacement[61]:

$$\rho_m \frac{\partial^2 \vec{v}}{\partial t^2} = (\vec{B}_o \cdot \nabla)^2 \vec{v} - \nabla[\frac{\partial}{\partial t} (P + \frac{B^2}{2})] \qquad (5\text{-}4)$$

where $P + (B^2/2)$ is the instantaneous total pressure. To eliminated the second term on the right hand side, we take the x-derivative of the divergence and subtract the result from the Laplacian of the x-component of this same equation. The final equation, satisfied by v_x, the velocity component along the direction in which the magnetic field varies, is[62]:

$$\nabla \cdot [\frac{\partial^2}{\partial t^2} - \frac{1}{\rho_m} (\vec{B}_o \cdot \nabla)^2] \nabla v_x = 0 \qquad (5\text{-}5)$$

The boundary condition to be applied is that $v_x \to 0$ as $|x| \to \infty$. We next Fourier-analyse this equation, taking $v_x = V(x) e^{-i\omega t + i(k_y y + k_z z)}$ and find that the equation satisfied by V(x) is

$$\frac{d}{dx} [(\omega^2 - \omega_A^2(x)) \frac{dV}{dx}] - k^2(\omega^2 - \omega_A^2(x)) V(x) = 0 \qquad (5\text{-}6)$$

where

$$k^2 = k_y^2 + k_z^2 \quad , \qquad (5\text{-}7)$$

$$\omega_A^2(x) = \frac{1}{\rho} (\vec{B}_o \cdot \vec{k})^2 = V_A^2(x)\, k^2 \cos^2 \theta \quad , \qquad (5\text{-}8)$$

$V_A(x)$ is the local Alfvén speed and θ is the angle between the direction of the magnetic field and the wave vector. The boundary conditions are $V(x) \to 0$ as $|x| \to \infty$.

As observed by Uberoi[61], this equation has exactly the same form of the equation studied by Barston[59], and the boundary coniditions are also identical. The theorems established by Barston which are of interest for us can be summarized as follows:

1) If $\omega_A^2(x)$ is an everywhere non-constant, continuous function, the spectrum is real and purely continuous and consists of those values of ω^2 that satisfy for some x the equation $\omega^2 = \omega_A^2(x)$. More generally, the continuous spectrum is given by the singularities of Eq. (5-6), that occur at the values of x such that

$$|V_A(x) \cos \theta| = \left| \frac{\omega}{k} \right| \qquad (5\text{-}9)$$

that is, at the positions for which the phase velocity is equal to the magnitude of the local Alfvén velocity component along the field line.

2) If $\omega_A^2(x)$ is constant in some interval, $\omega_A^2(x) = C^2$, then $\pm C$ lie in the discrete spectrum.

3) If ω belongs to the continuum and $\omega_A^2(x)$ is analytical, then in the neighborhood of x_s where $\omega_A^2(x_s) = \omega^2$, the solution of the differential Eq. (5-6) is singular and takes the form:

$$T(x) = A_1 E(x) + B_1[E(x) \ln|x-x_s| + (x-x_s)D(x)] \text{ for } x < x_s \tag{5-10a}$$

$$T(x) = A_2 E(x) + B_2[E(x) \ln|x-x_s| + (x-x_s)D(x)] \text{ for } x > x_s \tag{5-10b}$$

where $E(x)$ and $D(x)$ are regular, and A_1, B_1, A_2, B_2 are constants. The requirement that the solution must be an integrable function across the singularity is satisfied by the matching of the coefficients B_1 and B_2: $B_1 = B_2$, while the coefficients A_1 and A_2 remain arbitrary. Then, in addition to a logarithmic singularity, every eigenfunction may exhibit a step discontinuity at the point x_s. It is precisely the fact that the coefficients A_1 and A_2 are independent across a singularity that precludes any functional dependence of ω on k, and ω is free to range over the continuous spectrum. The relation between the constants A_1 and A_2 is determined by the boundary conditions, that can always be satisfied for any value of ω.

To see how these general results apply for a specific form of the function $\omega_A^2(x)$, we consider a configuration of particular interest, in which the z-component of the equilibrium magnetic field is constant, and the y-component varies linearly with the coordinate x. Then:

$$B_z = B_o \tag{5-11}$$

$$B_y(x) = B_o\,(x/L_s) \tag{5-12}$$

where L_s is a length scale that measures the change in direction of the field as we proceed across the field lines. A field like this is produced by a uniform current density along the z-direction:

$$J_z = \frac{B_o}{L_s} \tag{5-13}$$

This gives for the function ω_A^2 the quadratic dependence on the transversal coordinate:

$$\omega_A^2(x) = \frac{V_{Ao}^2\ k_y^2}{L_s^2}\ (x + \frac{k_z\ L_s}{k_y})^2 \tag{5-14}$$

where

$$V_{Ao}^2 = \frac{B_o^2}{\rho}\ .$$

Introducing in Eq. (5-6) the transformation

$$u = k\ (x + \frac{k_z\ L_s}{k_y})\ , \tag{5-15}$$

and defining the normalized frequency

$$\hat{\omega} = (\frac{k\ L_s}{k_y\ V_{Ao}})\ \omega\ , \tag{5-16}$$

where $k = \sqrt{k_y^2 + k_z^2}$, we obtain the following equation:

$$\frac{d}{du}\left[(\hat{\omega}^2 - u^2)\frac{dV}{du}\right] - (\hat{\omega}^2 - u^2)V = 0 \qquad (5\text{-}17)$$

As pointed out by Y.Y. Lau[63], this equation admits no unstable eigenmode solution. Since the function ω^2 is monotonic and non-constant over all its interval of definition, by Barston's theorems, no discrete eigenvalues exist. The (stable) spectrum is purely continuous and covers the infinite range $0 < \hat{\omega}^2 < \infty$. The "dispersion relation", in this case, is given by the parabolic curve:

$$\hat{\omega}^2 = u^2 \qquad (5\text{-}18)$$

that specifies the location of the layer in the plasma slab that resonates with the frequency ω. At these points, the solution is singular, but is still integrable -- as we mentioned before, it has to be interpreted not as a function in the usual sense, but as a distribution. This fact permits us to introduce the Fourier transform:

$$T(\xi) = \int_{-\infty}^{+\infty} V(u)\, e^{iu\xi}\, du \quad , \qquad (5\text{-}19)$$

that converts the differential equation Eq. (5-17) to:

$$\frac{d}{d\xi}\left[(1 + \xi^2)\frac{dT}{d\xi}\right] + \hat{\omega}^2(1 + \xi^2)T = 0 \qquad (5\text{-}20)$$

an equation identical to the "distilled" equation of the previous chapter if we take g = 0. In the case of a toroidal configuration, we had first to introduce averages to "clean-out" the equation from the periodicities coming from the geometry, and, in this sense, the "distillation" process can be described figuratively as a process of reduction to a planar geometry. The residue left from the averages of the coupling between the mode and the curvatures are isolated in an effective "gravity" (the terms depending on g) that is absent in the present model. The introduction of the Fourier transform here is equivalent to the use there of the ballooning transformation, since this one is no more than a superposition of Fourier transforms.

The analogy between both cases is made possible by the choice of a quadratic dependence of the square of the local Alfvén frequency ω_A on the transverse coordinate x. Note that, in the toroidal case, the shear is the only quantity in the equation that describes the structure of the mode along the field line that retains the information about the transverse inhomogeneities of the equilibrium field. In the planar model that we are considering now, the inhomogeneity comes from the rotation of the field lines across the surfaces where the magnetic field lies. If we measure the angular shift of the field from the z-axis by the q-like quantity:

$$\text{"q"} = \frac{B_y}{B_z} \qquad (5\text{-}21)$$

then the non-uniformity of the medium could as well be characterized by a shear parameter $\hat{s}$:

$$\hat{s} = \frac{d(\ell n\ "q")}{d(\ell n x)} = \frac{x}{L_s} \quad . \tag{5-22}$$

As we have seen in Chapter III, the quantity Σ, that contains the effects of shear, in an expansion around the magnetic axis to the order required to arrive at the "distilled" equation depends only linearly on the long variable ℓ. In the shear-Alfvén term of the ballooning equation, this quantity enters to the second power. This fact, plus the fact that the differential equation governing the mode is of the second order, decides the form of $\omega_A^2(x)$ that reproduces the "distilled" equation. Ultimately, the analogy rests on the assumption of a uniform current directed along the applied magnetic field in a plasma slab.

Equation (5-17) provides us an opportunity to look closely into the nature of the singularities. We assume that the regular piece of the solution in the vicinity of the point $u = \hat{\omega}$ can be expanded in power series as

$$V(u) = (u - \hat{\omega})^{\varsigma} [1 + C_1(u - \hat{\omega}) + C_2(u - \hat{\omega})^2 + \ldots]. \tag{5-23}$$

Then, by substitution in the equation, and identifying terms of equal powers, we obtain for non-vanishing $\hat{\omega}$ the indicial equation for the exponent:

$$s^2 = 0 \qquad (5\text{-}24)$$

and $C_1 = 0$, $C_2 = -1/2$. By the third of Barston's theorems in page 183, the singular part of the solution can then be represented as:

$$V(u) = \ell n\, |u - \hat{\omega}|\, [1 - (1/2)(u - \hat{\omega})^2 + \ldots] \qquad (5\text{-}25)$$

Fourier transforms of a function like this, understood in a generalized sense, exist, and it can be shown to be[64]:

$$\frac{e^{i\hat{\omega}\ell}}{\ell}\left(1 + \frac{i}{2\pi^2\ell^2} + \ldots\right), \qquad (5\text{-}26)$$

omitting a normalization constant. Then, it becomes apparent that the effect of the Fourier transformation is to map the singularities of Eq. (5-17) into the points $\ell = \pm\infty$ of Eq. (5-20). In fact, a theorem in the theory of generalized functions[65] states that for large ℓ, the expansion of $\tau(\ell)$ is given precisely by the above expression.

This correspondence between the asymptotic behavior of the solutions of the transformed equation, Eq. 5-20, and the singularities of the eigenmodes can also be seen in another, perhaps more direct way. If, in Eq. (5-20), we introduce the transformation

$$\tau(\ell) = \frac{F(\ell)}{\sqrt{1 + \ell^2}} \qquad (5\text{-}27)$$

we obtain for $F(\ell)$ the equation:

$$\frac{d^2F}{d\ell^2} + \left[\hat{\omega}^2 - \frac{1}{(1+\ell^2)^2}\right] F = 0 \quad . \tag{5-28}$$

The solutions of this equation can be conveniently represented as $e^{\pm i[\hat{\omega}\ell+\phi(\ell)]}$, where $\phi(\ell)$ is a function that, for large ℓ, gives a contribution to the phase that varies slower than $\hat{\omega}\ell$ and vanishes asymptotically. Note that the only singularities of Eq. (5-20) are located at infinity, and its solution is everywhere smooth and continuous. Going back to the space of the physical coordinate u, by taking the inverse transform of $T(\ell)$, we have:

$$V(u) = \frac{1}{2\pi} \int_{-\infty}^{+\infty} \frac{e^{i(\pm\hat{\omega}-u)\ell}}{\sqrt{1+\ell^2}} e^{\pm i\phi(\ell)} \, d\ell \tag{5-29}$$

This Fourier integral is a well-behaved function, except at the points $u = \pm\hat{\omega}$. When this happens, because $\phi(\ell) \to 0$ as $\ell \to \infty$, the integral diverges logarithmically.

The conclusion is that the dispersion relation for the continuum is determined by the asymptotic solution of the transformed equation. This applies equally well to the toroidal case, where the periodicities of the equilibrium involve necessarily the preliminary step of the ballooning transformation, that is a row of Fourier transforms. To investigate the asymptotic behavior of the ballooning equations, because of

the mixture of periodicities with the secularity associated to the shear, we have next to introduce a variable such as

$$\ell = \chi \oint \frac{\partial q_\ell}{\partial \psi} \, d\chi \tag{5-30}$$

distinct from the variable χ that is associated with the short scale variations of the solution. In general, the method of averages, that we illustrated in Chapter IV, will provide two coupled equations in the long variable, that describe the MHD spectrum of low frequency, long wavelength modes, both its unstable and stable sides. This lattest one may comprise discrete eigenfrequencies, that can be found only by a global treatment of the equations. The continuum, however, can be obtained in its entirety from the asymptotic solutions. From the previous analysis, it is clear that such solutions are of the form

$$T(\ell) \underset{\ell \to \infty}{\sim} \frac{e^{\pm i \Omega \ell}}{\ell} \tag{5-31}$$

where Ω is a function of the frequency and of the equilibrium quantities, that appear as averages over one cycle of the equilibrium. The local dispersion relation is then given by the values of Ω that make the phase of the Fourier integrals in the infinite series representation to vanish, corresponding to points in the domain of the physical space where the mode exhibits isolated logarithmic singularities. Namely, this local dispersion relation is

$$\Omega^2(\omega) = \left| \frac{S - n}{\oint (\partial q_\ell / \partial \psi)\, d\chi} \right|^2 \qquad (n=0, \pm 1, \pm 2, \ldots) \qquad (5\text{-}32)$$

where $S = N\omega$.

But before pursuing this theme of the continuous spectrum, let us reconsider the plasma slab model to amplify it and include some other interesting possibilities.

The Effect of Non-Uniform Gravity

The favorite artifice to simulate the effect of curvature of the field lines in a rectilinear model, like the slab that we are considering, is to introduce a gravitational force directed perpendicularly to the magnetic field that acts upon the heavy plasma. From a particle point of view, this analogy makes sense, because the particles that constitute the plasma, as they travel along a curved line, experience a centrifugal acceleration everywhere normal to the direction of the line and inversely proportional to the radius of curvature. From a fluid point of view, the effect of curvature finds its correspondent in the Raleigh-Taylor instability, where the gravity can de-stabilize the equilibrium of a heavy fluid supported by a less dense fluid. This is well known, and we shall not dwell on it.

In the previous section we showed how a plasma slab, carrying a uniform current, can simulate the shear in configurations with a rotational transform. We now propose to expand the model, by adding an artificial gravity, to simulate the

effects of curvature. Moreover, to reproduce the conditions prevailing in toroidal configurations, where the field lines see a varying curvature, that alternates from unfavorable to favorable with respect to the plasma pressure gradient, we allow for a non-uniform, periodically varying gravity. Also, we describe this gravity by two mutually perpendicular components, that model the normal and geodesic components of the curvature. A mode like this , in fact, was the basis of early investigations by B. Coppi on the ballooning instabilities[8,9,66].

We shall continue to assume a linear shear, generated by a uniform current distribution directed along the z-axis. The equilibrium field is then the same as specified by Eqs. (5-11) and (5-12), and varies slowly in the x-direction, with a scale length L_s. The magnetic pressure associated with this field is balanced by a density gradient with a profile characterized by a scale length r_p.

"Flux surfaces" are then represented by the planes perpendicular to the x-axis, where the field lines lie on. These are described by the straight lines

$$x = \text{constant} \tag{5-33}$$

$$y - \frac{xz}{L_s} = \text{constant} \tag{5-34}$$

The effect of the normal curvature on the perturbed quantities is simulated by a gravity $g_x(z)$, that points in the direction transverse to the "flux planes" and varies with the

z-coordinate.* Similarly, the geodesic curvature is represented by a gravitational force that, while being contained within the "flux surfaces", is also perpendicular to the field lines. In particular, at the plane x = 0, where the field lines are parallel to the z-axis, the only component of this force is $g_y(z)$, that is directed along the y-axis.

To keep a close analogy with the ballooning modes that we have been studying, we consider a mode of the form

$$\vec{\xi}(\vec{x}) = \hat{\vec{\xi}}(\vec{x}) \; e^{iN[y - (x/L_s)z] - i\omega t} \qquad (5\text{-}35)$$

where N is a large number ($N \gg 1$), and such that all fast variations across the field lines is contained in the phase factor. The amplitude $\hat{\vec{\xi}}(\vec{x})$ contains the much slower variation of the mode along the field lines, with a typical scale length of the same order of the period of the curvature, or, in our present terms, of the gravity.

In fact, we are interested in solutions that are periodic in z with the same period of the gravity, say, L_g. A quasi-mode, like the one of Eq. (5-35), involves obviously the same difficulties with respect to the question of periodicity that we found in the toroidal case, which, likewise, can be solved by recourse to the ballooning transformation. It is then understood that what we really mean is a superposition of quasi-modes:

---

*It would be more appropriate to introduce a coordinate ζ following the magnetic field line, and describe the variation of g in terms of this coordinate, rather than z. For simplicity, and with no loss of generality, we choose to describe the mode structure along the z-axis.

$$\vec{\xi} = e^{iN[y-(xz/L_s)]} \sum_{n=-\infty}^{+\infty} \hat{\vec{\xi}}(x,y,z+n\,L_g) e^{-i[N(x/L_s)]n\,L_g} \quad (5\text{-}36)$$

and that we are considering only the quasi-mode corresponding to n=0, from which the overall, periodic mode can be constructed a posteriori. As we discussed in Chapter II, z here does not represent actually the coordinate of the physical space, but its (Fourier) conjugate. However, because of the invariance of the periodic quantities under the ballooning transformation, it is still appropriate to keep the same notation and to think in terms of the coordinate space and field lines.

The equation describing the structure of the mode along the field line can be derived as in Chapter II. Of the original set of MHD equations, the equation of motion is modified to include the gravitational force on the perturbed density:

$$-\rho_m \omega^2 \vec{\xi} = -\nabla P_1 + \vec{J}_1 \times \vec{B} + \vec{J} \times \vec{B}_1 + \rho_1 \vec{g} \quad (5\text{-}37)$$

Gravity, however, is not included in the static equilibrium, that is satisfied, in the slab geometry, by

$$\nabla \left(P + \frac{B^2}{2}\right) = 0 \quad (5\text{-}38)$$

To eliminate the high-frequency modes, we assume, as before, that the perturbed pressure is given by

$$P_1 = - \vec{B}_o \cdot \vec{B}_1 \quad , \tag{5-39}$$

meaning that the total pressure (the sum of the fluid and magnetic pressures) remains constant in the perturbed state as well. To further decouple the analysis of the shear-Alfvén waves and instabilities of the analysis of slow sound waves, we consider only incompressible oscillations ($\nabla \cdot \vec{\xi} = 0$). Using the continuity equation,

$$\rho_1 + \nabla \cdot (\rho_o \vec{\xi}) = 0 \quad , \tag{5-40}$$

this last assumption permits us to evaluate the perturbed density as

$$\rho_1 = - \vec{\xi} \cdot \nabla \rho_o \quad . \tag{5-41}$$

For simplicity, we refer to the field lines lying on the y-z plane, that are parallel to the z-axis. To lowest order in an expansion in powers of the small parameter 1/N, the mode equation along these lines is:

$$\rho_m \frac{\omega^2}{B_o^2} (1 + \frac{z^2}{L_s^2}) T + \frac{d}{dz}[(1 + \frac{z^2}{L_s^2}) \frac{dT}{dz}] - \frac{1}{B_o^2} \frac{dP}{dx} [g_x(z) +$$

$$+ \frac{z}{L_s} g_y(z)] T = 0 \tag{5-42}$$

which is to be solved under the boundary condition that $\tau(z) \to 0$ as $|z| \to \infty$.

We specify now the gravity functions. For the "normal" gravity, we choose

$$g_x(z) = g_n(h + \cos k_y z) \tag{5-43}$$

where g_n is a constant, $k_g = (2\pi/L_g)$ and h is a constant, such that g_n h represents the average value of the curvature around the torus. For the geodesic component, in order to simulate properly the equilibrium conditions in a toroidal confinement, we choose a form that averages out to zero over a cycle of the equilibrium, and is shifted in phase by $\pi/2$ with respect to the normal gravity:

$$g_y(z) = g_n \sin k_g z \tag{5-44}$$

With this, we expect that the sheared Alfvén waves and gravitational instabilities in a plasma slab represent a model of the corresponding waves and pressure gradient-curvature driven instabilities to be found in toroidal geometry. In fact, if in Eq. (5-42) we introduce the replacements:

$$k_g z \to \theta, \quad \frac{z}{L} \to \hat{s}\theta, \quad dz \to R_o q_o d\theta, \quad L_s \to \frac{q_o^2}{(r/R_o)(dq/dr)},$$

$$\frac{dP}{dx} \to \frac{dP}{dr}, \quad g_n \to \frac{2}{R_o}, \quad k_g \to \frac{2\pi}{R_o q_o} \tag{5-45}$$

we obtain the following equation:

$$r^2(1+\hat{s}^2\theta^2)\tau = \frac{d}{d\theta}\left[(1+\hat{s}^2\theta^2)\frac{d\tau}{d\theta}\right] + G(h + \cos\theta + \hat{s}\theta\sin\theta)\tau \qquad (5\text{-}46)$$

which is a more general version of Eq. (2-60) in Chapter II, and describes the modes in a toroidal configuration characterized by circular concentric flux surfaces[11]. The dimensionless parameters r^2 and G were defined by Eqs. (3-82) and (4-22).

The general outline of Eq. (5-42) is familiar, from what we have seen in Chapter IV. It is a Hill's equation, one involving periodic coefficient functions, and can be solved by a perturbative technique that requires the introduction of two scale lengths. To take care of the periodicities in the short scale L_g, we define a variable η:

$$\eta = k_g z \qquad (5\text{-}47)$$

and treat separately the secular behavior of the solution by means of a "long" variable, defined as:

$$\xi = \frac{z}{L_s} \qquad (5\text{-}48)$$

In terms of these two independent variables, Eq. (5-42) becomes:

$$r_p^2(1+\ell^2)T = (1+\ell^2)\frac{\partial^2 T}{\partial \eta^2} + \frac{1}{k_g L_s}\frac{\partial}{\partial \ell}\left[(1+\ell^2)\frac{\partial T}{\partial \eta}\right] + \frac{1}{k_g L_s}(1+\ell^2)\frac{\partial^2 T}{\partial \ell \partial \eta}$$

$$+ \frac{1}{k_g^2 L_s^2}\frac{\partial}{\partial \ell}\left[(1+\ell^2)\frac{\partial T}{\partial \ell}\right] + G_p[h + \cos\eta + \ell \sin\eta]T \qquad (5\text{-}49)$$

where

$$r_p^2 = -\frac{\rho_m \omega^2}{k_g^2 B_o^2} \qquad (5\text{-}50)$$

and

$$G_p = -\frac{g_n}{k_g^2 B_o^2}\frac{d\rho}{dx} . \qquad (5\text{-}51)$$

We adopt as expansion parameter the quantity $(k_g L_s)^{-1}$ that measures the ratio of the connection length to the shear length scale, and is much less than one for a configuration with weak shear. The solution is then expanded as:

$$T = T_o(\ell,\eta) + \frac{1}{k_g L_s} T_1(\ell,\eta) + \frac{1}{(k_g L_s)^2} T_2(\ell,\eta) + \ldots \qquad (5\text{-}52)$$

and is required to be periodic in the variable η with period 2π. We assume that the parameters entering Eq. (5-49) can be ordered as $G_p \sim h \sim (k_g L_s)^{-1}$, $r_p^2 \sim (k_g L_s)^{-2}$, and write, formally,

$$G_p = \sqrt{2}\, G_1 (k_g L_s)^{-1} \qquad (5\text{-}53a)$$

$$h = (h_1/\sqrt{2})(k_g L_s)^{-1} \qquad (5\text{-}53b)$$

$$r_p^2 = r_2^2 (k_g L_s)^{-2} \tag{5-53c}$$

where G_1, h_1, r_2^2 are numbers of order unity and the factor $\sqrt{2}$ was introduced in the definitions for convenience.

The solution follows exactly the same steps as in the previous chapter, but since $\ell/\eta = (k_g L_s)^{-1}$ is now a first order quantity in the expansion parameter, we need to carry out the expansions only to the second order to obtain the eigenvalue equation. The lowest order equation, $(1+\ell^2)\ (\partial^2 T_o/\partial\eta^2) = 0$ just tells us that T_o is a function of ℓ. The first order equation is then simply:

$$(1+\ell^2)\ \frac{\partial^2 T_1}{\partial\eta^2} + G_1\sqrt{2}\ [\cos\eta + \ell \sin\eta]T_o = 0 \tag{5-54}$$

and is solved by

$$T_1 = \frac{G_1\sqrt{2}}{1+\ell^2}\ [\cos\eta + \ell \sin\eta]T_o \tag{5-55}$$

The next order equation, after being averaged out over its periodicities on η, already gives an equation for T_o:

$$r_2^2\ (1+\ell^2)T_o = \frac{d}{d\ell}\ [(1+\ell^2)\ \frac{dT_o}{d\ell}] - B_p\ T_o \tag{5-56}$$

where

$$B_p = G_1\ (-h_1 - G_1) \tag{5-57}$$

The structure of this equation differs from the structure of the "distilled" equation for toroidal geometry in that the

specifically ballooning term, of the form $A/(1+\ell^2)$, is missing. The asymptotic solutions of Eq. (5-56) are of the form $1/\ell^{2\gamma}$, where the exponent γ is given by:

$$\gamma = \frac{1}{4} \pm \frac{1}{4} \sqrt{1 - 4\, G_1(h_1+G_1)} \tag{5-58}$$

and instabilities, of the flute type, appear when the discriminant becomes negative. Explicitly, the stability criterion is:

$$G_1^2 + h_1 G_1 - 1/4 < 0 . \tag{5-59}$$

Now, in a torus, the depth of the magnetic well is measured by the parameter:

$$h = \frac{r}{R_o} \left(\frac{1}{q_o^2} - 1\right) \tag{5-60}$$

Recalling the definitions of G_1 and h_1 given by Eq. (5-53) and substituting L_s and $d\rho/dx$ according to the prescription of Eq. (5-45), Eq. (5-59) can be recast as:

$$\frac{1}{4} \left(\frac{q'}{q_o}\right)^2 + \frac{2P'}{rB_o^2} (1 - q_o^2) < 0 \tag{5-61}$$

where primes denote derivatives with respect to r, and we have dropped terms of order β^2. In this expression, we recognize immediately the Mercier criterion under the more familiar form

that was given to it by Shafranov and Yurchenko[67]. If the stabilization by the magnetic well vanishes, so that $h_1 = 0$, we retain higher order effects of the pressure gradient, and the criterion becomes $G_1 < 1/2$, or, introducing the substitutions that are appropriate to establish the analogy with a torus,

$$- 2P' \frac{R_o q_o^2}{B_o^2} < \pi\sqrt{2}\,\hat{s} \qquad (5\text{-}62)$$

The reason why the model fails to simulate the true ballooning instabilities can be found in the orderings specified by Eq. (5-53). We recall that, in the derivation of the "distilled" equation for the toroidal equilibrium, we had to assume that the pressure gradient and the shear are related by $\hat{s} \sim G^2$, as indeed is the correct dependence among these equilibrium quantities in an expansion about the magnetic axis. Here, however, we have assumed a linear relation of the form $\hat{s} \sim G$, that leads prematurely to an eigenvalue equation for the modes, and, therefore, contains only the dominant interchanges. We stress that, if $q_o = 1$ and the stabilizing effects of the magnetic well are suppressed, this is the only consistent ordering, and the stability criterion is given by Eq. (5-62).

For a nonvanishing magnetic well, however, it is still possible to manufacture an equation to describe the ballooning instabilities and save the model configuration of circular concentric flux surfaces, if we give the appropriate treatment to Eq. (5-46). For this, we reintroduce the original orderings among the small parameters, putting, as we did in Chapter IV,

$$\hat{s} = \frac{G^2}{4g} \tag{5-63a}$$

and

$$r^2 = r_4^2 G^4 \tag{5-63b}$$

where g and r_4^2 are numbers of order unity. To allow for a full range of possibilities, we write the equilibrium parameter h as

$$h = h_a G + h_b G^3 \tag{5-64}$$

since we now have resources to include higher order effects of the pressure gradient in the final equation. This is, in fact, the simplest device to arrive at an eigenvalue equation with the desired structure.*

We introduce two variables θ and $\ell = \hat{s}\theta$ assumed to be independent, and expand the function T in powers of G. Going over the steps that by now should be well known, we find that T_o depends only on the stretched variable and that T_1 is again given by:

$$T_1 = \frac{T_o}{1+\ell^2} (\cos\theta + \ell \sin\theta) \tag{5-65}$$

---

*A similar treatment was given by H.R. Strauss, who considered a linear dependence of h on G in his investigations of the effects of finite resistivity on the growth rates of ballooning modes[68].

To second order, however, we find an equation as

$$(1+\ell^2)\,(\partial^2 T_2/\partial\theta^2) + (\cos\theta + \ell\sin\theta)T_1 + h_a T_o = 0 \qquad (5\text{-}66)$$

and the requirement that T_2 must be a periodic function of θ gives a constraint on the equilibrium parameter h_a:

$$h_a = -\frac{1}{2} \qquad (5\text{-}67)$$

The solution of Eq. (5-66) is then

$$T_2 = \frac{T_o}{(1+\ell^2)^2}\left[\left(\frac{1-\ell^2}{8}\right)\cos 2\theta + \frac{\ell}{4}\sin 2\theta\right] \qquad (5\text{-}68)$$

To the next order, we obtain

$$(1+\ell^2)\frac{\partial^2 T_3}{\partial\theta^2} + \frac{1}{4g}(1+\ell^2)\frac{\partial^2 T_1}{\partial\theta\,\partial\ell} + \frac{1}{4g}\frac{\partial}{\partial\ell}\left[(1+\ell^2)\frac{\partial T_1}{\partial\theta}\right] +$$

$$+ (\cos\theta + \ell\sin\theta)T_2 - \frac{T_1}{2} = 0 \qquad (5\text{-}69)$$

where we have already substituted h_a by $(-1/2)$. This automatically guarantees the periodicity of T_3, which is

$$T_3 = \frac{1}{2g}\frac{T_o}{1+\ell^2}\cos\theta + \left[\left(\frac{1}{2g} - \frac{7}{16}\right)\ell\sin\theta - \left(\frac{7}{16} + \frac{\ell^2}{2g}\right)\cos\theta\right]T_o\,, \qquad (5\text{-}70)$$

omitting terms that involves derivatives of T_o and terms in $\cos 3\theta$ and $\sin 3\theta$, that will average out to zero in the final equation. This one, obtained by taking the averages over one period of the equilibrium of the fourth-order expanded equation, is:

$$\frac{d}{d\ell}\left[(1+\ell^2)\frac{dT_o}{d\ell}\right] + \left(\frac{A}{1+\ell^2} - B\right)T_o = \hat{\Gamma}^2 (1+\ell^2)T_o \qquad (5\text{-}71)$$

where

$$A = 4g - \frac{7}{2} g^2 \qquad (5\text{-}72a)$$

$$B = 16\, h_b\, g^2 \qquad (5\text{-}72b)$$

and we have defined the dimensionless growth-rate parameter as

$$\hat{\Gamma}^2 = \Gamma_4^2 \frac{G^4}{\hat{s}^2} \qquad (5\text{-}73)$$

Then, at least formally, we were able to reproduce the structure of the mode equation that we laborously derived for toroidal geometry taking into account all the intricacies of the equilibrium. Clearly, the "ballooning term" $A/(1+\ell^2)$ appears as a result of the linear dependence of the equilibrium parameter h on the pressure gradient. The "interchange term" -B, in this formulation, appears as a result of higher order effects of the equilibrium on the mode, as it is indeed necessary if the specifically ballooning characteristics of the instability are not to be masked. If, however, we re-establish the predominance of this term, by ordering a posteriori

$$h_b \sim \frac{1}{G} \frac{r}{R_o} \left(\frac{1}{q_o^2} - 1\right) \tag{5-74}$$

with $G \ll r/R_o$, we again make the interchanges overwhelm the ballooning instabilities. It is not difficult to show that, in this case, the stability criterion, once more, takes the precise form of Eq. (5-61).

The Continuum in the Vicinity of the Axis

After this digression, we return to the theme of the continuum. To illustrate the ideas developed in the previous sections, we consider in some detail the spectrum of the Alfvén waves and slow compressional acoustic waves as described by the second order differential "distilled" equation derived in Chapter IV. As we have seen, the spectrum is given by solving the local dispersion relation at the singular points in the domain of the physical poloidal variable, which are associated with the oscillating asymptotic behavior of the eigenfunctions in the conjugate space of the variable. In the limit of large values of ℓ, the solution of Eq. (4-42) is:

$$T(\theta) = \frac{e^{\pm i \Omega \hat{s} \theta}}{\sqrt{1 + \hat{s}^2 \theta^2}} , \tag{5-75}$$

where Ω^2 is given by Eq. (4-44), and we have replaced ℓ by $\hat{s}\theta$. The representation of the eigenmode in the physical space involves a summation of the Fourier integrals

$$\int_{-\infty}^{+\infty} \frac{e^{-i(S-n \pm \Omega\hat{s})\theta}}{\sqrt{1+\hat{s}^2\theta^2}}\, d\theta = \frac{2}{\hat{s}} K_o\left(\left|\frac{S-n}{\hat{s}} \pm \Omega\right|\right) \qquad (5\text{-}76)$$

where K_o is a modified Bessel function, which exhibits a typical logarithmic singularity at the points where the argument vanishes. The local dispersion relation is then

$$\Omega^2 = \left(\frac{S-n}{\hat{s}}\right)^2 \qquad (n=0, \pm 1, \pm 2, \ldots) \qquad (5\text{-}77)$$

or, substituting Ω^2 as given by Eq. (4-44),

$$\hat{\Gamma}^2 \left(1 + \frac{2q_o^2}{1 + (V_{Ao}^2/V_s^2)\,\hat{s}^2\,\hat{\Gamma}^2}\right) = -\left(\frac{S-n}{\hat{s}}\right)^2 . \qquad (5\text{-}78)$$

Introducing the notation

$$\hat{\omega}_s^2 = \frac{\omega^2 (R_o q_o)^2}{V_s^2} \qquad (5\text{-}79)$$

and recalling that

$$\hat{\Gamma}^2 = -\frac{\omega^2 (R_o q_o)^2}{\hat{s}^2\, V_{Ao}^2} ,$$

we can recast the last expression as

$$\hat{\omega}_s^4 - \left[1 + 2q_o^2 + \frac{V_{Ao}^2}{V_s^2}(S-n)^2\right]\hat{\omega}_s^2 + \frac{V_{Ao}^2}{V_s^2}(S-n)^2 = 0 \qquad (5\text{-}80)$$

a quadratic equation with two real, positive roots, given by

$$\hat{\omega}_s^2 = \frac{1}{2}\left\{1+2q_o^2 + \frac{V_{Ao}^2}{V_s^2}(S-n)^2 \pm \sqrt{\left[1+2q_o^2 + \frac{V_{Ao}^2}{V_s^2}(S-n)^2\right]^2 - \frac{4V_{Ao}^2}{V_s^2}(S-n)^2}\right\} \qquad (5\text{-}81)$$

We refer to the larger root, corresponding to the positive sign, as the Alfvén branch of the spectrum, and to the smaller root, obtained by taking the negative sign, as the slow magneto-acoustic branch. The gap between the two branches is $\Delta\hat{\omega}_s^2 = 1+2q_o^2$.

Precisely on the magnetic axis, where the shear vanishes, the frequencies of the slow sound waves degenerate at $\hat{\omega}_s^2 = 0$ and the spectrum reduces to the Alfvén branch, with a characteristic parabolic-like dispersion relation,

$$\hat{\omega}_A^2 = (S - n)^2 \qquad (5\text{-}82)$$

where $\hat{\omega}_A$ is the frequency normalized to the Alfvén speed:

$$\hat{\omega}_A^2 = \frac{\omega^2(R_o q_o)^2}{V_{Ao}^2} \qquad (5\text{-}83)$$

In general, the behavior of the Alfvén branch is dominated by the factor $(S-n)^2$. For example, in the vicinities of the mode rational surfaces, where this factor is small, the roots of the quadratic equation can be conveniently expressed as:

$$\hat{\omega}_s^2 = \frac{V_{Ao}^2}{V_s^2}(S-n)^2 \quad , \tag{5-84}$$

$$\hat{\omega}_A^2 = \frac{V_s^2}{V_{Ao}^2}(1 + 2q_o^2) + \left(\frac{4q_o^2}{2q_o^2 + 1}\right)(S-n)^2 \tag{5-85}$$

It is interesting to note that in the limit $\gamma_c \to \infty$, which makes the ratio of the velocities V_{Ao}^2/V_s^2 to approach unity, the frequencies of the slow sound waves and the Alfvén waves are respectively:

$$\hat{\omega}_s^2 = (S-n)^2 \tag{5-86}$$

$$\hat{\omega}^2 = \frac{V_s^2}{V_{Ao}^2}(1 + 2q_o^2) \quad , \tag{5-87}$$

showing that, at the rational surfaces, the modes assume characteristics similar to the incompressible ones. Far from the mode rational surfaces ($S-n \gg 1$), the Alfvén branch is again parabolic:

$$\hat{\omega}_A^2 = 2q_o^2 \left(\frac{V_s^2}{V_{Ao}^2}\right) + (S-n)^2 \qquad (5\text{-}88)$$

while the slow magnetoacoustic branch approaches a constant value:

$$\hat{\omega}_s^2 = 1 \quad , \qquad (5\text{-}89)$$

that can be identified as an accumulation point of the stable spectrum, at which all surfaces in the plasma resonate.

These features can be found in Figs. 5.2a and 5.2b, where we plotted the two branches of the spectrum for specific values of the equilibrium parameters. We chose $q_o = 1$, and the local beta, defined as $\beta = 2P/B_o^2$ was taken to be 0.1, so that the ratio of the characteristic speeds is $V_{Ao}^2/V_s^2 = 13$, assuming $\gamma_c = 3/5$. The value of S_o, in the plots, is arbitrary, and the values of n run from 0 to 5. By varying the value of β, each of the lines in this figure would generate a band, which would represent the contribution to the continuum of all resonating surfaces covered by the respective range of values of β. An example of a graph of this type can be found in Ref. 77. In our case, the artifice by which we incorporated the compressibility effects in the "distilled" equation, by treating the quantity V_{Ao}^2/V_s^2 formally as of order ρ^{-4}, makes us to be sure that we cannot extend the analysis too far from the axis. At any rate, our aim here was only to illustrate the general ideas about the continuum spectrum using the simple analytical model afforded by the "distilled" equation.

Fine Scale Effects

A question of interest is to know if more detailed descriptions of the plasma, e.g., the kinetic equations, would lead to a stable spectrum with a discrete structure. This is tantamount to asking the question if, by inclusion of effects that lie outside the frame of the ideal MHD, as those arising from the finite gyroradius of the individual particles that constitute the plasma and the existence of trapped particles, the singularities of the (stable) eigenmodes would be eliminated.

The definitive answer to this question, of course, can be provided only by a full kinetic treatment of the problem, which is not the approach that we are adopting in this thesis. However, without abandoning the context of MHD, it is still possible to assess the consequences of the fine scale effects on the mode structure by a slight modification of our equations. By fine scale effects, we mean effects that are seen by the waves with a wavelength comparable to the ion gyroradius. Indeed, Timofeev[69], in his paper on the stability of Alfvén waves in an inhomogeneous plasma slab, pointed out that if the spatial structure of the perturbations in the ideal fluid is described by the normal mode equation:

$$\hat{L}\, V = 0 \ , \qquad (5\text{-}90)$$

Figure 5.2a: The Continuous Spectrum of Alfvén Waves in the Vicinity of the Magnetic Axis for $\beta = 0.1$, $q_o = 1$.

Figure 5.2b: The Continuous Spectrum of Slow Sound Waves in the Vicinity of the Magnetic Axis for $\beta = 0.1$, $q_o = 1$.

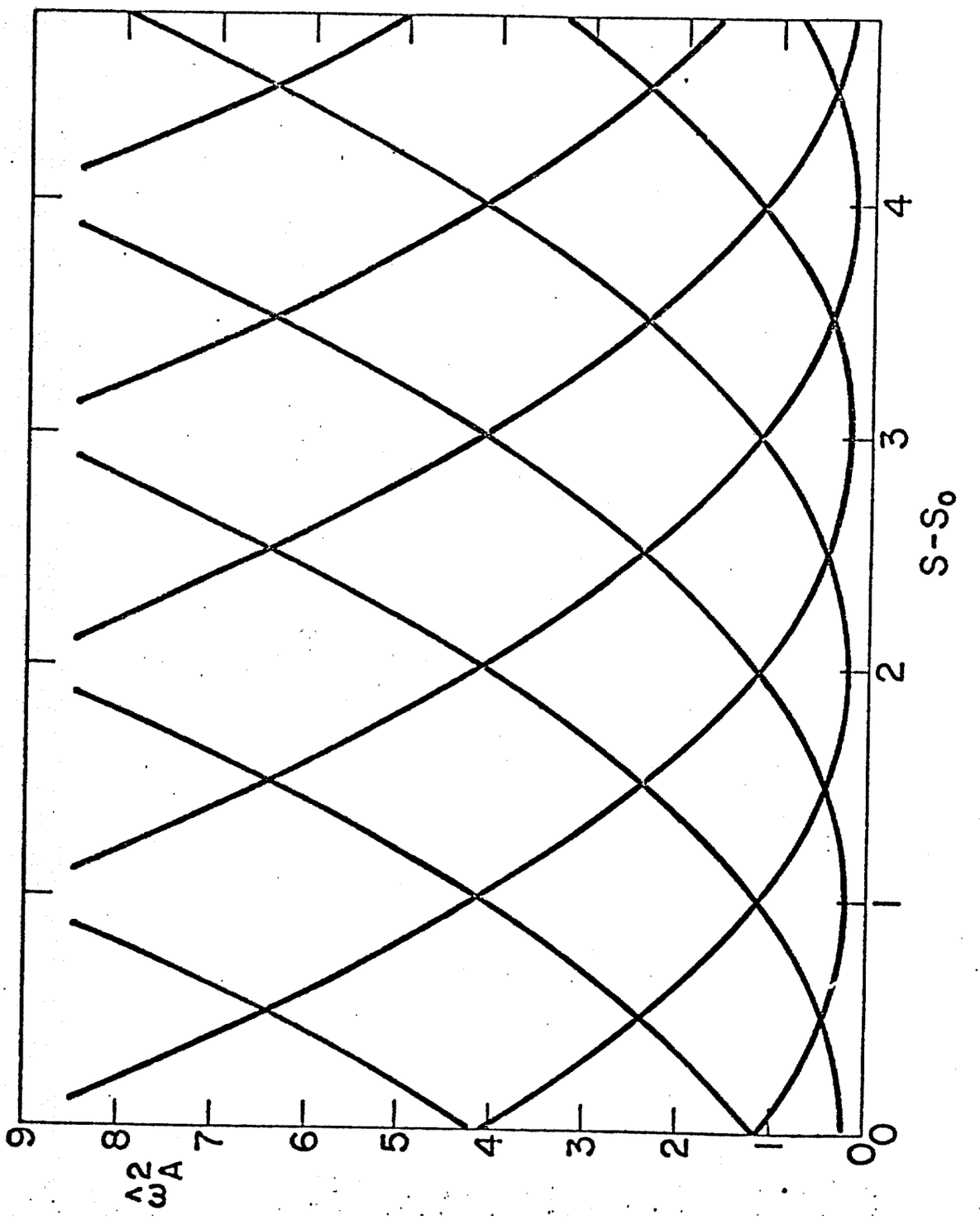

Figure 5.2a

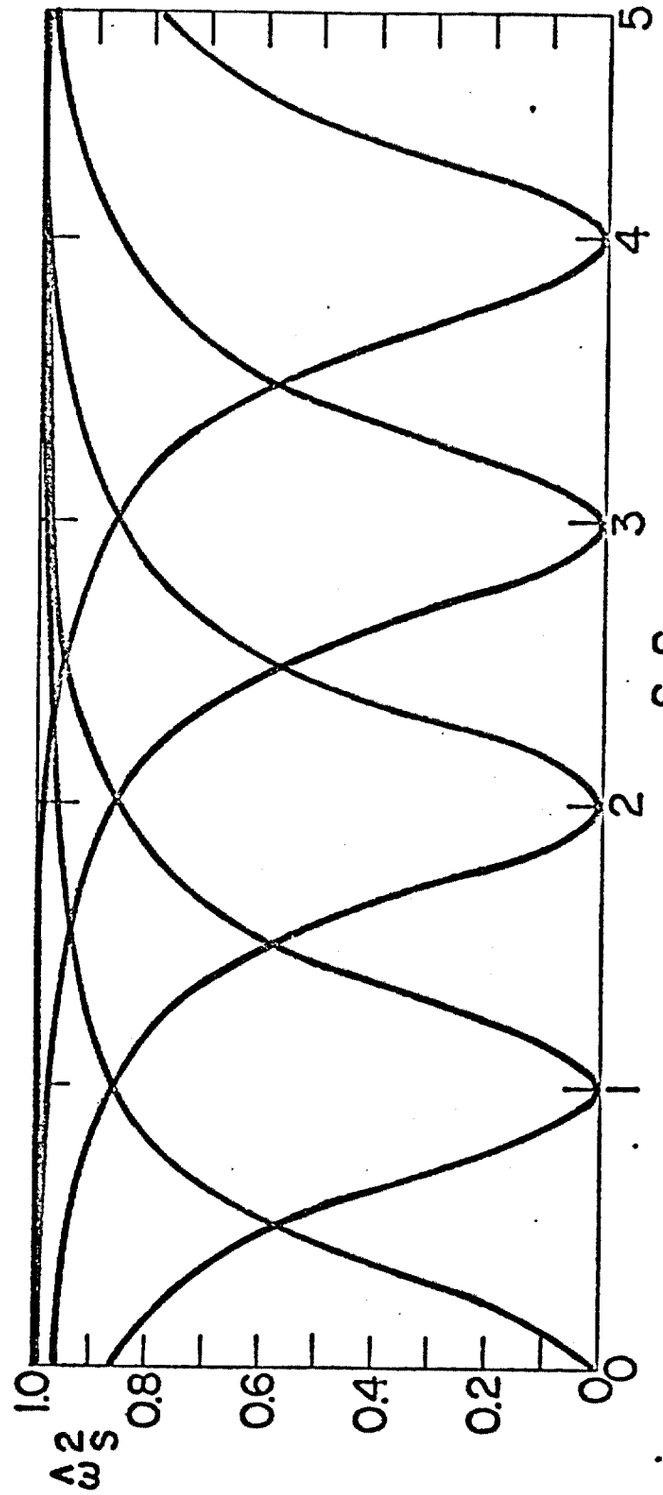

Figure 5.2b

where $\hat{L}$ is a second-order differential operator, then to take into account the effects of the finite Larmor radius, we have to replace Eq. (5-90) by:

$$\omega^2 \alpha \frac{\partial^4 V}{\partial x^4} + \hat{L} V = 0 \qquad (5\text{-}91)$$

Here, x represents the direction along which the plasma is non-homogeneous and the factor α is proportional to the square of the gyroradius of the ions of the bulk plasma:

$$\alpha = \frac{7}{4} \rho_i^2 \qquad (5\text{-}92)$$

*

Following this prescription, we re-examine the problem of the normal modes in the plane stratified medium, by considering the equation:

$$\omega^2 \alpha \frac{d^4 V}{dx^4} + \frac{d}{dx}\left[(\omega^2 - \omega_A^2(x))\frac{dV}{dx}\right] - k^2[\omega^2 - \omega_A^2(x)]\, V = 0 \qquad (5\text{-}93)$$

instead of Eq. (5-6). In the case of a uniform current distribution directed along the z-axis, using the same transformation and defining the dimensionless frequency the same way as before, this equation becomes:

$$\lambda^2 \hat{\omega}^2 \frac{d^4 V}{du^4} + \frac{d}{du}\left[(\hat{\omega}^2 - u^2)\frac{dV}{du}\right] - (\hat{\omega}^2 - u^2)\, V = 0 \qquad (5\text{-}94)$$

---

*The coefficient given by Timofeev, actually is $\alpha = [(7/4) - i\delta]\rho_i^2$, where δ is a correction that depends on the effective collision frequency of trapped electrons. We are neglecting this further effect.

where

$$\lambda^2 = \alpha k^2 = \frac{7}{4} \rho_i^2 k^2 \qquad (5\text{-}95)$$

Rosenbluth and Rutherford[70], investigating the excitation of Alfvén waves by high-energy ions in tokamaks, had also found that the correction to the ideal operator is a fourth-order derivative term, with exactly this same proportionality factor.

We now introduce the Fourier transform of the perturbation, defined by Eq. (5-19), and we obtain the equation:

$$\frac{d}{d\ell} \left[(1 + \ell^2) \frac{dT}{d\ell}\right] + \hat{\omega}^2 \left[(1 + \ell^2) - \lambda^2 \ell^4\right] T = 0 \qquad (5\text{-}96)$$

that can be further converted to

$$\frac{d^2F}{d\ell^2} + \left[\hat{\omega}^2 \left(1 - \frac{\lambda^2 \ell^4}{1+\ell^2}\right) - \frac{1}{(1+\ell^2)^2}\right] F = 0 \qquad (5\text{-}97)$$

using again the transformation of the dependent variable defined in Eq. (5-27). For small values of ℓ, the solution in general exhibits oscillations. In the asymptotic limit $\ell^2 >> 1$, this equation can be approximated by

$$\frac{d^2F}{d\ell^2} + \hat{\omega}^2 (1 - \lambda^2 \ell^2) F = 0 \quad , \qquad (5\text{-}98)$$

the familiar equation for a quantum-mechanical harmonic oscillator. In this region of values of ℓ, the oscillations still remain for $\lambda^2 \ell^2 < 1$, while for $\lambda^2 \ell^2 > 1$ it vanishes

exponentially. Then it appears that, by inclusion of the fine scale effects, the function $F(\ell)$ becomes square integrable, and the solution is regularized around the point where we had, in the previous ideal case, a logarithmic singularity. This, otherwise, can be seen directly from Eq. (5-94), where the points $u = \pm \hat{\omega}$ are now ordinary points of the differential equation. In the neighborhood of these points, over a range that depends on the size of the coefficient multiplying the highest-order derivative term, a "boundary layer" develops, where the solution increases sharply, but remains always bounded.

The analytical treatment of the exact equation is difficult. If, however, we assume that Eq. (5-98) is a reasonably good global approximation of Eq. (5-97), then the eigenvalues, corresponding to stable, well-behaved normal modes, can be estimated as

$$\hat{\omega} = 2\lambda \left(n + \frac{1}{2}\right) \qquad (n=0, 1, 2, \ldots) \qquad (5\text{-}99)$$

This approximation holds better for large values of $\hat{\omega}$, in which case the term $1/(1+\ell^2)^2$ in Eq. (5-97) is negligible also in the range of small values of ℓ. But regardless the question of accuracy of this result, the important fact is that the continuum, by virtue of the non-vanishing gyroradius of the ions, has apparently been split into infinitely many discrete eigenvalues, separated by

$$\hat{\Delta\omega} \sim 2\lambda \sim 7\, \rho_i\, k\,. \qquad (5\text{-}100)$$

These conclusions, however, have to be seen with caution. Pursuing the analogy that we found between the plasma slab and the vicinities of the magnetic axis of a toroidal confinement, we may reinterpret ℓ in Eqs. (5-20) and (5-97), as the "stretched" variable of a "distilled" equation, and k_ℓ as physically meaning $k_\perp$, the transverse wave-number of the mode. Now, the validity of MHD theory is restricted to the description of phenomena for which $k_\perp \rho_i << 1$. We may expect that the quasi-fluid model discussed in this section permits us to extend this range to roughly $k_\perp \rho_i \sim 1$, and this gives the limit of validity of Eqs. (5-97) and (5-98) as $\lambda^2 \ell^2 \sim 1$. It turns out, however, that it is exactly in this range of values of ℓ that the solutions change from oscillating to an evanescent behavior. Then, it is not clear if the model really supports the inclusion of fine-scale effects to the extent that is required to decide if the basic properties of the continuous medium are modified or not. A similar doubt was raised in Ref. 71, where the consideration of a quadratic form of the mode equations indicated that the inclusion of the finite Larmor radius term does not seem to provide the asymptotic behavior that is needed to regularize the eigenmodes. With the matter as yet undecided, we may only say that the tendencies predicted by this model point in the direction that kinetic effects in the range $k_\perp \rho_i > 1$, that cannot be simulated properly by fluid-like equations, ultimately will lead to well-behaved stable normal modes, associated with a discrete structure of the spectrum.

The Time-Dependent Equation

We now return to the realm of pure MHD to study the temporal evolution of disturbances of the Alfvén-type[72]. The substitution $\omega^2 \rightarrow -(\partial^2/\partial t^2)$ transforms Eq. (4-42) into a second-order partial differential equation both in time and in the space-like variable, of the hyperbolic type, that can be solved for suitable initial conditions. However, even without solving the initial value problem, a great deal of information about the transient behavior of the disturbances can be obtained from the normal mode equation. For this, it is convenient to use the transformation defined by Eq. (5-27), that converts Eq. (4-42) into

$$\frac{d^2}{d\xi^2} F(\xi) = [V(\xi) + \hat{r}^2] F \qquad (5\text{-}101)$$

where

$$V(\xi) = \frac{B}{1 + \xi^2} - \frac{A - 1}{(1 + \xi^2)^2} \qquad (5\text{-}102)$$

Equation (5-101) has the same form of an equation describing the steady-state motion of a quantum mechanical wave-particle in a potential field $V(\xi)$. Concepts as scattering and transmission of incident waves can then be used to gain some insight into the characteristics of propagation of wave-packets constructed by superposition of single-frequency modes. The shape of the equivalent potential $V(\xi)$ is determined by the curvature functions A and B, which depend, or their turn, on the

equilibrium through the independent parameters g and β_p. To simplify the analysis, we may consider the limit $\beta_p \to \infty$, which reduces the dependence to a single parameter without modifying the structure of the potential.

Perhaps the most convenient way to visualize the changing effects of the equilibrium on this potential as g is varied is by means of a turning point analysis. If we write $\hat{\Omega}^2 = -\hat{\Gamma}^2$, with $\hat{\Omega}^2 > 0$ for stable modes, these are determined as the roots of the equation $V(\ell_T) = \hat{\Omega}^2$. Explicitly, we have:

$$\ell_T^2 = \frac{B - 2\hat{\Omega}^2 \pm \sqrt{B^2 - 4(A-1)\hat{\Omega}^2}}{2\hat{\Omega}^2} \tag{5-103}$$

The number of turning points seen by the incident wave on the potential barrier depends both on the frequency and on the specific equilibrium conditions, and, as it is apparent from the above expression, may be four, two or zero. For this discussion, it is convenient to introduce the normalized squared frequencies:

$$\hat{\omega}_1^2 = \frac{B^2}{4(A-1)} \tag{5-104}$$

$$\hat{\omega}_2^2 = B - A + 1 \tag{5-105}$$

which are plotted, as a function of g, in Fig. 5.3. For most of the first stable region, $\hat{\omega}_1^2$ is negative, and the two terms of $V(\ell)$ add together to produce a potential with the shape of a

hill. The frequency $\hat{\omega}_2^2$ is precisely the height of this hill, and separates the higher frequencies, which are little disturbed by the barrier, from the lower ones, that undergo a substantial amount of scattering. Note that for all this region, the value of the $\hat{\omega}_2^2$ is below unity, so that the behavior of propagating wavepackets will be controlled mostly by the time-harmonic components that do not see the barrier. Also, increase of g has the effect of reducing the height of the hill, as we approach the first threshold of instability. When we reach, however, the value g = 0.279, the squared frequency $\hat{\omega}_1^2$ changes sign, so that the second term in Eq. (5-102) subtracts from the first; with a slight increase in g (precisely at g = 0.284), the competition between the two terms, because of their different dependence on ξ, has the net effect of producing <u>two</u> potential hills, around a local minimum at ξ = 0. This gives rise to the possibility of four turning points, as for the modes with (squared) frequencies that lie below the top of the twin hills. This condition is stated as $\omega^2 < \hat{\omega}_1^2$. In the first stable regime, the range of values of g for which this profile of the potential occurs is quite narrow, since at g = 0.301, we reach already marginal stability.

In this description of the equilibrium conditions by means of an equivalent potential, unstable eigenmodes can be viewed as "bound" states. Note that in the interval $0.29 < g < 1.84$, where $\hat{\omega}_2^2$ is negative, the shape of $V(\xi)$ is dominated by a "well" around ξ = 0 surrounded by two shallow hills. The difference

Figure 5.3: Sketch of the Several Frequency Domains for Equilibria Characterized by Circular Flux Surfaces in the Vicinity of the Axis and $\beta_p = \infty$.

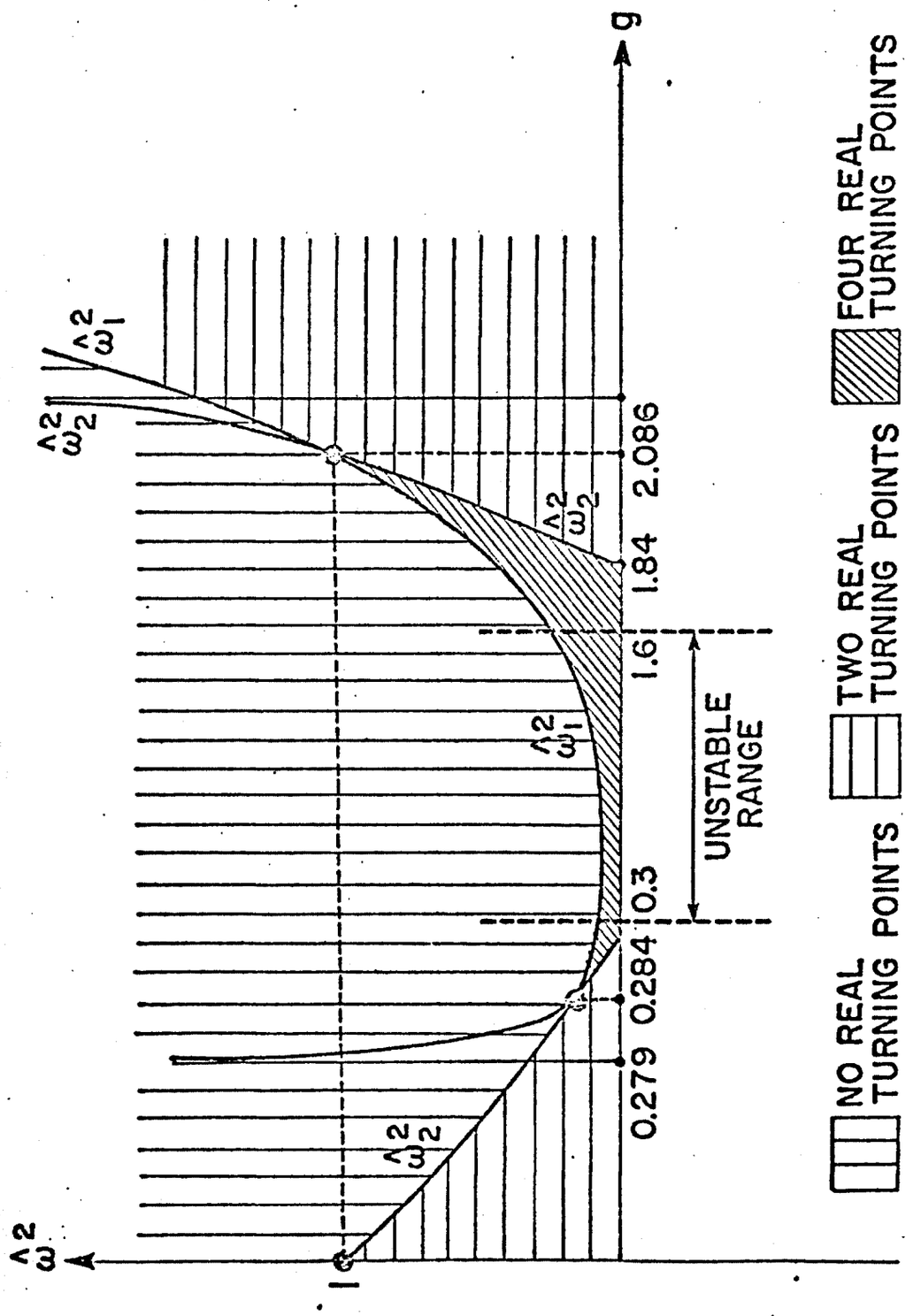
g
$\hat{\omega}_1^2$
$\hat{\omega}_2^2$
$\hat{\omega}_2^2$
$\hat{\omega}_1^2$
$\hat{\omega}_2^2$
$\hat{\omega}^2$
A
I
2.086
1.84
1.6
0.3
0.284
0.279
UNSTABLE RANGE
NO REAL TURNING POINTS
TWO REAL TURNING POINTS
FOUR REAL TURNING POINTS

between the above boundaries and the actual critical values of g for marginal stability ($g_I = 0.301$, $g_{II} = 1.6$) can be explained by the minimum depth of the "well" required for the existence of "bound" states. In the vicinity of the second threshold of instability, therefore, this form of the potential (two local maxima around a shallow "well") still persist for a relative wide range of values of g. Only at g = 2.086, where the two curves $\hat{\omega}_1^2$ and $\hat{\omega}_2^2$ intercept, the potential resumes the form of a simple hill. Further increase of g has the effect of increasing more and more the peak of the potential, that is given again by $\hat{\omega}_2^2$. Generally speaking, as we increase g above ~2, we may expect that the harmonics of wave packets that see two turning points will become increasingly important, and a larger fraction of the spectral components will experience reflection from the barrier.

These trends of the equivalent potential with the equilibrium parameter g can be visualized in Fig. 5.4, where we plotted V(ℓ) for g = 0 (first stable region), g = 1 (corresponding to instability), g = 1.6 (second threshold of marginal stability) and g = 3 (second stable region).

In the asymptotic limit of large ℓ, the solution of Eq. (5-101), in the geometrical optics approximation is

$$F(\ell) \sim \exp\left(\pm i\hat{\Omega} \int^{\ell} \sqrt{1 - \frac{V(\ell)}{\hat{\Omega}^2}}\, d\ell\right) \qquad (5\text{-}106)$$

and therefore the group velocity of a wave packet with a narrow distribution of frequencies about $\hat{\Omega}$ is

$$V_g = \frac{1}{\sqrt{1 - \frac{V(\ell)}{\hat{\Omega}^2}}} \quad . \tag{5-107}$$

For large values of ℓ, under any equilibrium condition, $V(\ell)$ vanishes, and the velocity of propagation is uniform and equal to unity. As far as the potential $V(\ell)$ is not seen, no distortion of the original waveform occurs. In the first stable regime, as we have shown, except for conditions approaching instability, the potential barrier takes the shape of a quite shallow hill, and fairly localized around $\ell = 0$. Then, for most of the time, the wavelets follow the asymptotic pattern. Only as the disturbances come close to the origin at $\ell \sim 1$, and start to "climb" the potential hill, new effects appear. The velocity of propagation is augmented, and the initial shape starts to distort because of the increasing importance of the low frequency components that are reflected back. But since these are restricted to $\hat{\Omega}^2 < 1$, the barrier is not able to force the wave packet to recede entirely. Rather, the collision is followed by a partial transmission in addition to the scattering backwards. On the other hand, deep into the second stable region (i.e., for $g > 2$), the effects of $V(\ell)$ are felt on a wider range of ℓ, and the top of the hill overlooks a larger fraction of wavelets. Since the curvature function B is now large, the phase velocity of the modes becomes a strong function of frequency and position. Then, dispersive effects start to appear much earlier, and we may anticipate a pronounced acceleration and distortion of the disturbances as they initiate the travelling towards the origin. In this case of a "hard" potential, the collision effectively detains the incoming pulse;

Figure 5.4: Shape of the Equivalent Potential V(ℓ) for Different Equilibria.

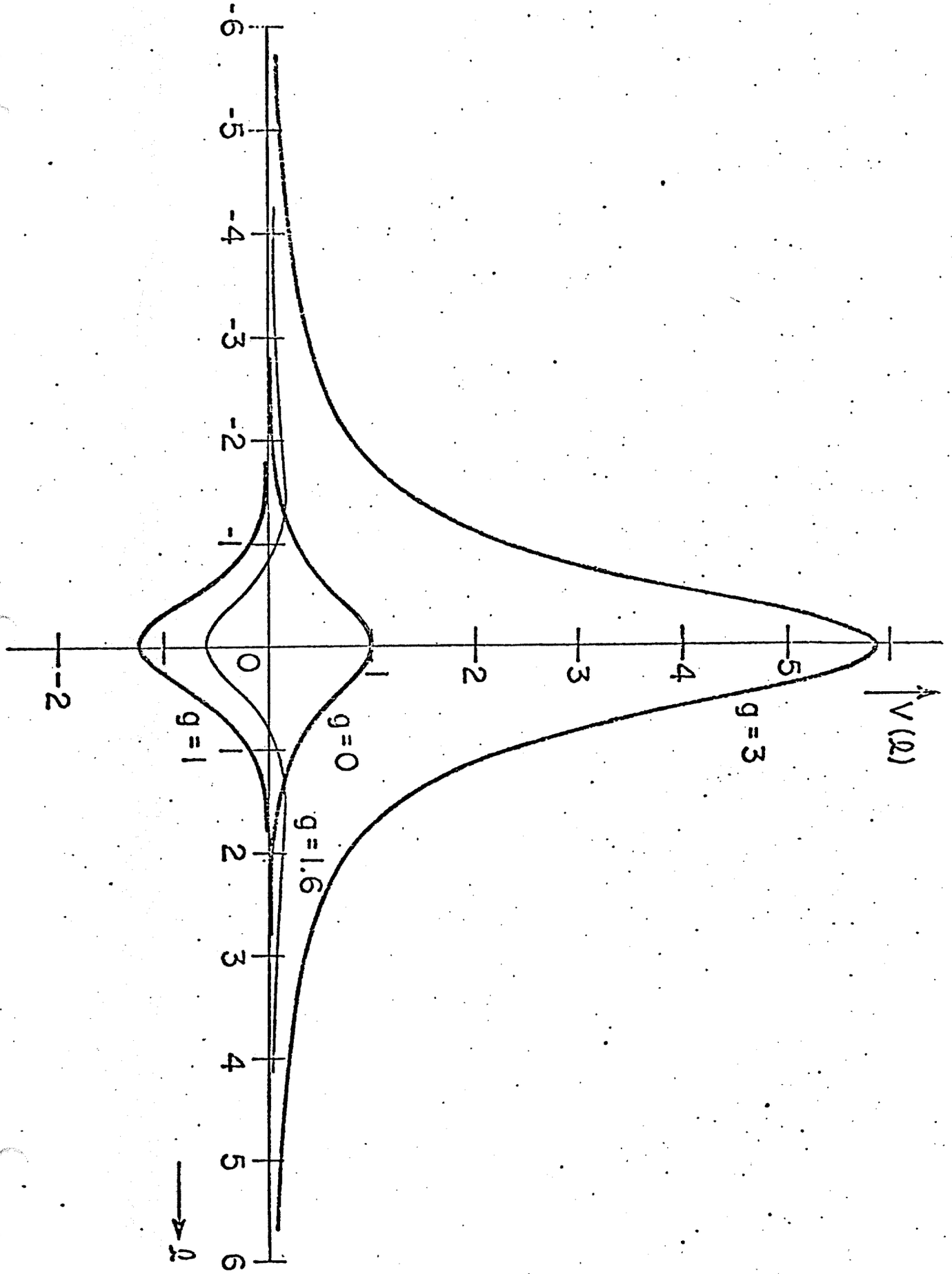
-6
-5
-4
-3
-2
-1
0
1
2
3
4
5
6
-2
0
1
2
3
4
5
V(Ω)
g=1
g=0
g=1.6
g=3
Ω

transmission across the barrier will still occur, but the main effect will be reflection. But perhaps the most interesting situation arises from those equilibria in the neighborhood of the instability, where the potential, as seen by the approaching pulse, first increases, and then deeps into a "valley". As we have seen, this configuration is found in the stable ranges $0.29 \lesssim g < 0.30$ and $1.6 < g \lesssim 2$. Then, acceleration is followed by retardation, and, for $1.6 < g \lesssim 1.8$, where $V(\ell)$ indeed becomes negative between the hills, the velocity of propagation becomes even less than in the asymptotic range of ℓ. This effect can be interpreted as the "trapping" of the wavelets with sufficiently low frequencies to see the four turning points, making the pulse temporarily captive into the potential "valley" between the hills.

In this discussion, we restricted our attention to the stable configurations, but it is not difficult to see what happens in the case of unstable equilibria. The pulse that we have been following starts its motion in the asymptotic region, reaches the negative "well", is slowed down and begins to increase exponentially without limit, developing into an instability around the origin.

It is interesting to note that the WKB condition for the points of marginal stability, obtained as an integral of the eikonal in Eq. (5-106) between turning points:

$$\oint |V(\ell)|^{1/2}\, d\ell = \int_{-\ell_T}^{+\ell_T} \sqrt{A-1-B(1+\ell^2)}\, \frac{d\ell}{1+\ell^2} = (n+\tfrac{1}{2})\pi \qquad (5\text{-}108)$$

where $\ell_T^2 = (A-1-B)/B$ for $\hat{\Omega} = 0$, gives:

$$\sqrt{A-1} - \sqrt{B} = \frac{1}{2} + 2n \qquad (n=0, 1, 2, \ldots) \qquad (5\text{-}109)$$

a result that has the same form of the correct eigenvalue condition (Eq. (4-58)).

In fact, growth of the approaching disturbance occurs also in the stable regimes, but not exponentially. We did not mention this important effect up to now, that we wish to examine using directly the time-dependent solution. An analytical solution of the partial differential equation for given appropriate initial conditions, in full generality, is difficult because of the intractable form of its dependence on the spatial variable, ultimately because of the "equivalent potential". However, for the effect that we have in mind, this is not really necessary. We may consider only the asymptotic limit, that makes $V(\ell)$ to vanish, and eliminates the curvature as one of the two sources of inhomogeneities of the medium, the other one, that we retain, being the shear. This brings us back again to the same equation that applies to the plane stratified medium.

In the limit of large ℓ, the solutions of the reduced equation, Eq. (5-101), are simply plane waves, of the form $e^{\pm i\Omega\ell}$, as indicated by Eq. (5-106). By an integral superposition, they can be made to reproduce any initial waveform and velocity. We choose, for simplicity, to describe the motion of a pulse initially located at $\ell_o >> 1$, sufficiently narrow to be

approximated by an impulsive function $\delta(\ell-\ell_o)$, and with zero initial velocity. In this case, it is not difficult to see that the appropriate Green's function for the Fourier-transformed problem (in time) is

$$F(\ell) = e^{\pm i\hat{\omega}|\ell-\ell_o|} \quad . \tag{5-110}$$

Recalling the relation between F and τ_o (Eq. (5-27), and applying the initial conditions, the Fourier integral of Eq. (5-110) over $\hat{\omega}$ gives finally the time-dependent solution:

$$\tau_o(\ell,t) = \frac{1}{2}\sqrt{\frac{1+\ell_o^2}{1+\ell^2}}\,[\delta(t-\ell+\ell_o)+\delta(t+\ell-\ell_o)] \tag{5-111}$$

where t, here, is a normalized time, measured in units of $\hat{s}$ $V_{Ao}/R_o q_o(1+2q_o^2)$.

Some of the features of this solution we found already by means of the normal mode analysis, namely, the conservation of the shape of the original pulse, and the uniform velocity of propagation. As it occurs typically for hyperbolic equations, the initial pulse splits in two half-pulses, travelling in opposite directions, one towards the increasing values of ℓ, and the other towards the origin. This lattest one amplifies in time, by a factor $\sqrt{(1+\ell_o^2)/(1+\ell^2)}$, while the amplitude of the half moving the other way is decreased by the same factor. This time-dependent solution was first obtained by Y.Y. Lao[63], who also pointed out the similarity between the transient growth of

stable perturbations in a current carrying plasma and in a hydrodynamic shear flow[73].

The explanation usually given to the transient amplification of a convective disturbance is that the shear acts to produce a temporary focusing on the constituent wavelets. This geometric effect of the field lines can be easily visualized by referring once more to the plane stratified medium. It is sufficient, for the purpose of physical interpretation, to consider the ordinary Alfvên waves. These can be obtained by taking the x-component of the curl of Eq. (5-4):

$$\left[\frac{\partial^2}{\partial t^2} - V_A^2(x) \left(\frac{\vec{B}_o}{B_o} \cdot \nabla \right)^2 \right] \vartheta_x = 0 \qquad (5\text{-}112)$$

where we wrote $\vec{\vartheta} = \nabla \times \vec{v}$ for the vorticity, and can be considered formally to be a particular subset of solutions of the more general equation, Eq. (5-5) (replacing ∇v_x by ϑ_x). For simplicity, we assume that the scale of variation of the mode in the z-direction is much larger than along the other coordinates, to eliminate dependences on z. This reduces the equation to:

$$\left[\frac{\partial^2}{\partial t^2} - V_A^2(x)\, b_y^2(x)\, \frac{\partial^2}{\partial y^2} \right] \vartheta_x(x,y,t) = 0 \qquad (5\text{-}113)$$

where $b_y(x) = B_{oy}/B_o$ is the cosine of the angle between the magnetic field and the y-axis and is a function of x only. In general, the solutions are of the form

$$\vartheta_x = \vartheta_x (x, y \pm b_y(x)\, V_A(x) t) , \qquad (5\text{-}114)$$

so that, on a given "flux surface" x=constant, the modes propagate along the y-direction at the local speed $b_y(x)\, V_A(x)$. The nonuniform transversal distribution of velocities tends to produce a temporary alignment in the x-direction of magnetic ripples traveling along adjacent field lines, leading to a transient amplification of the fluctuation. At subsequent times, because the ripples again interfere incoherently, the amplitude eventually decays (Fig. 5.5). From an analytical point of view, the $1/\ell$ behavior of the amplitude at large distances is clearly related to the logarithmic singularities of the shear-Alfvên continuum, and this is another way of saying that amplification and damping are consequences of the non-uniformity of the medium, in this case represented by the shear.

As the pulse approaches the origin, in addition to dispersive effects introduced by the equivalent potential, as distortion of shape and change in velocity, we expect that the amplification rate is no longer uniform and departs from the simple asymptotic formula $\sqrt{(1+\ell_0^2)/(1+\ell^2)}$. It is useful, for this discussion, to consider an "energy" conservation relation that can be obtained from the time-dependent equation. If we multiply the reduced equation

$$\frac{\partial^2 F}{\partial t^2} = \frac{\partial^2 F}{\partial \ell^2} + V(\ell)\, F \qquad (5\text{-}115)$$

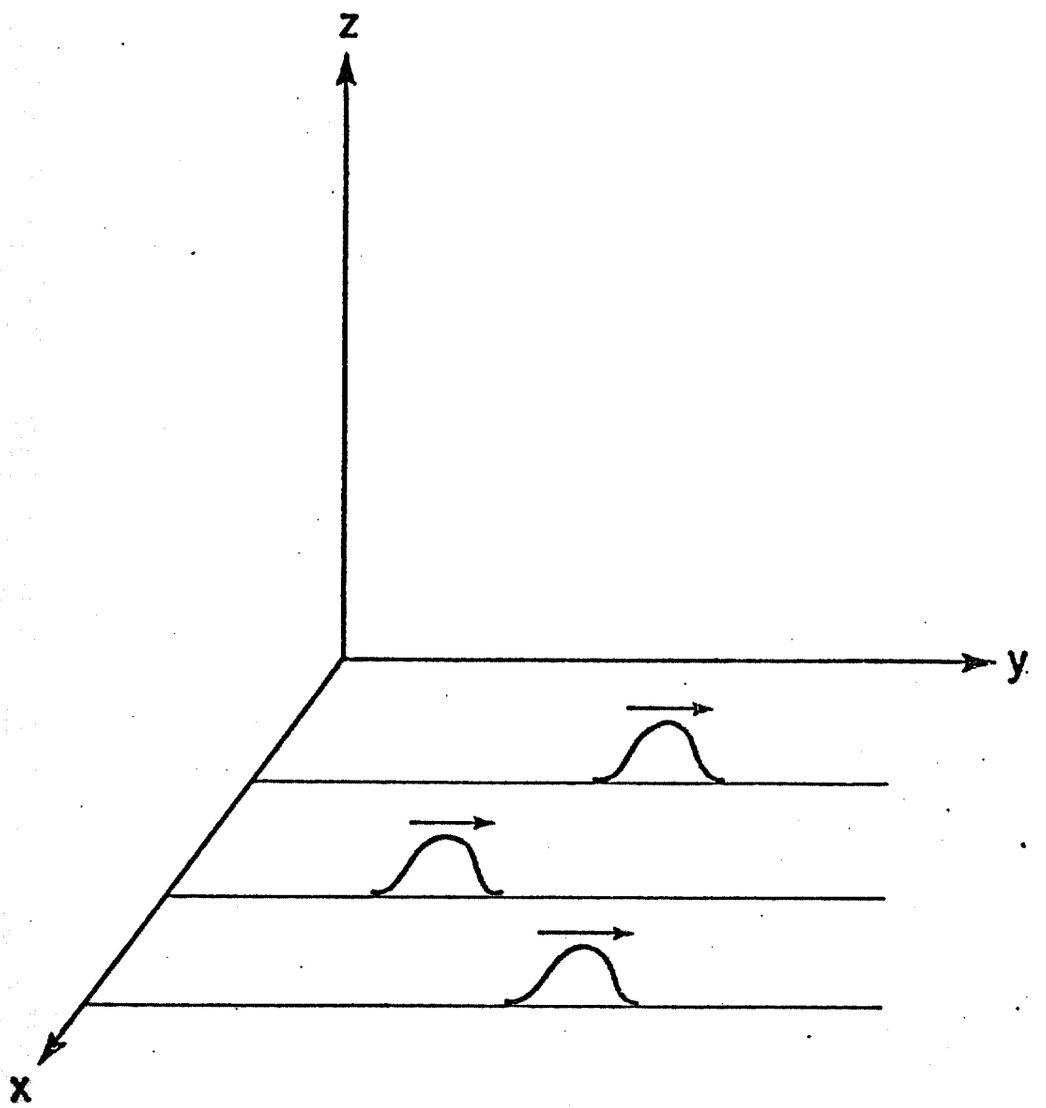

Figure 5.5: Interpretation of the Transient Growth of Stable Perturbations as a Focusing Effect on Magnetic Fluctuations Caused by Shear.

by $(\partial F/\partial t)$ and integrate over ℓ, after a partial integration, we get:

$$\frac{d}{dt} \int_{-\infty}^{+\infty} [(\frac{\partial F}{\partial t})^2 + (\frac{\partial F}{\partial \ell})^2 + V(\ell)F^2] \, d\ell = 0 \qquad (5\text{-}116)$$

Let us consider first a toroidal equilibrium with vanishingly small pressure gradient ($g \sim 0$), which is equivalent to the plasma slab with no gravity. In this case, we still have a potential $V(\ell) = 1/(1+\ell^2)$, that is due entirely to the shear, with the shape of a fairly low hill around the origin. At remote regions, this potential is not seen, and the solutions of Eq. (5-115) are of the form $[(1/2)\delta(\ell-\ell_o \pm t)]$; in terms of F, rather than of τ_o, the amplitude is conserved, since the transformation defined by Eq. (5-27) eliminates the shear amplification factor $1/\sqrt{1+\ell^2}$. As the pulse approaching the origin starts to "climb" the hill, the velocity is increased, and, based on the balance of terms of the above constant of motion, we may argue that the amplitude F is decreased with respect to its asymptotic value. The total (normalized) time taken by the perturbation to travel from ℓ_o to $\ell \sim 0$ will be less than ℓ_o. As we introduce a small amount of pressure gradient into the configuration, the potential is just depressed by the curvature term $-A/(1+\ell^2)^2$, since the small contribution from the B-term, that depends only quadratically on g, is not sufficient to change significantly its shape. Then the approaching pulse experiences essentially the same effects, but

to a lesser degree than in the pressureless case, so that, in relative terms, there is an enhancement of the fluctuations and a delay in the travelling time. We expect that further increases of g, that brings the equilibrium closer to the first threshold of instability, will reinforce more and more these trends, until we reach g ~ 0.28 where A = 1, and the piece of the potential coming from the shear is cancelled out. Around this value of g, the pulse reaches the vicinities of the origin with about the same size it had in the asymptotic region, spending a migration time approximately equal to ℓ_o. The potential barrier, by then, is almost transparent, and produced only by the B-curvature term. In the narrow range that is still left in the first stable region, the potential starts to gain the characteristics of a negative well. For $\ell \lesssim 1$, $V(\ell)$ changes sign and concomitant to a significant retardation, the amplification rate, inside the potential "valley", becomes larger than unity. Finally, in the unstable range $0.3 < g < 1.6$, $V(\ell)$ plays the role of an external source that feeds energy into the mode; increase of F, according to Eq. (5-116), is balanced by further increase of F, and the amplitude grows exponentially, evolving into an instability.

Sizeable amplification and slowing down can be expected to occur in the stable regimes operating close to the second threshold of instability, in particular in the range $1.6 < g < 1.84$, where a negative well between two surrounding shallow hills is still found. At values of g larger than 2., the equivalent potential is a simple hill, but with an important

contribution of the term $B/(1+\ell^2)$. From there on, increase of the pressure gradient quickly reduces the level of fluctuations, as this means further stabilization of the configuration.

In Fig. (5.6), we display the evolution of a pulse, obtained by numerical integration of Eq. (5-115), for a few equilibria. To show the transient amplification produced by the shear, we plotted T_o instead of F. The initial shape, in all cases, is a Gaussian

$$2\, e^{-[(\ell-\ell_o)/\sigma]^2} \qquad (5\text{-}117)$$

with width $\sigma = 2$ centered at $\ell_o = 15$, and the initial velocity was taken to be zero. Note that the initial pulse is subsequently divided into two half pulses with unity amplitude each, traveling in opposite directions. For comparison, we selected three equilibria, corresponding to g = 0 (equivalent to the plasma slab with no gravity), g = 0.25 (first stable regime), and g = 3.00 (second stable regime). After the discussion in this section, the interpretation of the events represented in this figure should be clear. In the third case, the picture at t = 15 catches the moment when the pulse, stopped by the potential, is inverted, and then, for larger times, reflected back. In the other two cases, with a less hard potential, we may see that the "break" of the inciding pulse is followed by its splitting into smaller pulses that spread, wave-like, in both directions.

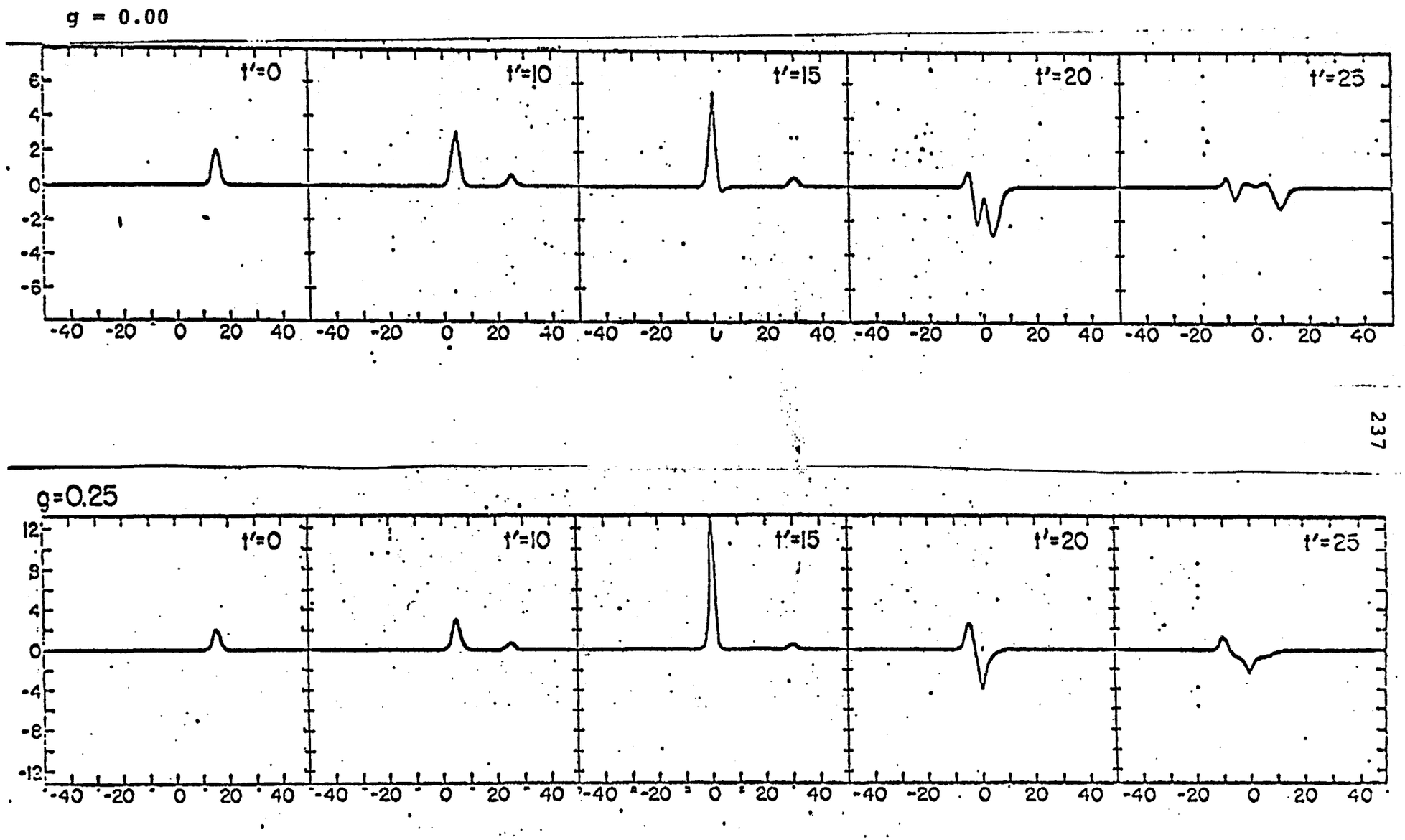

Fig. 5.6: Time Evolution of a Pulse

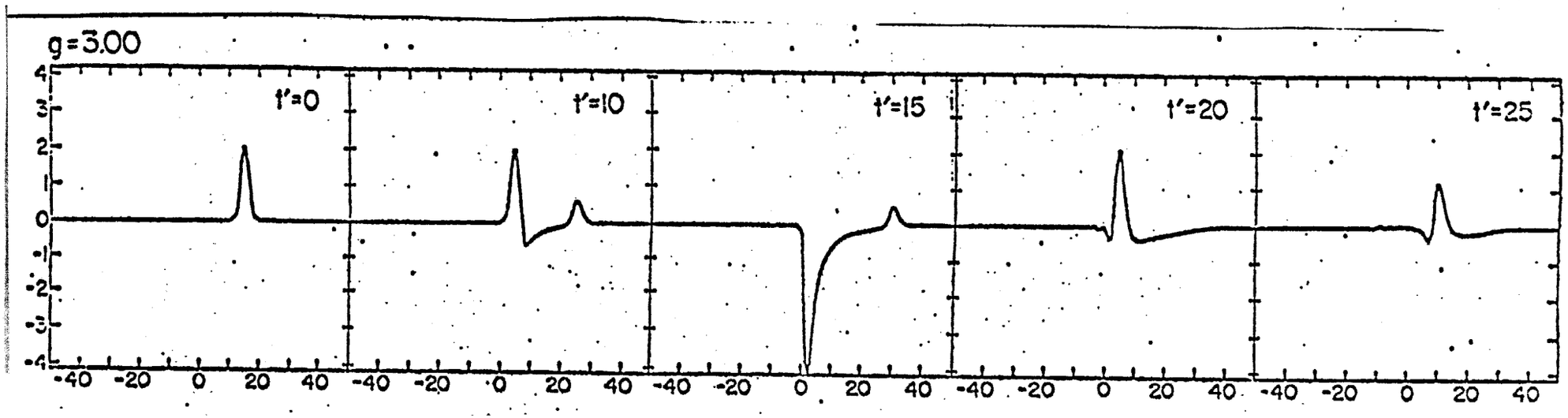

Fig. 5.6(cont'd): Time Evolution of a Pulse

In Fig. 5.7 we plotted the total amplification, defined as the ratio of the maximum amplitude that is reached by the inciding pulse to the initial amplitude, and in Fig. 5.8, the time T at which the maximum amplitude was recorded, that is essentially the time spent by the pulse to travel from $\ell_o = 15$ to the origin. Note that the asymptotic formula predicts a total amplification of approximately 15, to occur at time $T \sim 15$. In fact, as we have discussed before, this happens only for equilibria close to the conditions of instability, when the contributions coming from the two terms entering the function $V(\ell)$ tend to cancel one another.

The initial position was chosen to be $\ell_o = 15$ not only because it ~~leys~~ lies in the asymptotic region of the potential, without being too large to overload the numerical computations with uninteresting events, but also because it represents typically the MHD limit of validity of the mode equation. We recall that this limit is given by $k_\perp \rho_i < 1$, where

$$k_\perp = N\, v(\phi - \int^{\theta} q_\ell \, d\theta) \simeq \hat{s}_\theta \, k_\theta \qquad (5\text{-}118)$$

is the transverse component of the displacement vector. Since the poloidal wavenumber is something like $k_\theta \simeq - N(q_o/r)$, this condition implies a maximum value for the variable $\ell = \hat{s}_\theta$,

$$\ell_{max} \sim \frac{1}{Nq_o} \frac{r}{\rho_i} \qquad (5\text{-}119)$$

Figure 5.7: Maximum Amplification of a Pulse Initially Located at $\ell_o = 15$ as a Function of the Equilibrium Parameter g.

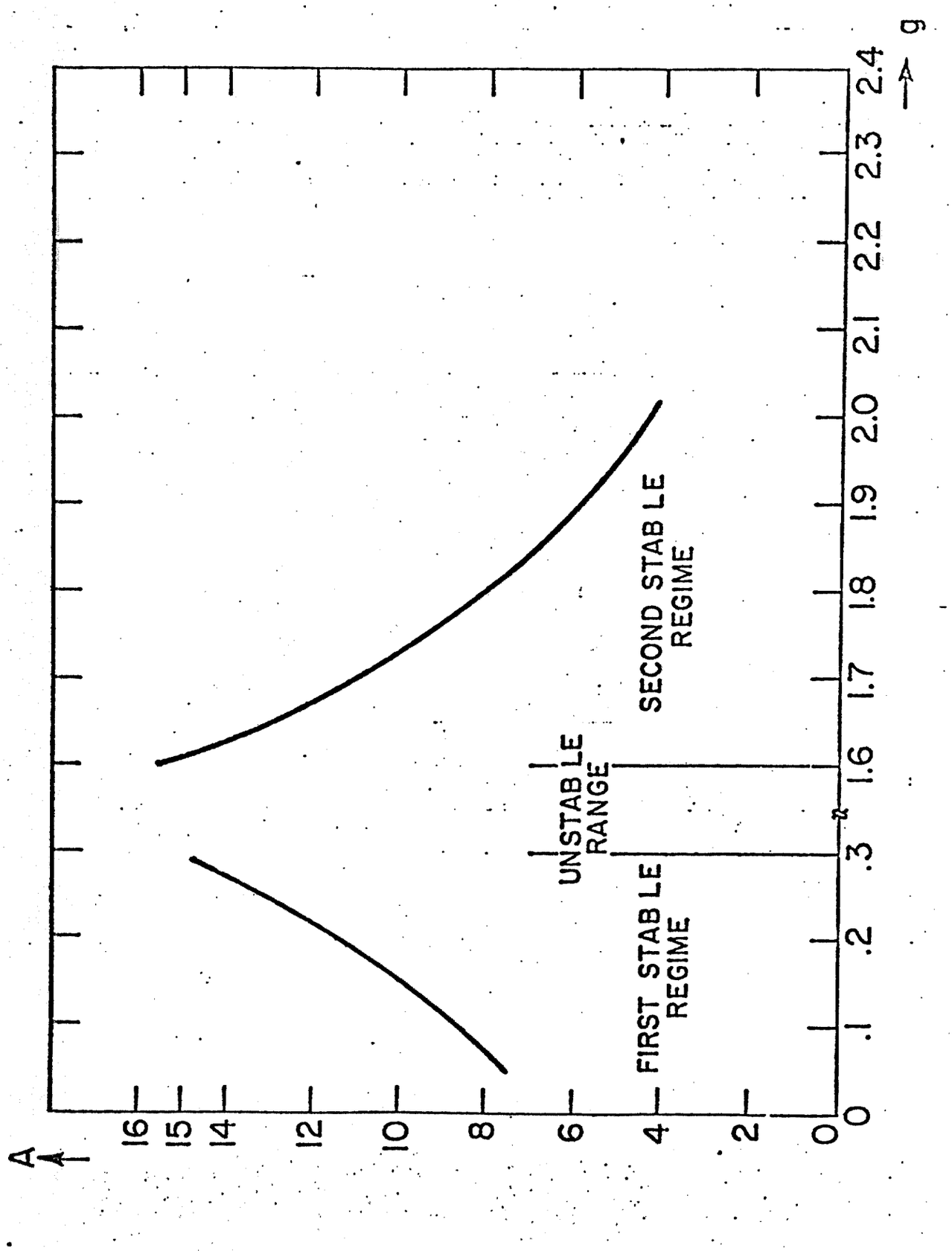
A
16
15
14
12
10
8
6
4
2
0
0
.1
.2
.3
1.6
1.7
1.8
1.9
2.0
2.1
2.2
2.3
2.4
g
FIRST STAB LE REGIME
UNSTAB LE RANGE
SECOND STAB LE REGIME

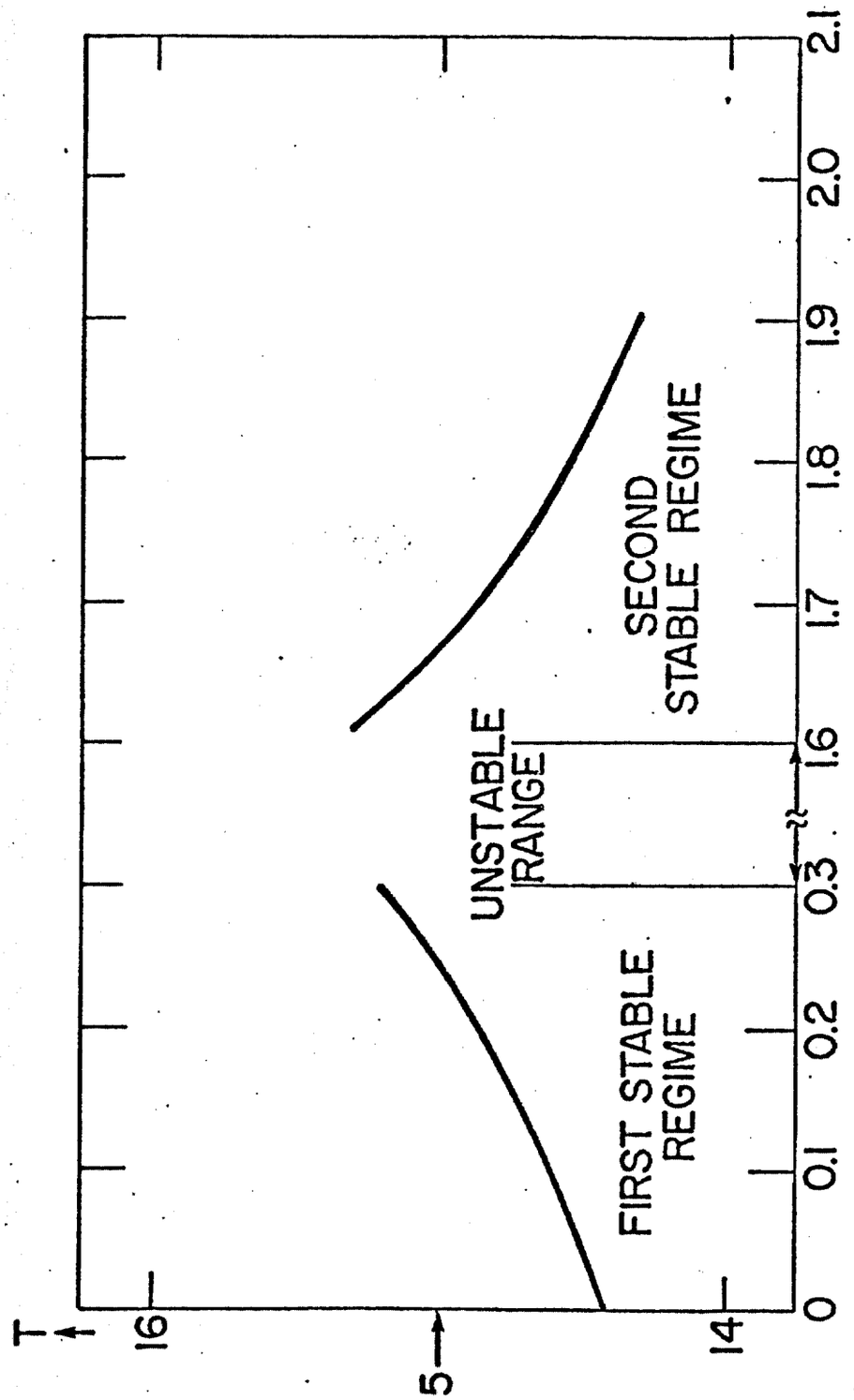

Figure 5.8: Time for a Pulse Initially Located at ℓ_o = 15 to Reach the Origin as a Function of the Equilibrium Parameter g.

For example, in a plasma column with ion temperature $T_i \sim 5$ keV, toroidal magnetic field $B_\phi \sim 70$ kG, the ion gyroradius is $\rho_i \sim 0.07$ cm. At a distance $r = 5$ m from the magnetic axis, we find that, for modes with toroidal number $N = 5$, the above relation determines a maximum range for the extended poloidal variable

$$\ell_{max} \approx 14.$$

The maximum amplification of the perturbations, of course, depends both on the equilibrium conditions and on the initial distribution, as it appears in the ℓ-space. By choosing the upper MHD limit for ℓ_o, we may have a glimpse at its order of magnitude, and, as the present study indicates, it seems to remain at modest levels, except for those equilibria operating on the border of instability. More precise information about the initial conditions to be applied to the wave equation would require an investigation about the possible source of the excitations, and this is a question we shall not address in this thesis. We may conject, however, that if any sources of energy are present, as 3.5 MeV α-particles in D-T fusion reactors, or neutral energetic beams, as those injected in current-day hydrogen experiments, the rate of amplification of the shear-Alfvén perturbations that will be excited and the instability boundaries will be altered. In connection with this problem, we observe that preliminary studies of the resonant interaction of fusion-born α-particles with the modes we considered here, as

the one reported in Ref. (71) suggest that, for large ℓ, the amplification is not significantly enhanced. We may expect, however, that for small values of ℓ, in particular for equilibria in the neighborhood of instability, this conclusion does not hold. This would make the range of physical parameters that characterize the unstable configurations expand, shifting the boundaries for the transition of shear-Alfvén waves to ballooning modes.

Finally, as a caveat, we remind the reader that the results in this section are restricted to a very particular class of equilibria not only by the geometry of the flux surfaces, but also by the high poloidal beta limit considered, that permitted us to conduct the discussion in terms of a single equilibrium parameter. In practice, high-beta tokamaks are achieved by a process that involves flux-conservation, and under this constraint, the value of poloidal beta is never very high[74]. It would not be difficult to extend the analysis to low and moderate values of β_p, by including the correcting functions δ_1 and δ_2 in the expression of the effective potential (see Eqs. (4-23)), but we shall leave this task to others.

Appendix 5A

Note on the Numerical Solution of the Wave Equation

For partial differential equations of the hyperbolic type, the recommended method of numerical solution is the method of characteristics[75]. In very loose terms, the characteristic curves (or simply characteristics) associated with a partial differential equation can be thought of as a set of natural coordinate. When, by an appropriate change of variables, the differential equation is re-expressed in terms of the characteristic coordinates, the form that results — called "canonical form" — in many cases of practical interest is simpler than the original one. The transformation is not always convenient or desirable for numerical applications, as in the case of elliptic equations, where two intersecting families of characteristic curves can be found, but they are not real, and in the case of parabolic equations, where they are real, but degenerate into a single family. For hyperbolic equations, however, the two families are both real and distinct, and provide a natural grid, over which the solution can be determined, given suitable initial conditions, by a step-by-step numerical procedure. The advantage of the use of characteristic coordinates, in this case, is not restricted to the simplicity of the form that the equation may take, and of the numerical schemes of integration. For one thing, the method is free of restrictive conditions to ensure stability and convergence. And, since discontinuities

may propagate along characteristics, it becomes obligatory when the initial conditions are specified by discontinuous functions, a situation that cannot be handled by other methods, as finite differences.

We want to solve numerically by the method of chacteristics the partial differential equation:

$$F_{\ell\ell} - F_{tt} = - V(\ell)F \qquad (5A\text{-}1)$$

given the values of F, F_ℓ and F_t at the time t = 0.* Or, more generally, we want to use the prescribed values of these quantities to determine the second order derivatives uniquely, in such a way that the differential equation is always satisfied.

Assuming that the derivatives of F_ℓ and F_t exist, we may write:

$$d(F_\ell) = F_{\ell\ell}\, d\ell + F_{\ell t}\, dt \qquad (5A\text{-}2)$$

$$d(F_t) = F_{\ell t}\, d\ell + F_{tt}\, dt \qquad (5A\text{-}3)$$

---

*The theory of hyperbolic equations demands that the curve in the (t,ℓ) plane over which the "initial" values are specified does not coincide with a characteristic line, otherwise the solution does not exist generally, or may exist if certain special conditions are satisfied, but then it is not unique (76). The axis t=0 is not a characteristic line, and we may be sure that the solution exists and is unique.

These two equations, together with Eq. (5A-1), constitute a set of algebraic equations for the quantities $F_{\ell\ell}$, $F_{\ell t}$, F_{tt}, which admit a unique solution, unless the determinant of the system, given by

$$\begin{vmatrix} d\ell & dt & o \\ o & d\ell & dt \\ 1 & o & -1 \end{vmatrix} \tag{5A-4}$$

vanishes. This condition turns out to be

$$(dt)^2 - (d\ell)^2 = 0 \quad \text{or} \quad \frac{dt}{d\ell} = \pm 1$$

and defines the characteristic curves for the differential equation that are then the straight lines $\ell \pm t$ = constant (Fig. 5.9). But we want to proceed exactly along these lines, to follow the evolution of the initial perturbation. Then, in order to make possible the solution of the system of equations, we have to impose the condition that the other determinants also vanish. This means, for example, that

$$\begin{vmatrix} d\ell & dt & d(F_\ell) \\ o & d\ell & d(F_t) \\ 1 & o & -VF \end{vmatrix} = 0 \tag{5A-5}$$

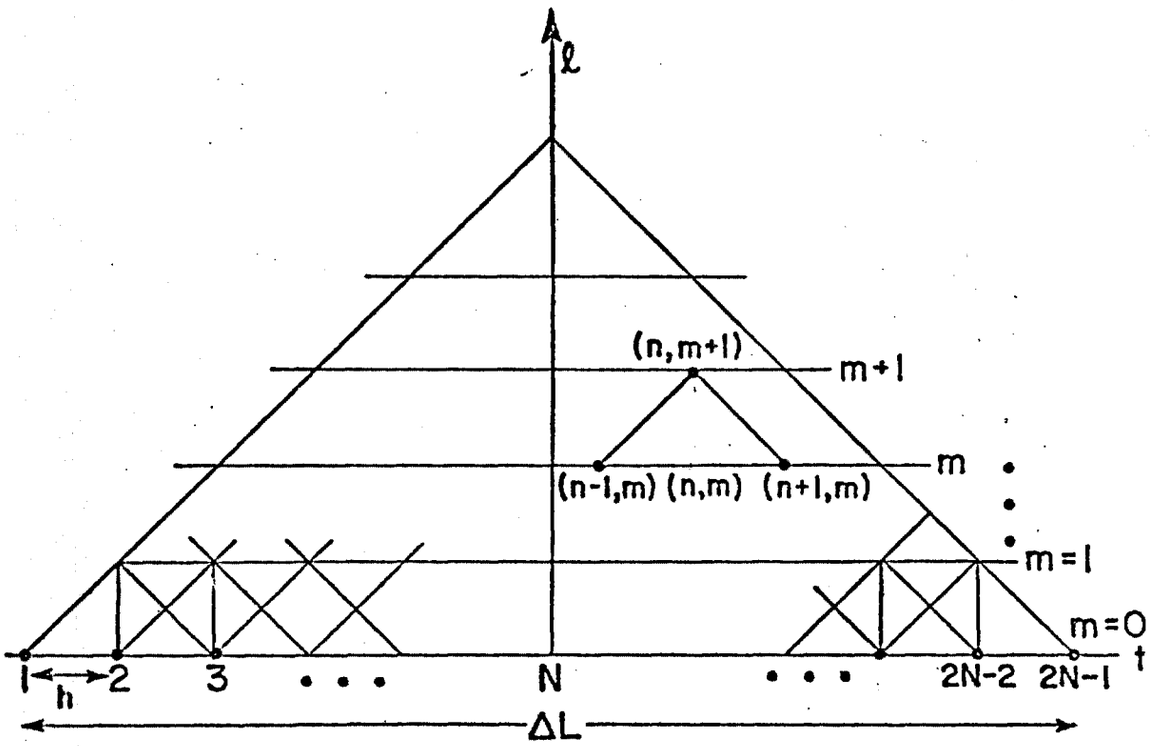

Figure 5.9: Characteristic lines in the (t,) Plane.

which provides the compatibility condition:

$$-VF\, d\ell + d(F_t)\, \frac{dt}{d\ell} - d(F_\ell) = 0 \qquad (5A\text{-}6)$$

This equation (the equation along the characteristics), complemented by the differential relation:

$$dF - F_\ell\, d\ell - F_t\, dt = 0 \qquad (5A\text{-}7)$$

can now be used to determine numerically the solution of the original problem over the characteristic grid.

Along the family $t - \ell$ = constant, Eq. (5A-6) becomes

$$-VF\, d\ell + d(F_t) - d(F_\ell) = 0 \; . \qquad (5A\text{-}8)$$

Replacing the differentials by finite differences between two grid points, labeled (n, m+1) and (n-1, m) in Fig. 5.9, this equation can be approximated by

$$-\frac{1}{2}\,[V(n)\,F(n,m+1) + V(n-1)F(n-1,m)]h + [F_t(n,m+1) - F_t(n-1,m)]$$

$$-\;[F_\ell(n,m+1) - F_\ell(n-1,m)] = 0 \qquad (5A\text{-}9)$$

where $h = \Delta\ell$ is the distance separating two consecutive points along the line $t = 0$ over which the initial conditions are defined.

Similarly, the equation along the characteristics $t + \ell =$ constant is:

$$-VF\, d\ell - d(F_t) - d(F_\ell) = 0 \qquad (5A\text{-}10)$$

and the discrete version, between two adjacent grid points $(n,m+1)$ and $(n-1,m)$ is:

$$+ \frac{1}{2}\,[V(n)\,F(n,m+1) + V(n-1)F(n+1,m)]h - [F_t(n,m+1) - F_t(n+1,m)]$$

$$- \quad [F_\ell(n,m+1) - F_\ell(n+1,m)] = 0 \qquad (5A\text{-}11)$$

Finally, Eq. (5A-7) can be used on either of the two characteristic lines across the point $(n,m+1)$ to furnish the missing relation among unknown quantities. Choosing the characteristic with positive slope, we have:

$$F(n,m+1) - F(n-1,m) - \frac{1}{2}\,[F_\ell(n,m+1) + F_\ell(n-1,m)]h$$

$$- \frac{1}{2}\,[F_t(n,m+1) + F_t(n-1,m)]h = 0 \qquad (5A\text{-}12)$$

We have now three algebraic equations for the function F and its derivatives F_ℓ and F_t at the grid point $(n,m+1)$, <u>id est</u>, at the time $t = (m+1)h$, that can be solved if the values at the nearest neighboring grid points corresponding to time $t = mh$ are known. Explicitly, the solution is given by:

$$F(n,m+1) = \frac{1}{1-(h^2/4)V(n)} \left\{ F(n-1,m) + \frac{h}{2} [F_\ell(n+1,m) + F_t(n+1,m) \right.$$

$$\left. + F_\ell(n-1,m) + F_t(n-1,m)] + \frac{h^2}{4} V(n+1) F(n+1,m) \right\} . \quad (5A-13a)$$

$$F_\ell(n,m+1) = \frac{1}{2} [F_\ell(n-1,m) + F_\ell(n+1,m) - F_t(n-1,m) + F_t(n+1,m)] +$$

$$+ \frac{h}{4} [V(n+1) F(n+1,m) - V(n-1) F(n-1,m)] \quad (5A-13b)$$

$$F_t(n,m+1) = -\frac{1}{2} [F_t(n-1,m) + F_t(n+1,m) + 3 F_\ell(n-1,m) +$$

$$+ F_\ell(n+1,m)] + \frac{h}{4} [V(n-1)F(n-1,m) - V(n+1)F(n+1,m)] +$$

$$+ \frac{1}{1-(h^2/4)V(n)} \left\{ F_\ell(n+1,m) + F_t(n+1,m) + F_\ell(n-1,m) + F_t(n-1,m) \right.$$

$$\left. + \frac{h}{2} [V(n+1)F(n+1,m) + V(n)F(n-1,m)] \right\} \quad (5A-13c)$$

and is correct to order h^2 (75).

After the values of F have been recurrently computed, the function τ_o can be evaluated at each grid point by means of the relation

$$\tau_o(n,m) = \frac{F(n,m)}{\sqrt{1 + n^2h^2}} \quad (5A-14)$$

that follows from the transformation introduced by Eq. (5-27).

For the initial value of F, we choose a form that gives for γ_o a Gaussian pulse:

$$F\,(t=0) \;=\; 2\, e^{-[(\ell-\ell_o)^2/\sigma^2]}\,\sqrt{1+\ell^2} \qquad (5A\text{-}15)$$

centered at $\ell = \ell_o$ and with width $\sim\sigma$. The spatial derivative at the axis $t = 0$ is then given by

$$F_\ell(t=0) \;=\; \left[\frac{\ell}{1+\ell^2} \;-\; \frac{2(\ell-\ell_o)}{\sigma^2}\right] F(t=0). \qquad (5A\text{-}16)$$

In all solutions reported previously, the initial time derivative was taken to be zero:

$$F_t(t=0) \;=\; 0\;, \qquad (5A\text{-}17)$$

but this restriction could be easily lifted up.

This is a typical initial value problem, for which boundary conditions do not intervene. Of course, in numerical computations, the infinite domain of definition of the spatial variable is just a finite interval, large enough to cover the potential function in all its extension, up to the regions where it decays asymptotically and becomes negligible. This makes it possible to watch the evolution of initially localized disturbances during all stages of the interesting events since it starts its migration from remote regions towards the origin. In general, as we proceed in time with the numerical solution of a wave

equation, the finite domain over which the solution is spatially defined shrinks. This is, obviously, a consequence of the fact that the characteristic lines are the "carriers" for the propagation of the disturbances. Thus the characteristics across the extremes of the interval on the axis t=0 in Fig. 5.9, over which the initial values are actually specified, limit the extension of the intervals of definition at subsequent times. After a time Δt has elapsed, the initial interval ΔL is reduced to $\Delta L - 2\Delta t$. Care has to be taken to guarantee that, for the maximum time the solution is to be determined, this range is still large enough. On the other hand, since the initial pulse is highly localized, it is not desirable to overload the computations with an extended range that, for most of the time, remains idle.

For all cases studied numerically, it was found that the requirements of economy, good definition of the solution and accuracy of the computations can be comfortably well accomodated with a choice of numerical parameters typically as

$\Delta L \sim 100$, equally divided at each side of the origin;

$h \sim 5 \times 10^{-2}$, which gives ~2000 initial grid points;

$\Delta t_{max} \sim 30$, corresponding to ~600 time steps.

For an initial narrow pulse located at $\xi_o = 15$, and the equivalent potential $V(\xi)$ of Eq. (5-102), everything of interest happens within the above time limit and is contained inside the available space.

Chapter VI

CONCLUSIONS

Since the year of 1977, that marks the beginning of the period of intense research on ballooning modes, a great deal of progress has been reached. Numerical work showed that, for local values of the inverse rotational transform larger than unity, the unstable region does not extend to the axis, and the first stable region merges with the second. As illustrated in Fig. 6.1, this corresponds to a stable area in the parameter space with low values of shear and both low and high pressure gradients. At the present moment, work is in progress at M.I.T. and Princeton[78,79,80] to verify if, by generating flux conserving sequences of equilibria, profiles can be produced that would take advantage of the available "window" to achieve high values of beta.

Although ballooning modes are the most feared of the MHD instabilities, they have been elusive to experimental observation. S.C. Prager *et al.*[81], from the University of Wisconsin, reported the stable confinement of a plasma with values of beta higher than 8 percent, against predictions based on the ideal MHD theory that the threshold for ballooning would be reached. Similarly, the experiments in the ISX-B Tokamak, at the Oak Ridge National Laboratory, failed to detect signs of MHD activity, challenging also the predictions of the fluid theory. In a talk given at MIT in September, 1980, D.J. Sigmar interpreted this negative result as a consequence of the strong

anisotropic effects in the bulk plasma caused by the powerful neutral beam that is used to heat the plasma. In addition, the large gyroradius of the ionized particle would have acted as a further stabilizing effect.

To our knowledge, the only reported experimental evidence of ballooning modes comes from Columbia University[82]. Curiously enough, the data obtained there from Torus II indicate not only MHD instabilities with characteristics of a ballooning mode, but also that they appear when the plasma is cooled and beta is decreased. If we realize that in Torus II the plasma is initially formed with an average beta as high as 10 percent, we may be inclined to accept the interpretation of the Columbia group, that the device was operating in the second stable region, and upon cooling, crossed the theoretically predicted second stability boundary into the unstable region.

Many concrete situations of practical interest, as the one of the ISX experiment, can be analyzed only with the apparatus of the kinetic theory. The ideal MHD theory, however, does not lose its interest and usefulness. In the first place, it provides a simple framework that, as the history of ballooning modes shows, has permitted the community of physicists to attack and solve a large number of crucial theoretical problems. In the second place, from a strictly practical point of view, the ideal fluid theory gives a low bound for stability thresholds, that remains a useful reference and basis for design.

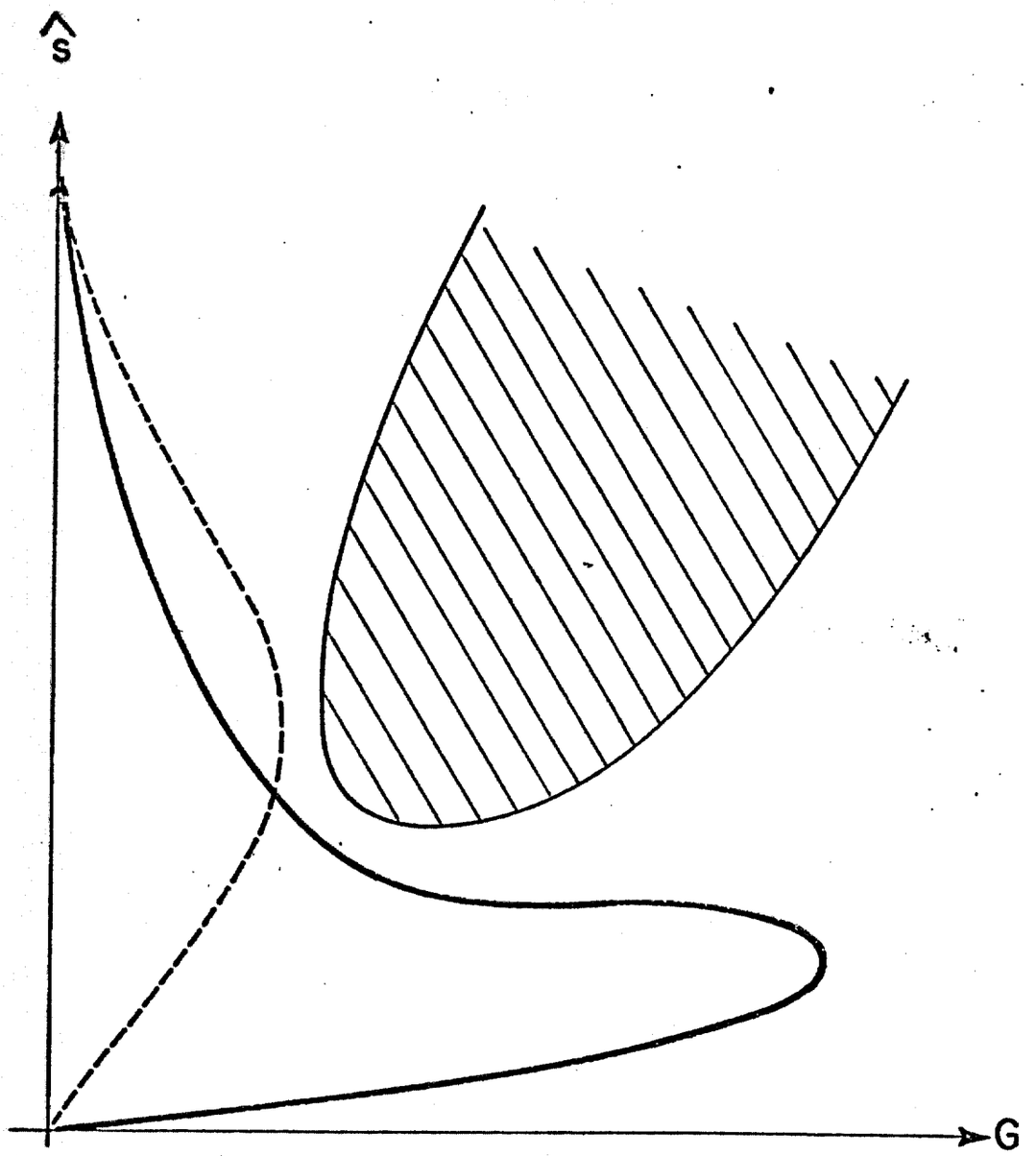

Figure 6.1: Equilibrium Profiles in the First Stable Region (Dashed Line) and Partially in the Second Stable Region (Solid Lire).

REFERENCES

1. Ribe, F.L., Rev. of Modern Phys., V.47, No. 1 (1975) 7.
2. Metz, N.D., Science 192 (1976) 1320.
3. Bateman, G., in MHD Instabilities, The MIT Press (1978) Cambridge, Massachusetts and London, England, page 163.
4. Mukhoratov, V.S., Shafranov, V.D., Nucl. Fusion 11 (1971) 605.
5. Clark, J.F., Sigmar, D.J., Phys. Rev. Lett. 38 (1977) 70.
6. Dory, R.A., Peng, Y.-K.M., Nucl. Fusion 17 (1977) 21.
7. Todd, A.M.M., Chance, M.S., Greene, J.M., Grimm, R.C., Johnson, J.L., Manickam, J., Phys. Rev. Lett. 38 (1977) 826.
8. Coppi, B. and Rosenbluth, M.N., in Plasma Physics and Controlled Nuclear Fusion Research 1965, Paper CN-21/105 (Publisher International Atomic Energy Agency, Vienna, 1965).
9. Furth, H.P., Killeen, J., Rosenbluth, M.N., Coppi, B. in Plasma Physics and Controlled Nuclear Fusion Research 1965, Paper CN-21/106 (Publisher International Atomic Energy Agency, Vienna, 1965).
10 Kulsrud, R.M., in Plasma Physics and Controlled Nuclear Fusion Research 1965, Paper CN-21/113 (Publisher International Atomic Energy Agency, Vienna, 1965).
11. Coppi, B., Phys. Rev. Lett. 39 (1977) 939.
12. Dobrott, D., Nelson, D.B., Greene, J.M., Glasser, A.H., Chance, M.S., Frieman, E.A., Phys. Rev. Lett. 39 (1977) 943.

13. Lee, Y.C., VanDam, J.W., in Proceedings of the Finite Beta Theory Workshop, 93 (Coppi, B., Sadowsky, W., Eds.) Publisher: U.S. Department of Energy, Washington, D.C. (1978).

14. Glasser, A.H. in Proceedings of the Finite Beta Theory Workshop, 55 (Coppi, B., Sadowsky, W., Eds.) Publisher: U.S. Department of Energy, Washington, D.C. (1978).

15. Pegoraro, F. and Schep, T., Rijnhuizen Report IR78/001, Association Euratom-FOM (FOM-Institut voor Plasmafysica, Rijnhuizen, Jutphaas, The Netherlands, 1978).

16. Connor, J.W., Hastie, R.J., Taylor, J.B., Phys. Rev. Lett. 40 (1978) 396.

17. Connor, J.W., Hastie, R.J., Taylor, J.B., Proc. R. Soc. Lond. A. 365 (1979) 1.

18. Chance, M.S., Dewar, R.L., Frieman, E.A., Glasser, A.H., Greene, J.M., Grimm, R.C., Jardin, S.C., Johnson, J.L., Manickam, J., Okabayashi, M., Todd, A.M.M., Report PPPL-1468 (1978) Princeton University.

19. Coppi, B., in Proceedings of the Finite Beta Theory Workshop, 31 (Coppi, B., Sadowsky, W., Eds.) Publisher: U.S. Department of Energy, Washington, D.C. (1978).

20. Coppi, B., Ferreira, A., Mark, J.W.-K., Ramos, J.J., Nucl. Fusion 19 (1979) 715.

21. Coppi, B., Filreis, J., Mark, J.W.-K., in Plasma Physics and Controlled Nuclear Fusion Research (Proc. 7th Int. Conf. Innsbruck, 1978) Vol. 1, IAEA, Vienna (1979) 793.

22. Mercier, R., in Plasma Physics and Controlled Nuclear Fusion Research (Proc. 7th Int. Conf. Innsbruck, 1978) Vol. 1, IAEA, Vienna (1979) 701.

23. Sykes, A., Turner, M.F., Fielding, P.J., Haas, F.A., in Plasma Physics and Controlled Nuclear Fusion Research (Proc. 7th Int. Conf. Innsbruck, 1978) Vol. 1, 625.

24. Zakharov, L.E., in Plasma Physics and Controlled Nuclear Fusion Research (Proc. 7th Int. Conf. Innsbruck, 1978) Vol. 1, 689.

25. Strauss, H.R., Park, W., Monticello, D.A., White, R.B., Jardin, S.C., Chance, M.S., Todd, A.M.M., Glasser, A.H., Nucl. Fusion 20 (1980) 638.

26. Coppi, B., Lectures on High Temperature Plasma Physics (M.I.T., September, 1977).

27. Antonsen Jr., T.M., Lane, B., Phys. Fluids 23 (1980) 1205.

28. Callen, J.D., Dory, R.A., Phys. Fluids 15 (1972) 1523.

29. Bateman, G., Phys. Phys. Fluids 15 (1972) 68.

30. Greene, J.M., and Johnson, J.L. in Advances in Theoretical Physics, Ed. K.A. Breuckner (Academic Press, New York, 1965) Vol. 1, p. 195.

31. Furth, H.P., Killen, J., Rosenbluth, M.N., Coppi, B., Culham IAEA Conf., 1 (1965) 103.

32. Greene, J.M., in Theory of Magnetically Confined Plasmas, 3 (Proceedings of the Course held in Varenna, Italy, 1977; Coppi, B., Stringer, T., Pozzoli, R. and Sindoni, E., Carnihan, J.P., Leotta, G.G., Eds). Published for the Commission of the European Communities by Pergamon Press (1979).

33. VanDam, J.W., Ph.D. Thesis, University of California, Los Angeles (1979).

34. Friedman, B., in Lectures on Applications-Oriented Mathematics, p. 37 (Edited by Victor Twersky, University of Illinois, Chicago) Copyright 1969 by Holden-Day, Inc.

35. Coppi, B., Filreis, J., Pegoraro, F., Ann. Phys. 121 (1979) 1.

36. Antonsen Jr., T.M., private communication.

37. Goedbloed, J.P., Phys. Fluids 18 (1975) 1258.

38. Todd, A.M.M., Manickam, J., Okabayashi, M., Chance, M.S., Grimm, R.C., Greene, J.M., and Johnson, J.L., Nucl. Fusion 19 (1979) 743.

39. Newcomb, W.A. Ann. Phys. 10 (1960) 232.

40. Dewar, R.L., Chance, M.S., Glasser, A.H., Greene, J.M., Frieman, E.A., Report PPPL-1587 (1979) Princeton University.

41. Dewar, R.L., Manickam, J., Grimm, R.C., Chance, M.S., Report PPPL-1663 (1980) Princeton University.

42. Weinberg, S., Phys. Rev. 126 (1962) 1899.

43. Bender, C.M., and Orszag, S.A., in Advanced Mathematical Methods for Scientists and Engineers, Mc-Graw Hill Book Company (1978), p. 484.

44. Solovev, L.S., Sov. Phys. JETP 26 (1968) 400.

45. Laing, E.W., Roberts, S.J., Whipple, R.T.P., J. Nuclear Energy, Part C: Plasma Phys. 1 (1959) 49.

46. Solovev, L.S., and Shafranov, V.D., in Reviews of Plasma Physics, Vol. 5 (Consultants Bureau, New York, 1970), p. 221.

47. Galvão, R., Ph.D. Thesis, Massachusetts Institute of Technology (1975), p. 109.

48. Ramos, J.J., J. Plasma Phys. 22 (1979) 97.

49. Ramos, J.J., Antonsen, T., Coppi, B., and Ferreira, A. 1979 Sherwood Meeting on Theoretical Aspects of Controlled Thermonuclear Research, Paper 2C34.

50. Lortz, D., Nührenberg, J., 1979 Sherwood Meeting on Theoretical Aspects of Controlled Thermonuclear Research, Paper 2B18.

51. Coppi, B., Ferreira, A., Ramos, J.J., Phys. Rev. Lett. 44 (1980) 990.

52. Lortz, D., Nührenberg, T., Nucl. Fusion 19 (1979) 1207.

53. Abramowitz, in Handbook of Mathematicl Functions, 753, M. Abramowitz and I.A. Segun, Eds., Dover Publications, Inc. (1965) New York.

54. Antonsen, Jr., T.M., private communication.

55. Mikhailovskii, A.B., in Theory of Plasma Instabilities (Consultants Bureau, New York, 1974), Vol. 2, p. 178.

56. Abramowitz, M. and Segun, I.A., op. cita, p. 555.

57. Abramowitz, M. and Segun, I.A., op. cita, p. 355.

58. Coppi, B., Ferreira, A., Ramos,J.J., Massachusetts Institute of Technology (RLE) Report PRR-79/26, Cambridge, Mass. (1979). To be published in the Proceedings of the Workshop on Physics of Plasmas Close to Thermonuclear Conditions (Coppi, B., Sadowsky, W., Eds., U.S. Department of Energy, Washington, D.C., 1980).

59. Barston, E.M., Ann. Phys. 29 (1964) 282.

60. Pao, Y.Y., Nucl. Fusion 15 (1975) 631.

61. Uberoi, C., Phys. Fluids 15 (1972) 1673.

62. Pridmore Brown, D.C., Phys. Fluids 9 (1966) 1290.

63. Lau, Y.Y., Phys. Rev. Lett. 42 (1979) 779.

64. Lighthill, M.J., in Fourier Analysis and Generalized Functions, p. 40 (Cambridge University Press, Cambridge, Mass. 1958).

65. Lighthill, M.J., op. cita, p. 52.

66. Coppi, B., Report MATT-471, Plasma Physics Laboratory, Princeton University (1966).

67. Shafranov, V.D. and Yurchenko, E.I., Sov. Phys. JETP, 26 (1968) 682.

68. Strauss, H.R., Bull. of the Am. Phys. Soc., Vol. 25, No. 8 (October 1980) Paper 5Q14.

69. Timofeev, A.V., Sov. J. Plasma Phys. 2 (1976) 280.

70. Rosenbluth, M.N., Rutherford, P.H., Phys. Rev. Lett. 34 (1975) 1428.

71. Coppi, B., Pegoraro, F., Comments on Plasma Physics and Controlled Fusion, Vol. V, 4 (1979) 131.

72. Coppi, B., Ferreira, A., Massachusetts Institute of Technology (RLE) Report PRR-80/1, Cambridge, Mass. (1980). To be published in Proceedings of the Workshop on Physics of Plasmas Close to Thermonuclear Conditions (Coppi, B., Sadowsky, W., Eds., U.S. Department of Energy, Washington, D.C. 1980).

73. Orr, W. McF., Proc. R. Irish Acad. A, 27 (1979) 69.

74. Mizoguchi, T., Kammash, T., Sigmar, D.J., Report TN 37830 (1978) Oak Ridge National Laboratory.

75. Ames, W.F., in Numerical Methods for Partial Differential Equations, page 180 (Academic Press, New York, NY, 1977).

76. Hilderbrand, F.B., Advanced Calculus for Applications, p. 417 (Prentice Hall, Inc., Englewood Cliffs, N.J. 1976).

77. Chance, M.S., Greene, J.M., Grimm, R.C., Johnson, J.L., Nucl. Fusion 17 (1977) 65.

78. White, R.B., Monticello, D., Park, W., Strauss, H., Jardin, S., and Chance, M., Internatioanl Center for Theoretical Physics, Autumn College on Plasma Physics (1979), Paper SMR/61-59.

79. Sugiyama, L. and Mark, J. W.-K., Massachusetts Institute of Technology (RLE) Report PRR-80/7, Cambridge, Mass. (1980).

80. Ramos, J.J. and Sugiyama, L., private communication.

81. Prager, S.C., Halle, J.H., Phillips, M.W., Post, R.S., and Twichell, J.C., Report distributed at the Conference of the American Physical Society, Boston, Mass., November 1980.

82. Chu, C.K., Elkin, D., Georgin, G., Gross, R.A., Johnston, S., Kashani, A., Lui, H.C., Machida, M., Marshall, T.C., Navratil, G.A., Peseckis, F., Weber, P.G. and Yamazaki, K., 8th International Conference on Plasma Physics and Controlled Nuclear Fusion Research, Paper IAEA-CN-38/L-4-2.